

DISSERTATION

**EXPERIMENTAL STUDY ON MITIGATION OF
LIQUEFACTION-INDUCED GROUND DEFORMATION BY
USING GRAVEL AND GEOSYNTHETICS**

Graduate School of
Natural Science and Technology
Kanazawa University

Division of Environmental Design

Student ID Number: 1524052018

Name: Hendra Setiawan

Chief Advisor: Prof. MIYAJIMA Masakatsu

Date of Submission: June 2018

博 士 論 文

EXPERIMENTAL STUDY ON MITIGATION OF
LIQUEFACTION-INDUCED GROUND DEFORMATION
BY USING GRAVEL AND GEOSYNTHETICS

砕石とジオシンセティックスを用いた液状化による地盤変形
の抑制に関する実験的研究

金沢大学大学院自然科学研究科

環境デザイン学専攻

Student registration No.: 1524052018

Name: Hendra Setiawan

Supervisor: Prof. MIYAJIMA Masakatsu

SUMMARY

Soil liquefaction has been observed during past major earthquakes, and in several occurrences, it caused extensive damage. Its devastating effects sprang to the attention of engineers since 1964 by the catastrophic earthquake in Alaska, US, and followed by the Niigata earthquake, Japan. Since these two devastating earthquakes, liquefaction has been studied extensively by engineers around the world, especially in the earthquake-prone countries. There are frequent reports regarding the damage to the constructions in the previous earthquakes, such as the 1964 Niigata earthquake Japan (Ishihara and Yoshimine, 1992; Bhattacharya et al., 2014), 1995 Great Hanshin earthquake Kobe Japan (Tokimatsu and Asaka, 1998), 1999 Chi-Chi earthquake Taiwan (Chu, et al., 2004), 2010 Chile earthquake (Verdugo and Gonzalez, 2015), 2011 Tohoku Pacific earthquake Japan (Tokimatsu, et al., 2012; Miyajima, 2013), 2010-2011 Christchurch earthquake New Zealand Potter, et al., 2015), 2015 Nepal earthquake (Gautam et al., 2017), and the 2016 Kumamoto earthquake Japan (Bhattacharya et al., 2018).

Ground deformation is one of the unpleasant forms of liquefaction. Mainly, ground deformation caused by liquefaction could be observed in two different configurations, namely horizontal ground movements and vertical ground displacements. These two liquefaction-triggered ground displacement may cause massive damage to constructions built on it.

Lateral spreading is the term used to state the liquefaction-induced horizontal movements of the ground that mainly appears in the gently sloping ground. When lateral spreading appears, the ground rips, opening surface cracks and fissures across the slope. In the previous earthquake, lateral spreading has forced damages to engineering structures, for example, as reported by Motamed and Towhata (2010) in the 1964 Niigata earthquake, the 1983 Nihonkai-Chubu earthquake, and the 1995 Kobe earthquake.

Furthermore, soil liquefaction also decreases the strength of the soil. If the residual soil strength reaches the amount that is insufficient to support the constructions built above it, the settlement will occur. The magnitude of the settlement is influenced by several factors, such as peak ground acceleration (PGA) and the soil density. Occasionally, the ground composed of soils with different relative densities, the imbalanced settlement could appear. In the severe conditions, this condition leads to extensive damages and cause significant

effects on society, such as impassable roads and tilted buildings. Tokimatsu et al. (2012) presented liquefaction-induced damage to buildings in Urayasu City during the 2011 Tohoku Pacific earthquake. In contrary, it is important to keep some vital constructions such as evacuation roads and shelters still usable during earthquakes.

Over the last few decades, many methods have been suggested to alleviate the ground movements caused by liquefaction, for instance, as reported by Yoshida et al. In 2013. They clarified that the use of wooden piles could increase the resistance of the ground against liquefaction due to the increase of ground density by piling and the dissipation of excess pore water pressure along the surface of the piles. Correspondingly, Murakami et al. (2010) pointed out that, the use of the gravel and geosynthetics effectively reduced the settlement of the embankment during liquefaction. Lateral spreading of the gently sloping ground Previously, a conventional countermeasure such as cement solidification and sand compaction pile have been employed to reinforce liquefiable ground. However, since these methods are costly and complicated, its use becomes limited, and can not be widely applied, for example, constructions such as small planar roads and residential houses would not be able to afford these costly methods.

In this study, laboratory experiments were performed to investigate the effectiveness of gravel in conjunction with geosynthetics to mitigate liquefaction-induced ground deformation, both horizontal and vertical deformations. The performance of the proposed methods quantitatively observed by using a sequence of 1-g shaking table test. The result of this study will provide a recommendation regarding the effective and affordable techniques to mitigate the ground deformation induced by liquefaction. This proposed technique is expected to complement the existing methods and can be widely applied.

ACKNOWLEDGMENTS

The achievement during my doctoral course at Kanazawa University in the last three years would not be possible without the support from many parties, including teachers, colleagues, friends, and family members.

First and foremost, I want to thank my main supervisor, Professor MIYAJIMA Masakatsu for his complete support. He with great enthusiasm, unlimited patience and full of energy has guided me in my doctorate studies, always encouraged me to solve the obstacles while I am doing my research. Thank you for your continuous support and advice. Your enthusiasm and energy made me feel that the time I passed in our laboratory was one of the best phases of my life.

I would also express my deepest thanks to my dear professors in Earthquake Engineering Laboratory; DR. IKEMOTO Toshikazu and DR. MURATA Akira for their great support, advice, and guidance during my study time.

I would like to thank the committee members of my dissertation: Professors MIYAJIMA Masakatsu, IKEMOTO Toshikazu, KOBAYASHI Shunichi, FUKADA Saiji from Kanazawa University, and Professor HASHIMOTO Takao from Kokushikan University for their helpful discussions and critical reading.

I enjoyed the environment of the laboratory, and it gave a positive influence on my study progress. Therefore, I feel I am indebted to all of my friends and colleagues particularly the liquefaction group members: Mr. SUGITA Wataru, Mr. MATSUNO Kenji, and the one and only Ms. SERIKAWA Yuko, for their helpful and support while doing liquefaction experiments. Also, I would like to thank Mr. ISHIDA Akihisa for helped me in my early time in Kanazawa. Moreover, of course, last but not least, Ustadz Rama, for created Indonesian atmosphere in our laboratory. My deepest thank also goes to my friend the members of “2015 KU-DIKTI”.

I would like to thank also Directorate of Resources for Science, Technology, and Higher Education, Ministry of Research, Technology and Higher Education of Indonesia for providing me the scholarship.

My sincerest gratitude goes out to my family for their support, encouragement, and unflinching love throughout my life. I attribute my success to their reassuring love and sacrifice.

EXPERIMENTAL STUDY ON MITIGATION OF LIQUEFACTION-INDUCED GROUND DEFORMATION BY USING GRAVEL AND GEOSYNTHETICS

TABLE OF CONTENTS

SUMMARY	i
ACKNOWLEDGMENTS	iii
LIST OF FIGURES	vii
LIST OF TABLES	x
1. INTRODUCTION	1
1.1 General Remarks	1
1.2 An Overview of Liquefaction Phenomenon.....	2
1.3 An Overview of Liquefaction-induced Ground Displacement.....	2
1.3.1 Horizontal Ground Displacement.....	3
1.3.2 Vertical Ground Deformation	3
1.4 Literature Review of Current Research on Liquefaction Phenomenon and Countermeasure Method	5
1.4.1 The Liquefaction Phenomenon and its Occurrence in Previous earthquakes.....	5
1.4.2 Liquefaction Countermeasure Method	7
1.5 Research Objectives and Scope	14
1.6 Research Significance.....	15
1.7 Thesis Organization	15
1.8 References.....	16
2. AN OVERVIEW OF LIQUEFACTION-INDUCED GROUND DEFORMATION IN THE PREVIOUS EARTHQUAKES	20
2.1 Introduction.....	20
2.2 The 2010 Chile Earthquake	20

2.3 The 2011 Great East Japan Earthquake	23
2.4 The 2010-2011 Canterbury Earthquakes, New Zealand.....	25
2.5 The 2016 Kumamoto Earthquake, Japan.....	27
2.6 Discussion.....	29
2.6 References.....	29
3. THE ALLEVIATION OF LATERAL SOIL MOVEMENT GENERATED BY LIQUEFACTION BY UTILIZING GRAVEL AND GEOSYNTHETICS	31
3.1 Introduction.....	31
3.2 Previous Studies on Lateral Spreading Caused by Liquefaction.....	33
3.3 Laboratory Tests on Mitigation of Lateral Ground Movements Induced by Liquefaction with Gravel and Geosynthetic	35
3.3.1 Instruments Used in the Experiment	35
3.3.2 Material Properties	35
3.3.3 Experimental Setup	37
3.3.4 Pull-Out Test	40
3.4 Experimental Results	42
3.4.1 Excess Pore Water Pressure	42
3.4.2 Lateral Ground Movements	46
3.4.3 Pull-Out Test	51
3.5 Conclusions.....	53
3.6 References.....	53
4. THE MITIGATION OF LIQUEFACTION-INDUCED VERTICAL GROUND DEFORMATION BY USING GRAVEL AND GEOSYNTHETICS.....	55
4.1 Introduction.....	55
4.2 Previous Studies on Liquefaction-Induced Ground Settlement.....	55
4.3 Laboratory Test of the Liquefaction-induced Vertical Ground Movements.....	57
4.3.1 Material and Instrument utilized	57
4.3.2 Experimental Set-up.....	57
4.4 Experimental Results and Discussion	59
4.4.1 Pore Water Pressures.....	60
4.4.2 Acceleration	61

4.4.2 Vertical Ground Deformation	64
4.5 Conclusions.....	69
4.6 References.....	70
5. CONCLUDING REMARKS	71
APPENDIX A.....	73

LIST OF FIGURES

1.1	Liquefaction-induced damages	2
1.2	Liquefaction-induced lateral spreading in the previous earthquakes	4
1.3	Liquefaction-induced settlements in the previous earthquakes	4
2.1	Post-liquefaction settlements in the 2010 Chile earthquake	21
2.2	Damaged road due to lateral spreading	21
2.3	Collapse of the Hospital overpass	22
2.4	Damaged ports due to lateral spreading	22
2.5	Boiled sand on the road in the 2011 Great East Japan earthquake	23
2.6	Damages caused by liquefaction in the 2011 Great East Japan earthquake	24
2.7	Liquefaction-induced lateral spreading in the 2011 Great East Japan earthquake	24
2.8	Tilted buildings due to liquefaction-induced differential settlements.....	26
2.9	Lateral spreading occurred in the 2010-2011 Canterbury earthquakes, New Zealand.....	26
2.10	Road surface cracks due to lateral spreading towards the Avon River.....	26
2.11	Buildings suffered from differential settlements due to liquefaction.....	28
2.12	Damaged buildings caused by liquefaction-induced ground deformation.....	28
2.13	Lateral spreading in the river bank of Kiyama River, Akitsu Town, Kumamoto.....	28
3.1	The lateral spreading due to liquefaction during the 1995 Kobe earthquake	32
3.2	The lateral spreading due to liquefaction during the 2010-2011 Canterbury earthquakes, New Zealand.....	33
3.3	The photograph of the instruments used	36
3.4	The photograph of the materials used	37
3.5	The plan view and cross-section of the unreinforced model.....	38
3.6	The side view of the reinforced models (Case 2 – Case 6).....	39
3.7	Pull-out test set up.....	41
3.8	Instruments used in the pull-out test	42
3.9	Excess pore water pressure time histories for P1	43
3.10	Excess pore water pressure time histories for P2.....	43
3.11	Excess pore water pressure time histories for P3.....	44

3.12	Excess pore water pressure time histories for P4.....	44
3.13	Excess pore water pressure time histories for P5.....	45
3.14	Pore water pressure ratio of 5 cases for P1 – P5	45
3.15	Ground surface lateral spreading measured for Case 1.....	47
3.16	Ground surface lateral spreading measured for Case 2.....	47
3.17	Ground surface lateral spreading measured for Case 3.....	48
3.18	Ground surface lateral spreading measured for Case 4.....	48
3.19	Ground surface lateral spreading measured for Case 5.....	49
3.20	Averaged ground surface lateral spreading.....	49
3.21	Ground surface lateral spreading measured for Case 6.....	51
3.22	Averaged ground surface lateral spreading of Cases 1, 3, and 6	51
3.23	Friction angle of the geosynthetics used	52
4.1	Damaged constructions due to liquefaction-induced ground displacements	56
4.2	The top view of the sandbox	58
4.3	The side view of the unreinforced ground (case 1).....	58
4.4	The side view of the gravel-reinforced ground (Case 2).....	59
4.5	The side view of the gravel and geosynthetic (type I and II) reinforced ground (Cases 3 & 4).....	59
4.6	Pore water pressures time histories in the loose sand condition (P1)	60
4.7	Pore water pressures time histories in the dense sand condition (P2).....	61
4.8	Acceleration time histories of no countermeasures ground (Case 1).....	61
4.9	Acceleration time histories of gravel-reinforced ground (Case 2).....	61
4.10	Acceleration time histories of gravel and geosynthetic type I-reinforced ground (Case 3).....	62
4.11	Acceleration time histories of gravel and geosynthetic type II-reinforced ground (Case 4).....	62
4.12	Amplification acceleration measured in the loose sand condition (A1)	63
4.13	Amplification acceleration measured in the dense sand condition (A2).....	64
4.14	Averaged residual vertical ground displacement	67
4.15	Differential settlements between the loose and dense sand zones	68
4.16	The ground surface inclination angle at the border line between loose and dense sand zones	68
A.1	The seismology of the 2016 Kumamoto earthquake, Japan	74

A.2	The recorded acceleration, velocity response, and response of the KMMH16 station at Mashiki town for the foreshock.....	75
A.3	The recorded acceleration, velocity response, and response of the KMMH16 station at Mashiki town for the mainshock	76
A.4	The residential houses damage in Mashiki town	76
A.5	The landslides during the 2016 Kumamoto earthquake	77
A.6	The fault movement during the 2016 Kumamoto earthquake	78
A.7	Liquefaction sites during the 2016 Kumamoto earthquake	79
A.8	Liquefaction-induced ground subsidence during the 2016 Kumamoto earthquake	79
A.9	The geologic map of Kumamoto city	81
A.10	J-SHIS Japan seismic hazard map.....	81
A.11	Location of the field survey	82
A.12	Topography classification map of the surveyed sites	82
A.13	Measurement locus of the house	83
A.14	The location of the surveyed area and borehole in Akitsu town.....	84
A.15	The tilt angle and tilt direction measured in Akitsu town.....	85
A.16	One of the tilted houses in Akitsu town.....	85
A.17	The lateral spreading occurred at Kiyama Riverbank, Akitsu town	86
A.18	The summary of the structural type and damage level of buildings in Akitsu town	86
A.19	The pile-supported house which experienced minor inclination in Akitsu town	87
A.20	The location of the surveyed area and borehole in Chikami-Karikusa towns	88
A.21	The location of the surveyed area and borehole in Chikami-Karikusa towns	88
A.22	The guiding pillar of former Chikami bridge.....	89
A.23	The inclination angle and its direction measured in Chikami town.....	90
A.24	The summary of the structure type and damage level several buildings In Chikami town.....	90
A.25	The inclination angle and its direction measured in Karikusa town	91
A.26	The summary of the structure type and damage level buildings in Karikusa town	92

LIST OF TABLES

3.1 Instrument's specifications	35
3.2 Index properties of materials used.....	36
4.1 Residual settlement for Case 1	64
4.2 Residual settlement for Case 2	65
4.3 Residual settlement for Case 3	65
4.4 Residual settlement for Case 4	66

1. INTRODUCTION

1.1 General Remarks

Liquefaction is one of the most complex and important topics in geotechnical earthquake engineering. This phenomenon has come to the attention of experts since 1964. In the previous time, liquefaction does not attract much attention since it does not cause casualties compared to the collapse of buildings and slopes failure. Furthermore, liquefaction is not considered a threat to public safety as it often occurs in areas not widely utilized by society. In March 1964, the Good Friday earthquake ($M = 9.2$) occurred in Anchorage, Alaska, followed by the Niigata earthquake ($M = 7.5$) in Japan, in June. Both earthquakes caused serious liquefaction-induced damage, such as bridge and building failures, slope failures, and flotation of buried structures. Ever since then, studies on mechanism and prediction of liquefaction as well as countermeasure methods were initiated.

Constructions, such as roads and buildings, which built on the soft liquefiable ground, may be damaged by liquefaction during earthquakes that cause large ground deformation. The damages that occur, among others, the tilted buildings, and the road surface deformation. Figure 1.1 (a) shows the damaged road construction of the Joban Motorway near Mito, Ibaraki, due to liquefaction occurred in the Great East Japan Earthquake in 2011. The tilted residential house due to liquefaction can be seen in Figure 1.1 (b), which occurred in the 2016 Kumamoto Earthquake, Japan. On top of that, in the severe conditions, road surface deformation can lead to impassable roads. However, for the vital roads such as main roads, evacuation routes, it is indispensable to guarantee the accessibility of these valuable roads during earthquakes. Hence, for that reason, it is essential to restrain liquefaction-induced ground deformation by economical and easy methods.

This chapter carries a review of relevant studies. An overview of the liquefaction phenomenon is presented in Section 1.2. In Section 1.3, the discussion is focused on ground displacement due to liquefaction, either vertical or horizontal displacement. Section 1.4 reviews and summarizes the literature on liquefaction phenomenon, liquefaction-induced ground displacement, and its countermeasure methods.



Figure 1.1 Liquefaction-induced damages:
 (a) The damaged road in the 2011 Great East Japan earthquake
 (b) Tilted residential house in the 2016 Kumamoto earthquake

1.2 An Overview of Liquefaction Phenomenon

The term liquefaction, originally invented by Mogami and Kubo (1953). Seismic liquefaction occurs in the saturated loose sandy ground. During shaking, saturated cohesionless soils tend to densify, and causes excess pore pressures to increase and effective stresses to decrease with time. As a result, in a complete loss of effective stress condition, sand has neither shear strength and consequently develops large deformation.

There are frequent reports regarding the damage to the constructions due to liquefaction and ground movement in the previous earthquakes, such as 1964 Alaska America, 1964 Niigata Japan ([Ishihara](#) and Yoshimine, 1992; Bhattacharya et al., 2014), 1995 Great Hanshin Earthquake Kobe Japan (Tokimatsu and Asaka, 1998), 1999 Chi-Chi Earthquake Taiwan (Chu, et al., 2004), 2010 Chile Earthquake (Verdugo and Gonzalez, 2015), 2011 Tohoku Pacific Earthquake Japan (Tokimatsu, et al., 2012; Miyajima, 2013), 2010-2011 Christchurch Earthquake New Zealand (Potter, et al., 2015), 2015 Nepal Earthquake (Gautam, et al., 2017), and 2016 Kumamoto Earthquake Japan (Bhattacharya, et al., 2018). However, the significant liquefaction and ground deformation damage have not only occurred under very strong earthquakes, but also under moderate levels of earthquake motion.

1.3 An Overview of Liquefaction-induced Ground Displacement

The adverse effects of liquefaction take many forms, such as ground deformation. There are some different appearances of ground deformation, for instance, lateral spreading of slightly

inclined ground, and settlement of the ground. These liquefaction-induced ground deformation may cause extensive damage to highways, railroads, pipelines, and buildings.

1.3.1 Horizontal Ground Displacement

Lateral spreading is the term used to refer to the development of horizontal ground displacement due to liquefaction that mainly occurs in the marginally sloping ground. Saturated loose cohesionless soils are prone to excess pore water pressure and liquefaction during earthquakes, and consequently, lateral displacements may occur. When lateral spreading occurs, the ground tears, opening surface cracks and fissures across the slope. This type of stretching of the ground can introduce significant lateral forces into foundation elements and built structures. If the foundation is not strong enough to resist the movement, the lateral spread causes it to extend. Furthermore, lateral spreading close to a waterway can cause damage to the surrounding land and the buildings it supports. Typically, the degree of lateral movement lessens as the distance from the waterway increases.

Lateral spreading has imposed damages to structures during previous large earthquakes, for instance, the 1964 Niigata, the 1983 Nihonkai-Chubu, and the 1995 Kobe earthquake (Motamed and Towhata, 2010) and the 2010-2011 Canterbury earthquakes (Cubrinovski and Robinson, 2016). Figure 1.2 (a) displays the lateral spreading that occurred along river road in Richmond, Christchurch, in the 2011 Christchurch earthquake, New Zealand (Heather and Wright, 2011). Figure 1.2 (b) shows the collapse of the Showa Bridge in Niigata after the 1964 earthquake. Lateral spreading was observed in the loose sands of the riverbanks, and it is suspected that it caused the failure of the bridge (Agaiby and Ahmed, 2016).

1.3.2 Vertical Ground Deformation

Landfilled ground occasionally liquefies due to large earthquakes and triggers ground deformation and may devastate constructions built on top of it. Liquefaction occurrence will cause the strength of the soil to support the structure reduced. If the strength decreases to an amount that is insufficient to hold the structure, large subsidence takes place. The magnitude of the settlement is influenced by several factors, such as Peak Ground Acceleration (PGA) and the relative density of the soils.



(a)



(b)

Figure 1.2 Liquefaction-induced lateral spreading in the previous earthquakes:
 (a) Richmond, Christchurch, in the 2011 Christchurch earthquake,
 (b) the collapse of Showa Bridge in the 1964 Niigata earthquake

There are several reports related to the damage due to liquefaction-induced ground subsidence in the previous major earthquakes. For example, Tokimatsu et al. (2012) presented liquefaction-induced damage to buildings in Urayasu City during the 2011 Tohoku Pacific earthquake, and Verdugo and Gonzalez (2015) described the liquefaction-induced ground damages during the 2010 Chile earthquake. Figure 1.3 (a) shows the liquefaction-induced large-scale settlement of the approach fills at Raqui 2 Bridge during the 2010 Chile earthquake (Anon., 2011). Figure 1.3 (b) illustrates the bridge damage due to liquefaction-induced ground settlement within the fill of the approach and displacements of abutment side walls in 2009 West Sumatra earthquake, Indonesia (Kusumastuti et al., 2010).



(a)



(b)

Figure 1.3 Liquefaction-induced settlements in the previous earthquakes:
 (a) Raqui 2 Bridge, Chile, in the 2010 Chile earthquake,
 (b) Padang, West Sumatra, Indonesia, in the 2009 West Sumatra earthquake

1.4 Literature Review of Current Research on Liquefaction Phenomenon and Countermeasure Method

Since 1964, when Alaska and Niigata earthquakes occurred, many researchers have studied on liquefaction phenomenon. In this thesis, the previous studies on liquefaction were classified into two groups: first, the nature of liquefaction phenomenon and its occurrence in the previous earthquake Reported, and second, the studies carried out in order to mitigate the liquefaction.

1.4.1 The Liquefaction Phenomenon and its Occurrence in the Previous Earthquakes

Hwang et al. (2003) investigated soil liquefaction during the 1999 Chi-Chi earthquake. They found that the sites where significant liquefaction occurred can be categorized as hydraulically-filled reclaimed land, riverbanks and nearby alluvial deposits, and alluvial deposits in old river channels or fans. Furthermore, on the liquefied horizontal ground, the ground subsidence and the sloping of the building largely swelled with the number of the stories, and buildings with pile foundations or underground basement suffered slight breakage.

Miyajima (2013) studied the performance of drinking water pipelines in liquefaction areas in the 2011 Great East Japan Earthquake. It is determined that the destruction level of drinking water pipeline in the filled land in Urayasu City be 1.60 cases/km, which comparable to the destruction level of pipeline buried in the reclaimed land of Kobe, Ashiya, and Nishinomiya Cities in the 1995 Kobe earthquake.

Potter et al. (2015) reported that in The 2010-2011 Canterbury earthquakes, in Christchurch, there was major destruction to the built environment due to liquefaction. A massive quantity of silt was ejected onto the surface. Approximately 900,000 tonnes of liquefaction silt were removed from the greater Christchurch area and washed into waterways, increasing the concentration of suspended sediment and causing impacts on water quality which reflected by the high level of bacteria (*Escherichia Coli*) in lower reaches. The ground height was changed in parts of Canterbury through settlement and tilting. Moreover, much of the underground infrastructure was damaged by the movement and liquefaction which causing lifeline failure.

Tokimatsu et al. (2015) conducted a field survey on building damage associated with geotechnical problems in the 2011 Tohoku Pacific earthquake and revealed conclusions as follows; 1. Liquefaction mainly appeared around Tokyo Bay and in the basin of Tone River inland areas reclaimed in relatively recent years. In some locations, grave sand boils, and ground subsidence of up to 50 cm triggered by liquefaction, leading to breakages such as the incline and the settlement of wooden and buildings reinforce with concrete on spread foundations, the uplift of underground structures and the collapses of roads. Liquefaction also caused a significant gap between pile-supported buildings and the surrounding ground, without structural damage was found in superstructures. Buildings on spread foundations having high rigidity, such as mat foundations, did not suffer structural damage to its superstructures, even when inclined.

Verdugo and Gonzalez (2015) reported liquefaction-induced ground damages during the 2010 Chile earthquake. They observed that liquefaction sites were found along the country, covering a prolongation close to 1000 km, which roughly reflects twice the size of the rupture zone. The farthest site with confirmation of liquefaction was observed at Llanquihue Lake, located at 550 km and 350 km from the epicenter and fault, in turn. Largest displacements were verified at the tip of the Arauco Peninsula, with an uplift of 1.8 m and a horizontal movement in the direction of the trench of 5.1 m.

Cubrinovski and Robinson (2016) investigated lateral spreading in 2010-2011 Christchurch earthquakes. According to their report, in these earthquakes, liquefaction appeared almost half of the urban area of Christchurch and the heaviest destruction to buildings and infrastructure was often associated with lateral spreading. The analysis, results, and interpretation of lateral spreads using measurements from detailed ground surveying at locations along the Avon River were presented.

Gautam et al. (2017) mentioned that soil liquefaction occurrence was found in the form of sand boils and lateral spreading in 12 locations during the 2015 Gorkha, Nepal earthquake. Also, numerical analysis based on geotechnical investigation records have been performed. Furthermore, by comparing existing vulnerability maps and their numerical analysis, together with field verification, it is confirmed that the existing susceptibility maps are unreliable.

Bhattacharya et al. (2018) discovered that during the 2016 Kumamoto earthquake, liquefaction was detected along the quadrangular strip between two rivers which was an old natural river dike. This liquefaction occurrence shows the significance of carrying out appropriate and sufficient ground improvement while reclaiming the ground. Furthermore, a study of the boiled sand showed that black volcanic soil liquefied.

1.4.2 Liquefaction Countermeasure Method

Akiyoshi et al. (1993) conducted the two-dimensional finite element program NUP2 liquefaction investigation of sandy ground enhanced by sand compaction piles. The numerical and experimental study performed showed that there might exist unsteady areas in the compressed zone near the unimproved area and an optimum compaction width to counterattack liquefaction of the ground for design objectives.

Zheng et al. (1996) evaluated the performance of sheet pile-ring countermeasure against liquefaction for oil tank site using the finite element numerical model. The results show that the numerical model could reproduce the observed earthquake reactions of the tank-ring-soil system and that the excess pore water pressure and the subsidence of the tank could be considerably decreased using this proposed method.

Haeri et al. (2000) performed a laboratory triaxial compression tests to ascertain the influence of geotextile strengthening on the mechanical performance of sand by means of varying the number of geotextile layers, type of geotextiles, confining pressure, and geotextile composition. The results demonstrated that geotextile existence enlarges the maximum strength, axial strain at failure, and ductility. However, it downgrades dilation.

Alawaji (2001) observed the vertical deformation and bearing capacity of the geogrid-strengthened sand of collapsible soil. Model load experiments were conducted using a circular plate of 100 mm diameter and Tensar SS2 geogrids. The width and depth of the geogrid were varied to ascertain its influences on the collapse settlement, deformation modulus, and bearing capacity ratios. The results showed a considerable disparity in the structural contribution of the tested geogrid which range from 95% decrease in subsidence, 2000% enlarge in elastic modulus, and 320% enhance in bearing capacity.

Boominathan and Hari (2002) studied the liquefaction strength of fly ash strengthened with disordered scattered fibers by conducting a series of stress-controlled cyclic triaxial experiments. The liquefaction strength is expressed regarding pore pressure ratio. The results show that the use of fiber elements enlarges the liquefaction resistance of fly ash remarkably and arrests the initiation of liquefaction even in models of the loose initial condition and consolidated with the low confining pressure.

Adalier et al. (2003) developed stone columns as liquefaction countermeasure in non-plastic silty soils by performing centrifuge investigations. The study focused on investigating the overall site stiffening consequences due to the stone column existence rather than the drainage effects. The results demonstrate that stone columns can be an efficient technique in the remediation of liquefaction-induced of nonplastic silty deposits, specifically under shallow foundations.

Orense et al. (2003) developed wall-type gravel drains as liquefaction countermeasure for underground structures. In this study, the implementation of reprocessed concrete crushed stones as gravel drain materials were measured by conducting two series of shaking table tests. The results showed that gravel drains, when appropriate grain size distribution is considered, effectively dissipate the excess pore water pressure underneath the structure, and consequently lessen the level of uplift.

Chang et al. (2004) performed a study of direct assessment of the usefulness of manufactured vertical drains in the liquefiable sand by a dynamic full-scale testing program. The effectiveness of the proposed mitigation method is evaluated experimentally by comparing the pore pressure generation, pore pressure dissipation, and vertical deformation from two reconstituted soil samples. The results showed that the drainage afforded by manufactured drains could considerably downgrade pore pressure generation, accelerate post-shaking pore pressure dissipation, and control related vertical displacement.

Takahashi and Takemura (2005) conducted centrifuge model experiments to study the dynamic performance of a pile-supported wharf, focusing on the failure process of the piles, the consequences of liquefaction on the permanent displacement of the wharf during earthquakes. In the parametric study, varying the thickness of the and layer under the rubble mound caused a change of the deformation mode of both ground and structures, and it is

revealed that a thicker liquefiable sand layer does not certainly trigger a larger distortion of soils and the structures.

Harada et al. (2006) developed a new drain method for protection of existing pile foundations from liquefaction effects by performed shaking table tests and on-site experiment. They found that when the intensity of earthquake motion is 200 gal or less, generation of excess pore water pressure is lessened and the pile bending moment is diminished, but if the intensity is greater, drainage impression avoids the disappearance of subgrade response. Moreover, drain type proposed can manage pore water pressure without blocking.

Liu and Song (2006) studied the working mechanism of cutoff walls in reducing uplift of large buried structures provoked by soil liquefaction by using the fully coupled dynamic finite element code DIANA Swandynne-II. They found that the insignificant effective unit weight of buried constructions, the generation of excess pore pressure and the flow of liquefied soil were the adequate and required conditions for buried constructions to uplift throughout an earthquake. Cutoff walls could control the flow or displacement of liquefied soils and prevent the uplift of underground structures, but they could not inevitably constrain the liquefaction of the surrounded soils.

Gallagher et al. (2007) investigated the colloidal silica treatment on the liquefaction and deformation resistance of loose, liquefiable sands during centrifuge in-flight shaking. Loose sand was saturated with colloidal silica grout and subsequently subjected to two shaking events to evaluate the response of the treated sand layer. The result showed that the improved soil did not liquefy during either shaking event.

Muntohar et al. (2008) carried out a study to mitigate liquefaction by using cement-column. It is concluded that of cement-column installation increased the strength of the ground the column, both radially and vertically and indicated that the risk of liquefaction is reduced.

Motamed and Towhata (2010) presented experimental results of a series of 1-g shake table tests on mitigation measures for a model consisting of 3 x 3 pile group and a sheet-pile quay wall in which the pile group was subjected to liquefaction-induced lateral spreading. In this study, three remedial techniques were deployed, namely sheet pile of floating type, sheet pile of fixed end type, and anchoring the quay wall to a new pile row. The results demonstrate

that by applying the proposed mitigation measures the seismic performance of both pile group and quay wall can be improved, as a result of a reduction in soil displacement and velocity of soil flow.

Valsamis et al. (2010) carried out a parametric investigation of horizontal ground deformation of the gently sloping liquefied ground. In this study, the main device used is a numerical methodology occupying a bounding surface plasticity model applied in a finite difference code, which has been comprehensively confirmed against 16 published centrifuge horizontal ground displacement experiments. The results show that important problem parameters are the mean ground acceleration, the period of strong shaking, the beginning of liquefaction, the corrected SPT blowcount, the depth of the sliding plane, the slope of the ground surface and the fines content of the liquefied soil layers.

Raisinghani and Viswanadham (2011) conducted a centrifuge model study on low permeable slope strengthened by hybrid geosynthetics. In this study, four centrifuge tests have been carried out on 2V:1H at 30 gravities. One unstrengthened, one model geogrid reinforced, and two hybrid geosynthetic reinforced incline models with a varying number of hybrid geosynthetic layers were verified. It was confirmed that the hybrid geosynthetic enlarge the steadiness of low permeable slope exposed to water table rise. The hybrid geosynthetic layers in the lowest half of the slope height play an important part in the dissipation of pore water pressure.

Liu et al. (2011) observed the static liquefaction performance of saturated fiber-reinforced sand in undrained ring-shear tests. The results indicate that the undrained shear performance of fiber-reinforced loose samples is not significantly affected by the existence of the fiber, but for medium dense and dense samples, the existence of fiber affects their undrained performance.

Azzam and Nazir (2012) proposed liquefaction mitigation using lateral confinement technique. The results demonstrated that the cell lessened the excess pore water pressure within the confined zone and the pore water pressure alleviation outside the confined block where the liquefaction is generated. Moreover, the maximum foundation acceleration of the confined footing soil system is decreased compared to the case of without cell confinement.

Haeri et al. (2012) carried out a large-scale 1-g shake table test to ascertain the reaction of a pile group to liquefaction-induced lateral spreading. It was found that the behavior of a group of piles without pile cap in an infinite mild slope far from a free face is different from those located behind a quay wall or close to a free face were reported by other studies.

Asgari et al. (2013) performed a numerical simulation of enhancement of a liquefiable soil layer utilizing stone columns and pile-pinning methods by employing three-dimensional finite element simulations using OpenSeesPL. The results are as follows: 1) risen superstructure mass tempts an enlarge in the lateral movement and highest bending moment and a lessen in the excess pore pressure. 2) the degree of variation in highest lateral deformation with structure weight enlarges approximately as the ground slope increases. 3) for any ground slope, lateral movement boosts as peak ground acceleration enlarges and the rate of increase is greater for a small slope angle.

Caballero and Razavi (2013) conducted a study on numerical simulation of mitigation of seismic liquefaction risk by preloading and its consequences on the behavior of constructions. The result showed that the usage of the preloading lessens the excess pore pressure generation into the soil profile and result in the reduction of liquefaction possibility when the mitigation technique is expended. Moreover, the preloading has an advantageous impact as well concerning the co-seismic relative subsidences.

Yoshida et al. (2013) reported experimental results of small-scale shaking table tests in a 1-g gravity field in order to mitigate liquefaction by using logs. It was clarified that the resistance of the ground against liquefaction was risen by using the wooden pile due to the upsurge of ground density by piling and the dissipation of excess pore water pressure along the surface of the piles. As a result, the level of subsidence of the house which was set on the improved ground by piling logs decreased.

Kang et al. (2013) researched centrifuge modeling and mitigation of manhole uplift due to liquefaction by testing 22 dynamic centrifuge models under 20g. It was found that excess pore water pressure is one of the influencing issues to the level of the manhole uplift. Based on this result, it was proposed to employ the backfill compression technique by shaking the manhole. The result shows that the uplift deformation in loose backfill was about 0.95 m, whereas in compressed backfill was only about 0.13 m.

Noorzad and Amini (2014) explored the behavior of randomly distributed fibers in increasing the liquefaction durability and shear modulus of loose and medium dense sand deposits by using stress-controlled cyclic triaxial examinations. The results indicated that the fiber existence appreciably enlarged liquefaction resistance of sand samples. The reinforcement effect in medium dense samples was found to be more considerable than that of looser samples. Furthermore, the shear modulus rises with the growing of fiber content.

Yukihiro et al. (2014) measured the usefulness of crashed tile in countermeasure against liquefaction by performing shaking table experiments. It is found that liquefaction can be lessened by using proposed materials. This is proven by the manhole which was backfilled by crashed tile floated only by 1/3 of the level detected in the case of without countermeasure.

Tang et al. (2015) carried out a numerical investigation on ground improvement for liquefaction mitigation by using stone columns encased with geosynthetics. In this study, three-dimensional finite element analysis was performed to explore the mitigation of mildly sloped saturated sand strata using encased stone column approaches. The results showed that the geosynthetics-encased stone column remediation lessened more lateral deformation, compared to the stone column. The ground stiffening was also improved as the stiffness and thickness of the geosynthetics, and the diameter of the column was enlarged.

Hernandez et al. (2015) carried out laboratory experiments on the cyclic undrained behavior of loose sand with cohesionless silt and its application to assessment of the seismic performance of subsoil. They concluded that when the rise of the fines contents up to F_{thr} reduces the liquefaction resistance. Furthermore, by using the volume compressibility, m_v , in place of SPT-N, FC reduces the liquefaction resistance of sand, and shear modulus of sand decreases as well with the progress of cyclic undrained shear.

Rasouli et al. (2015) investigated mitigation of vertical seismic deformation of light surface constructions by the induction of sheet-pile walls nearby the foundation by carrying out a series of 1-g shaking table tests in dissimilar groundwater levels. The results indicate that installing sheet-pile walls in fairly low groundwater level can stop settlement of structures completely.

Saez and Ledezma (2015) suggested liquefaction mitigation using secant piles wall under a large water tank by developed two-dimensional and three-dimensional numerical models. They found that although the mitigation strategy did not considerably decrease the liquefaction-induced vertical displacement, it enforced a relatively homogeneous distribution of these settlements, leading to less structural damage.

Chen et al. (2016) performed a study on the tensile force of geogrids inserted in the pile-reinforced embankment. In this study, a full-scale high-speed railway embankment model was formed. Water bags were dispensed around pile caps to initiate a model of the subsoil. The vertical movement of the subsoil was decided by the subsidence of the water bags. The results indicate that the spreading force of the embankment due to the embankment fill weight and the surcharge on the embankment vaguely enlarge the tensile force of the geogrid. Furthermore, the pile-soil differential settlement can considerably affect the tensile force of the geogrid.

Miranda et al. (2017) carried out a laboratory study on the effect of geotextile encasement on the performance of the stone column. The experiments were performed in a large instrumented Rowe-Barden oedometric cell. Results showed that the vertical stress reinforced by encased columns is about 1.7 times that sustained by the non-encased ones.

Rouholamin et al. (2017) performed a research on the effect of initial relative density on the post-liquefaction performance of sand by utilizing the cyclic triaxial equipment. Results of the test indicate that the stress-strain performance of sand in the post-liquefaction stage can be formed as a bi-linear curve using three parameters: the initial shear modulus (G_1), critical state shear modulus (G_2), and post-dilation shear strain ($\gamma_{post-dilation}$). It was found that the three parameters are reliant on the initial relative density of sands. Furthermore, it was observed that with the growth in the relative density of both G_1 and G_2 enlarge and $\gamma_{post-dilation}$ declines.

Ayoubi and Pak (2017) carried out a numerical study to determine the influence of different parameters on liquefaction-induced subsidence of shallow foundation placed on the two-layered soil. Results show that the existence of the dense layer can downgrade the settlement by up to 50% compared to uniform liquefiable layer.

1.5 Research Objectives and Scope

It is generally known that major earthquakes are usually followed by the occurrence of liquefaction. During past earthquakes, many important structures have been subjected to severe damage due to the deformation of the liquefied ground. Therefore, the main focus of this study is to determine the performance of gravel and geosynthetics to mitigate the liquefaction, in particular, the ground displacement triggered by liquefaction, both horizontal and vertical displacements.

In order to investigate the effectiveness of the suggested mitigation, a series of shaking table tests are carried out. The tests are performed in several different models, such as no countermeasure model, reinforced with gravel only, strengthened with geosynthetics only, and by using gravel along with geosynthetics. Through the shaking table test, parameters measured include acceleration, pore water pressures, and ground displacement. The effectiveness of projected mitigation is determined by analyzing the results obtained from the shaking table test.

Furthermore, the effectiveness of the proposed mitigation is also tested on two different ground conditions, i.e., in dense and loose conditions. The aim is to determine the performance of suggested mitigation on both soil conditions, which is the representation of soil conditions in nature. This test is also intended to be able to determine the level of success of planned mitigation to overcome the differential settlement, which often occurs in the ground due to various level of liquefaction occurrence on soils with different densities. The impacts that are often seen are the tilted building and the damage to the road surface as mentioned earlier.

Furthermore, there is also a variation on the geosynthetic used. In this study, two different geosynthetic types, both thickness, tensile strength, friction angle, and aperture size, were used to compare the effectiveness of the two geosynthetic types. Therefore, the pull-out test is performed on both geosynthetic types which will be used to determine the friction angle which has a massive influence on the effectiveness of gravel and geosynthetic use in this mitigation. This is because the geosynthetic friction angle affects the connection between

geosynthetic, sand and gravel. The stronger the bonds between the three, the more coherent the reinforcement layer will lead to ground deformation reduction.

This study is expected to produce a recommended reinforcement technique that can be used effectively to overcome ground deformation due to liquefaction. The simplicity of the proposed method is also intended to allow the method to be applied to residential houses that have limited funds to address the ground deformation problem. In addition, this method is also expected to be applied to conditions where sophisticated and heavy methods are impossible to perform, such as in remote areas where it is difficult to mobilize heavy equipment, as well as densely populated residential environments where several mitigation techniques causing noise and disturbance to existing constructions around the location to be repaired.

1.6 Research Significance

Research on earthquake-related disaster mitigation, particularly liquefaction has been widely practiced previously. Up to this moment, the study of liquefaction is still intensively conducted around the world, especially in countries prone to earthquakes. This is because liquefaction is a complex phenomenon and needs to be done in a comprehensive and sustainable study. To the author's knowledge, the use of gravel and geosynthetic is specifically aimed at overcoming ground deformation including lateral spreading and settlement due to liquefaction, in particular, for detached houses or buildings, is still very rare, and continues to grow rapidly to date. The method proposed in this study has several advantages over the methods proposed by previous researchers, among others: 1) more economical compared to other methods, such as vibration or sand piling, so it will be more affordable, especially if used for residential houses, where sometimes expensive and sophisticated techniques are not affordable; 2) more workable, due to it is easy to be executed; 3) less impact on surrounding environment.

Furthermore, one of the advantages of this study is the modest analysis due to the target is residential houses and people who cannot afford high costs of soil investigation. Of course, the resulting method is expected to be able to complement the previous techniques so that it can be one alternative in liquefaction mitigation.

1.7 Thesis Organization

This dissertation is organized into five chapters and delivers the findings of an investigation of the liquefaction phenomenon and the ground deformation triggered by liquefaction.

The first chapter presents a general overview of liquefaction and ground displacement due to liquefaction. A summary of the previous studies carried out on liquefaction and the methods of countermeasure liquefaction is also introduced in this chapter.

The liquefaction occurrence, particularly ground deformation triggered by liquefaction in the previous earthquakes is discussed in Chapter 2.

In Chapter 3, the mitigation of horizontal ground displacement caused by liquefaction by using gravel and geosynthetics is presented. In order to determine the effectiveness of this proposed mitigation in overcoming the liquefaction-induced lateral displacement, a series of shaking table test is implemented. The testing process, the materials and instruments used, and its results which include pore water pressures, acceleration, and lateral spreading are discussed in this chapter.

Chapter 4 illustrates the experimental results and analysis of the mitigation of vertical ground displacement due to liquefaction by using gravel and geosynthetics.

In Chapter 5, the summary, conclusion remarks of this study are described. Also, recommendations for future work are presented.

1.8 References

- Adalier, K., Elgamal, A., Meneses, J., and Baez, J.I., 2003, Stone columns as liquefaction countermeasure in non-plastic silty soils. *Soil Dynamics and Earthquake Engineering* 23 (2003), 571-584.
- Agaiby, S. W., and Ahmed, S.M., 2016, Learning from failures: A geotechnical perspective. *Proceedings of the International Conference on Forensic Civil Engineering, Nagpur, India. 21-23 January 2016.*
- Akiyoshi, T., Fuchida, K., Matsumoto, H., Hyodo, T., and Fang, H.L., 1993, Liquefaction analyses of sandy ground improved by sand compaction piles. *Soil Dynamics and Earthquake Engineering* 12 (1993), 299-307.
- Alawaji, H.A., 2001, Settlement and bearing capacity of geogrid-reinforced sand over the collapsible soil. *Geotextiles and Geomembranes* 19 (2001), 75-88.
- Anon., 2011, Post-earthquake reconnaissance report on transportation infrastructure: Impact of February 27, 2010, offshore Maule earthquake in Chile. Available at: <https://www.fhwa.dot.gov/publications/research/infrastructure/structures/11030/005.cfm>. Accessed at 4 May 2018.
- Asgari, A., Oliaei, M., and Bagheri, M., 2013, Numerical simulation of improvement of a liquefiable soil layer using stone column and pile-piling techniques. *Soil Dynamics and Earthquake Engineering* 51 (2013), 77-96.
- Ayoubi, P. And Pak, A., 2017, Liquefaction-induced settlement of shallow foundations on two-layered subsoil strata. *Soil Dynamics and Earthquake Engineering* 94 (2017), 35-46.
- Azzam, W.R. and Nazir, A.K., 2012, Liquefaction mitigation using lateral confinement technique. *Hindawi Publishing Corporation, Advances in Civil Engineering, Vol. 2010, Article ID 538274.*

- Bhattacharya, K., Tokimatsu, K., Goda, K., Sarkar, M., Shadlou, M., and Rouholamin, M., 2014, Collapse of Showa Bridge during 1964 earthquake: a quantitative reappraisal on the failure mechanisms. *Soil Dynamics and Earthquake Engineering*, Vol. 65, October 2014, 55-71.
- Bhattacharya, S., Hyodo, M., Nikitas, G., Ismael, B., Suzuki, H., Lombardi, D., Egami, S., Watanabe, G., and Goda, K., 2018, Geotechnical and infrastructural damage due to the 2016 Kumamoto earthquake sequence. *Soil Dynamics and Earthquake Engineering* 104 (2018), 390-394.
- Boominathan, A. And Hari, S., 2002, Liquefaction strength of fly ash reinforced with randomly distributed fibers. *Soil Dynamics and Earthquake Engineering* 22 (2002), 1027-1033.
- Caballero, F.L. and Razavi, A.M.F., 2013, Numerical simulation of mitigation of seismic liquefaction risk by preloading and its effects on the performance of structures. *Soil Dynamics and Earthquake Engineering* 49 (2013), 27-38.
- Chang, W.J., Rathje, E.M., Stokoe, K.H., and Cox, B.R., 2004, Direct evaluation of the effectiveness of prefabricated vertical drains in the liquefiable sand. *Soil Dynamics and Earthquake Engineering* 24 (2004), 723-731.
- Chen, R.P., Wang, Y.w., Ye, X.W., Bian, X.C., and Dong, X.P., 2016, Tensile force of geogrids embedded in pile-supported reinforced embankment: A full-scale experimental study. *Geotextiles and Geomembranes* 44 (2016), 157-169.
- Chu, D.B., Stewart, J.P., Lee, S., Tsai, J.S., Lin, P.S., Chu, B.L., Seed, R.B., Hsu, S.C., Yu, M.S., and Wang, M.C.H., 2004, Documentation of soil conditions at liquefaction and non-liquefaction sites from 1999 Chi-Chi (Taiwan) earthquake. *Soil Dynamics and Earthquake Engineering*, Vol. 24, Issues 9-10, 647-657.
- Cubrinovski, M. And Robinson, K., 2016, Lateral spreading: Evidence and interpretation from the 2010-2011 Christchurch earthquakes. *Soil Dynamics and Earthquake Engineering* 91 (2016), 187-201
- Gallagher, P.M., Pamuk, A., and Abdoun, T., 2007, Stabilization of liquefiable soils using colloidal silica grout. *Journal of Materials in Civil Engineering* 19 (1), 33-40.
- Gautam, D., de Magistris, F.S., and Fabbrocino, G., 2017, Soil liquefaction in Kathmandu valley due to 25 April 2015 Gorka, Nepal earthquake. *Soil Dynamics and Earthquake Engineering* 97, 37-47.
- Haeri, S.M., Kavand, A., Rahmani, I., and Torabi, H., 2012, Response of a group of piles to liquefaction-induced lateral spreading by large-scale shake table testing. *Soil Dynamics and Earthquake Engineering* 38 (2012), 25-45.
- Haeri, S.M., Noorzad, R., and Oskoorouchi, A.M., 2000, Effect of geotextile reinforcement on the mechanical behavior of sand. *Geotextiles and Geomembranes* 18 (2000), 385-402.
- Harada, N., Towhata, I., Takatsu, T., Tsunoda, S., and Sesov, V., 2006, Development of new drain method for protection of existing pile foundations from liquefaction effects. *Soil Dynamics and Earthquake Engineering* 26 (2006), 3297-312.
- Heather, B. and Wright, M., 2011, Half of the city's roads damaged. Available at <http://www.stuff.co.nz/national/christchurch-earthquake/4867370/Half-of-citys-roads-damaged>. Accessed 4 May 2018.
- Hernandez, Y.A., Towhata, I., Gunji, K., and Yamada, S., 2015, Laboratory tests on cyclic undrained. *Soil Dynamics and Earthquake Engineering* 79 (2015), 365-378.
- Hwang, J.H., Yang, C.W., and Chen, C.H., 2003, Investigations on soil liquefaction during the Chi-Chi earthquake. *Soils and Foundations*, Japanese Geotechnical Society, Vol. 43, No. 6, 107-123.

- Ishihara, K., and Yoshimine, M., 1992, Evaluation of settlements in sand deposits the following liquefaction during earthquakes. *Soil and Foundations*, Japan Society of Soil Mechanics and Foundation Engineering, Vol. 32, No. 1, 173-188.
- Kang, G.C., Tobita, T., Lai, S., and Ge, L., 2013, Centrifuge modeling and mitigation of manhole uplift due to liquefaction. *Journal of Geotechnical and Geoenvironmental Engineering* 139(3), 458-469.
- Kusumastuti, D., Suarjana, M., Sengara, I.W. and Rildova, 2010, Report on the West Sumatra earthquake of September 30, 2009. MCEER Bulletin, Vol. 24 No. 1, Spring 2010.
- Liu, H. And Song, E., 2006, Working mechanism of cutoff walls in reducing uplift of large underground structures induced by soil liquefaction. *Computers and Geotechnics* 33 (2006), 209-221.
- Liu, J., Wang, G., Kamai, T., Zhang, F., Yang, J., and Shi, B., 2011, Static liquefaction behavior of saturated fiber-reinforced sand in undrained ring-shear tests. *Geotextiles and Geomembranes* 29 (2011), 462-471.
- McCulloch, D. and Bonilla, M.G., 2013, Effects of the Earthquake of March 27, 1964, on the Alaska Railroad. Available at: <https://pubs.usgs.gov/pp/0545d/>. Accessed 4 May 2018.
- Miranda, M., Da Costa, A., Castro, J., and Sagaseta, C., 2017, Influence of geotextile encasement on the behavior of stone columns: Laboratory study. *Geotextiles and Geomembranes* 45 (2017), 14-22.
- Miyajima, M., 2013, Performance of drinking water pipelines in liquefaction areas in the 2011 Great East Japan earthquake. *International Journal of Landslide and Environment*, 1(1), 61-62.
- Motamed, R. And Towhata, I., 2010, Mitigation measures for pile group behind quay walls subjected to a lateral flow of liquefied soil: Shake table model tests. *Soil Dynamics and Earthquake Engineering* 30 (2010), 1043-1060.
- Muntohar, A.S., Widiannti, A., Oktoviar, E., Hartono, E., and Diana, W., 2008, Cement-column technique application on sandy soils. National Seminar of Science and Technology II (SATEK II), 17-18 November 2008, Lampung University, Indonesia.
- Noorzad, R. And Amini, P.F., 2014, Liquefaction resistance of Babolsar sand reinforced with randomly distributed fibers under cyclic loading. *Soil Dynamics and Earthquake Engineering* 66 (2014), 281-292.
- Orense, R.P., Morimoto, I., Yamamoto, Y., Yumiyama, T., Yamamoto, H., and Sugawara, K., 2003, Study on wall-type gravel drains as liquefaction countermeasure for underground structures. *Soil Dynamics and Earthquake Engineering* 23 (2003), 19-39.
- Potter, S.H., Becker, J.S., Johnston, D.M., and Rossiter, K.P., 2015, An overview of the impacts of the 2010-2011 Canterbury earthquakes. *International Journal of Disaster Risk Reduction*, Vol. 14, 6-14.
- Raisinghani, D.V., and Viswanadham, B.V.S., 2011, Centrifuge model study on low permeable slope reinforced by hybrid geosynthetics. *Geotextiles and Geomembranes* 29 (2011), 567-580.
- Rasouli, R., Towhata, I., and Hayashida, T., 2015, Mitigation of the seismic settlement of light surface structures by the installation of sheet-pile walls around the foundation. *Soil Dynamics and Earthquake Engineering* 72 (2015), 108-118.
- Rouholamin, M., Bhattacharya, S., and Orense, R.P., 2017, Effect of initial relative density on the post-liquefaction behavior of sand. *Soil Dynamics and Earthquake Engineering* 97 (2017), 25-36.

- Saez, E. And Ledezma, C., 2015, Liquefaction mitigation using secant piles wall under a large water tank. *Soil Dynamics and Earthquake Engineering* 30 (2010), 1043-1060.
- Takahashi, A. And Takemura, J., 2005, Liquefaction-induced large displacement of the pile-supported wharf. *Soil Dynamics and Earthquake Engineering* 25 (2005), 811-825.
- Tang, L., Cong, S., Ling, X., Lu, J., and Elgamal, A., 2015, Numerical study on ground improvement for liquefaction mitigation using stone columns encased with geosynthetics. *Geotextiles and Geomembranes* 43 (2015), 190-195.
- Tokimatsu, K. and Asaka, Y., 1998, Effects of liquefaction-induced ground displacements on pile performance in the 1995 Hyogoken-Nambu earthquake. Special issue of *Soils and Foundations*, Japan Geotechnical Society, September 1998, 163-177.
- Tokimatsu, K. and Katsumata, K., 2012, Liquefaction-induced damage to buildings in Urayasu City during the 2011 Tohoku Pacific earthquake. *Proceedings of the International Symposium on Engineering Lessons Learned from the 2011 Great East Japan earthquake*, March 1-4, 2012, Tokyo, Japan.
- Tokimatsu, K., Tamura, S., Suzuki, H., and Katsumata, K., 2012, Building damage associated with geotechnical problems in the 2011 Tohoku Pacific earthquake. *Soils and Foundations*, Japanese Geotechnical Society, 52(5), 956-974.
- Valsamis, A.I., Bouckovalas, G.D., and Papadimitriou, A.G., 2010, Parametric investigation of lateral spreading of the gently sloping liquefied ground. *Soil Dynamics and Earthquake Engineering* 30 (2010), 490-508.
- Verdugo, R. and Gonzalez, J., 2015, Liquefaction-induced ground damages during the 2010 Chile earthquake. *Soil Dynamics and Earthquake Engineering*, Vol. 79 (2015), 280-295.
- Wang, G., Wei, X., and Liu, H., 2015, Liquefaction evaluation of dam foundation soils considering overlying structure. *Journal of Rock Mechanics and Geotechnical Engineering* 7 (2015), 226-232.
- Yoshida, M., Miyajima, M., and Numata, A., 2013, Liquefaction countermeasure technique by using logs. *The progress of Geo-Disaster Mitigation Technology in Asia*, Part of The Environmental Science and Engineering Book series, 293-311.
- Yukihiro, M., Kenichi, M., and Feng, Z., 2014, Effectiveness of crashed tile in countermeasure against liquefaction. *International Journal of GEOMATE*, Vol. 7, No. 1 (SI. No. 13), 1003-1008.
- Zheng, J., Suzuki, K., and Ohbo, N., 1996, Evaluation of sheet-pile ring countermeasure against liquefaction for oil tank site. *Soil Dynamics and Earthquake Engineering* 15 (1996), 369-379.

2. AN OVERVIEW OF LIQUEFACTION-INDUCED GROUND DEFORMATION IN THE PREVIOUS EARTHQUAKES

2.1 Introduction

Soil liquefaction is one of the main impacts of the earthquake that may cause serious damage to constructions and lifelines. Of the late world, earthquakes have shown that the extensive damage is attributed to liquefaction. Liquefaction case pasts can be perceptible for the development of liquefaction phenomenon as well as to reduce the impacts of soil liquefaction.

The existence of liquefaction also causes massive damage to constructions and lifelines. One of the main causes of this structural damage is the ground deformation triggered by liquefaction. Some liquefaction-induced ground deformation occurrences were reported during previous earthquakes like the 2010 Chile earthquake, the 2010-2011 Canterbury earthquake, the 2011 Great East Japan earthquake, and the 2016 Kumamoto earthquake in Japan. The detailed information of the ground deformation caused by liquefaction in the past earthquakes mentioned above is described in the following section.

2.2 The 2010 Chile Earthquake

The gigantic earthquake of Magnitude 8,8 hit the Central-South region of Chile on February 27, 2010. Economically, the 2010 Chile earthquake has been the worst natural disaster in Chile's history, with a total cost of about 30 billion US dollars. This earthquake also caused near 600 casualties.

One of the reasons for resulting damages is linked with liquefaction and the substantial soil dislocations that are typical of this phenomenon. Liquefaction happened in some sites and caused major damages in road infrastructure, railroads system, ports, buildings and houses, irrigation channels, and tailing dams. Ramon Verdugo and Javiera Gonzalez (2015) carried a study and a field survey to observe the ground damages caused by liquefaction during this earthquake. They reported that ground deformation triggered by liquefaction caused the severe damages in some particular areas. They also observed the region affected by liquefaction covers an area with a length close to 1000 km in the North-South direction. Figures 2.1(a) and 2.1(b) describe the post-liquefaction settlements that developed on the ground surfaces and damage the roads and railways severely in Concepcion City, Chile.



Figure 2.1 Post-liquefaction settlements in the 2010 Chile earthquake:
(a) Costanera route in Concepcion City
(b) Near Concepcion City

Furthermore, horizontal ground deformation observed in some locations. Longitudinal rupture related with the lateral spreading were constantly detected for a couple of kilometers along the river banks. Figure 2.2 shows the characteristic cases of damages caused by lateral spreading on mild slopes, where shallow blocks of dry soil broke up internally, moving downward and floating above the liquefied soil. Around 45 km to the south of Santiago, lateral spreading caused the hospital overpass collapsed as shown in Figure 2.3. The horizontal displacement up to 87 cm was measured at the north abutment and generated the collapse of the bridge deck.



Figure 2.2 Damaged road due to lateral spreading



Figure 2.3 Collapse of the Hospital overpass

Lateral spreading triggered by liquefaction also affects pile foundations of several port facilities as shown in Figure 2.4. This port damage is generally linked with a huge economic loss, which is mainly caused by the stopped operations of the port.



Figure 2.4 Damaged ports due to lateral spreading:
 (a) Coronel Port, (b) Bocamina Port, (c) Fishermen's Port

2.3 The 2011 Great East Japan Earthquake

A gigantic M9.0 earthquake quaked northeastern Japan on March 11, 2011, at 2:46 pm. The Great East Japan Earthquake, placed off the Sanriku Coast, triggered the greatest motion ever noted in Japan. The earthquake caused a giant tsunami, which affected massive damage mainly in the Tohoku region and left around 20,000 people dead or missing.

Tokimatsu et al. (2012) conducted a field survey on liquefaction occurred in this earthquake and reported the result. They found that large soil liquefaction appeared around Tokyo Bay. Figures 2.5 – 2.6 shows the occurrence of liquefaction which triggered severe sand boils and ground subsidence up to 50 cm, leading to damage such as the tilt and the settlement of buildings and houses on spread foundations, and also gaps were formed between pile-supported buildings and the surrounding ground.

Furthermore, in the Tone River area, damage induced by liquefaction also happened. By the side waterways, liquefaction-induced lateral spreading appeared and caused the stream became narrow and the riverbed lifted, as shown in Figure 2.7(a). Moreover, the land following the embankment also settled significantly and moved horizontally, affecting damage to a bridge. Lateral spreading also caused the foundations of the houses and other buildings near the embankment tilted as if pushed toward the stream, as can be seen in Figure 2.7(b).



Figure 2.5 Boiled sand on the road in the 2011 Great East Japan earthquake



Figure 2.6 Damages caused by liquefaction in the 2011 Great East Japan earthquake:
 (a) A large settlement of the building
 (b) Tilted building
 (c) Ground settlement around the pile-supported building



Figure 2.7 Liquefaction-induced lateral spreading in the 2011 Great East Japan earthquake
 (a) Lateral ground spreading towards the river
 (b) Damaged house caused by lateral spreading

2.4 The 2010-2011 Canterbury Earthquakes, New Zealand

On 4 September 2010, a moment magnitude (M_w) 7.1 earthquake hit near the small town of Darfield in the Canterbury Plains of the South Island of New Zealand. 100 people were injured and luckily no associated deaths in this earthquake. An aftershock series was recorded, which included a disastrous M_w 6.3 earthquake on 22 February 2011 below the city of Christchurch, and caused at least 7171 people were injured, and 185 people were killed.

The earthquakes had substantial geotechnical characteristics with ground failures, and related damage is widespread through the city and the most noticeable damage feature outside the Central Business District (CBD). All four main events generated massive liquefaction specifically in the eastern suburbs of Christchurch. The liquefaction caused nearly 60,000 residential houses and buildings and also caused heavy damage to roads, bridges, and buried pipe networks of drinkable and wastewater systems of Christchurch. Ground deformation triggered by liquefaction namely settlement and lateral spreading are the main cause of these severe damages.

Cubrinovski et al. (2011) presented the soil liquefaction effects in the Central Business District. Figures 2.8(a) and 2.8(b) show the differential settlements triggered by liquefaction of constructions in this area. The building is shown in Figure 2.8(a) is a three-story building on shallow foundations that settled considerably at its front, resulting in significant differential settlements that leaned the building around 2 degrees. The building was also homogeneously dislocated laterally approximately 15 cm toward the side of major liquefaction near the front of the building (i.e., to the north). The building is shown in Figure 2.8(b) is located across the street to the north from the previous building. It is a six-story building on isolated footings with tie beams and perimeter grade beam. This foundation feature, together with the fact that the observations of liquefaction were most terrible at the southeast corner of the building, led to considerable differential settlements and stated structural distortion and cracking.

Correspondingly, in the following year, Cubrinovski et al. (2012) presented a study of lateral spreading and its impacts in urban areas in the 2010-2011 Christchurch earthquakes. Figures 2.9(a) and 2.9(b) show the inflight view of North Kaiapoi lateral spreading and cracks influencing residential houses located around 50 m away from the Kaiapoi River. Liquefaction-induced lateral spreading also triggered ground cracks and deformation of the road surface along the Avon River. The ground horizontally moved toward the river as shown in Figure 2.10.



Figure 2.8 Tilted buildings due to liquefaction-induced differential settlements



Figure 2.9 Lateral spreading occurred in the 2010-2011 Canterbury earthquakes, New Zealand

- (a) Aerial photo of liquefaction and lateral spreading impacts in the north of Kaiapoi
- (b) Lateral spreading cracks affected the residential house



Figure 2.10 Road surface cracks due to lateral spreading towards the Avon River

2.5 The 2016 Kumamoto Earthquake, Japan

At 21:25 JST on April 14, 2016, a strong earthquake of Mw 6.2 with a focal depth of 11 km below the ground surface struck along the Hinagu fault in Kumamoto Prefecture, on the island of Kyushu, Japan. This earthquake proved a foreshock. Two days later, on the Futagawa fault in the same area, a stronger earthquake of Mw7.0 occurred. Due to this earthquake, much damage was triggered by ground liquefaction, such as rupturing and cracking the ground surface and ground subsidence resulting in settlement of buildings and houses.

Bhattacharya et al. (2018) performed a study of geotechnical and infrastructural damage due to this earthquake sequence. Liquefaction was observed in Kumamoto Port, Akitsu River, Kamiezu Lake and a rectangular belt covering 2 km by 20 m between Shirakawa River and Midorikawa River in Kumamoto City. The possible explanation is that the area was an old natural river dike which was reclaimed. Figures 2.11(a) and 2.11(b) show the typical liquefaction damages in this area, which show several buildings suffered from differential settlements.

Harmoniously, Setiawan et al. (2017) also performed a field survey and reported the result on the structural damage of residential houses and buildings induced by liquefaction in this earthquake. Liquefaction mostly observed in Akitsu Town (Mashima residential area), Chikami Town, and Karikusa Town. 68 affected buildings were surveyed by measured its inclination. It was found that 72% of measured buildings tilted more than 0.6 degrees which could trigger health problems for the inhabitants. Figures 2.12(a) and 2.12(b) present the example of affected buildings caused by liquefaction-induced ground deformation in Akitsu Town. Lateral spreading also appeared in the Kiyama River as shown in the Figure 2.13. The complete results of the field reconnaissance by Setiawan et al. can be seen in the appendix section of this dissertation.



Figure 2.11 Buildings suffered from differential settlements due to liquefaction



Figure 2.12 Damaged buildings caused by liquefaction-induced ground deformation



Figure 2.13 Lateral spreading in the river bank of Kiyama River, Akitsu Town, Kumamoto

2.6 Discussion

Historical records of previous earthquakes show that severe damage is not only a result of the strong ground motion of the earthquake but could be because of geotechnical damage triggered by the earthquake, such as liquefaction. The earthquakes occurred around the world indicate that liquefaction may result in massive economic losses due to the damage of the structures and infrastructure its caused.

One of the liquefaction forms that cause much damage is ground deformation. The previous earthquake showed many buildings suffered damage with various levels due to ground deformation triggered by liquefaction. Roads, bridges, and underground structures also suffered the same impact. The damage to the building is not limited only to the large and heavy buildings, but also to light buildings, such as a residential house. As in the 2011 Great East Japan earthquake and the 2016 Kumamoto earthquake, liquefaction-induced ground deformation caused much damage to residential houses.

Therefore, it is necessary to develop a method to alleviate the liquefaction-induced ground deformation that can be afforded by the inhabitants, both regarding costs required and ease in applying it. Based on that consideration, in this study, geosynthetics along with gravel were offered to be used to mitigate the liquefaction-induced ground deformation

2.7 References

- Bhattacharya, S., Hyodo, M., Goda, K., Tazoh, T., and Taylor, C.A., 2011, Liquefaction of soil in the Tokyo Bay area from the 2011 Tohoku (Japan) earthquake. *Soil Dynamics and Earthquake Engineering* 31 (2011), 1618-1628.
- Bhattacharya, S., Hyodo, M., Nikitas, G., Ismael, B., Suzuki, H., Lombardi, D., Egami, S., Watanabe, G., and Goda, K., 2018, Geotechnical and infrastructural damage due to the 2016 Kumamoto earthquake sequence. *Soil Dynamics and Earthquake Engineering* 104 (2018), 390-394.
- Cubrinovski, M. And Robinson, K., 2016, Lateral spreading: Evidence and interpretation from the 2010-2011 Christchurch earthquakes. *Soil Dynamics and Earthquake Engineering* 91 (2016), 187-201
- Cubrinovski, M., Bray, J.D., Taylor, M., Giorgini, S., Bradley, Brndon., Wotherspoon, L., and Zupan, J., 2011, Soil liquefaction effects in the Central Business District during the February 2011 Christchurch earthquake. *Seismological Research Letters* Vol. 82, No. 6, 893-904.
- Cubrinovski, M., Robinson, K., Taylor, M., and Orense, R., 2012, Lateral spreading and its impacts in urban areas in the 2010-2011 Christchurch earthquakes. *New Zealand Journal of Geology and Geophysics*, Vol. 55, No. 3, 255-269.
- Potter, S.H., Becker, J.S., Johnston, D.M., and Rossiter, K.P., 2015, An overview of the impacts of the 2010-2011 Canterbury earthquakes. *International Journal of Disaster Risk Reduction*, Vol. 14, 6-14.

- Ramon Verdugo and Javiera Gonzalez., 2015, Liquefaction-induced ground damages during the 200 Chile earthquake. *Soil Dynamics and Earthquake Engineering* 79 (2015), 280-295.
- Setiawan, H., Serikawa, Y., Nakamura, M., Miyajima, M., and Yoshida, M., 2017, Structural damage to houses and buildings induced by liquefaction in the 2016 Kumamoto earthquake, Japan. *Geoenvironmental Disasters Journal* (2017) 4:13.
- Tokimatsu, K., Tamura, S., Suzuki, H., and Katsumata, K., 2012, Building damage associated with geotechnical problems in the 2011 Tohoku Pacific Earthquake. *The Japanese Geotechnical Society, Soils, and Foundations*, 2012; 52(5); 956-974.

3. THE ALLEVIATION OF LATERAL SOIL MOVEMENT GENERATED BY LIQUEFACTION BY UTILIZING GRAVEL AND GEOSYNTHETICS

3.1 Introduction

Lateral spreading is the expression used to refer to the development of large horizontal ground displacements due to earthquake-induced liquefaction, in the case of even small free ground surface inclination (e.g., 2-4%) or small topographic irregularities, e.g., river and lake banks (Valsamis et al., 2010). Previously, Bartlett and Youd (1992)²⁾ described that liquefaction-induced lateral spreading might occur on mild slopes of 0.3-5% underlain by loose sands where a shallow water table is present. Such soil deposits are prone to excess pore water pressure generation, liquefaction and consequently large lateral displacement during seismic excitations.

Landfilled ground occasionally liquefies due to large-scale earthquakes and triggers deformations on the ground surface and undermine construction on it, for example, the road (Takahashi et al., 2015). This phenomenon occurred because the liquefied layer is having low strength when shocked with large amplitude seismic waves, caused large movements to the road surface, and as a result, deformation of the road surface took place. Nevertheless, even though the road surface was composed of asphalt and roadbed and had high-strength if the ground under the road surface is liquefied, the strength (shear rigidity) of the road surface will be decreased and deformation will occur.

During previous earthquakes, there was much severe damage to engineering structures and infrastructures caused by horizontal soil movement of liquefied ground known as lateral spreading. The kinematic force of liquefied soil has been a cause of extensive damage during several destructive earthquakes such as the 1964 Niigata, the 1983 Nihonkai-Chubu, and the 1995 Kobe earthquakes (Motamed and Towhata, 2010). Similarly, Cubrinovski and Robinson (2016) examined the characteristics of lateral spreading caused in the 2010-2011 Canterbury earthquakes. They showed that in the 2010-2011 Canterbury earthquakes widespread liquefaction occurred over nearly half of the urban area of Christchurch. The most severe damage to buildings and infrastructure was often associated with lateral spreading and consequent large ground distortion and permanent ground displacements.

Past earthquakes have highlighted the fact that lateral movement has become better recognized and is important for civil engineering structures since it inflicts considerable lateral loads and may lead to widespread failures. For example, in the 1995 Kobe earthquake

and the 2010-2011 Canterbury earthquakes. **Figure 3.1** presents the lateral spreading incidences in the 1995 Kobe earthquake. **Figure 3.1(a)** shows the collapsed of ferry terminal caused by liquefaction and the quay wall moved outwards. **Figure 3.1(b)** The Nishinomiya Bridge collapsed due to liquefaction and triggered foundation deformations. Ground cracks behind the quay walls and parallel to the water edge are indicative of the lateral ground movements occurred. Furthermore, damages caused by liquefaction-induced lateral ground movements in 2010-2011 Canterbury earthquakes are shown in **Figures 3.2(a)** and **3.2(b)**.



Figure 3.1 The lateral spreading due to liquefaction during the 1995 Kobe earthquake
(a) The collapsed ferry terminal
(b) The collapsed Nishinomiya bridge



Figure 3.2 the lateral spreading due to liquefaction during the 2010-2011 Canterbury earthquakes

3.2 Previous Studies on Lateral Spreading Caused by Liquefaction

Many studies have been conducted related to liquefaction-induced lateral ground movements over the last few decades, and many methods have been recommended to solve this problem.

Conventional countermeasure such as sand compaction pile (SCP) and cement solidification have been used to improve the strength of liquefiable ground. However, since

these countermeasures are costly and the construction period is lengthened, liquefaction countermeasures are not carried out on small planar roads which are not as important as others structures, such as bridges. However, for important roads, such as main roads, emergency evacuation routes, and roads connected to important facilities, it is necessary to ensure their accessibility during earthquakes. For that reason, it is necessary to restrain liquefaction with economical methods that are simple to implement.

One of the recommended methods to alleviate liquefaction-induced lateral spreading is by use of gravel along with geosynthetics. Gravel, due to its high friction and drainage properties, is an effective technique used as a liquefaction countermeasure. Morikawa et al. (2014) showed that ground liquefaction could be reduced by using crushed tiles. Previously, Orense et al. in 2003 performed a study on wall-type gravel drains as a liquefaction countermeasure for underground structures. Similarly, in 2014, Chang et al. reported research on liquefaction characteristics of gap-graded gravelly soils in K_0 condition by conducting a series of undrained cyclic direct, simple shear tests. Moreover, geosynthetics, due to its high tensile strength, have been used worldwide to improve problematic liquefiable soils. Several studies related to the use of geosynthetics in liquefaction problems have been conducted, e.g., Vercueil et al. (1997) presented a study of the liquefaction resistance of saturated sand reinforced with geosynthetics. Similarly, Boominathan and Hari (2002) reported on the liquefaction strength of fly ash reinforced with randomly distributed geosynthetic fiber/mesh elements by performing a series of stress-controlled cyclic triaxial tests. Correspondingly, Noorzad and Amini (2014) also presented work on the liquefaction resistance of Babolsar sand reinforced with randomly distributed fibers under cyclic loading.

The use of a mix of gravel and geosynthetics is thought to be a good technique to mitigate liquefiable soil problems. Accordingly, Murakami et al. (2010) combined geosynthetics and gravel in order to restrain liquefaction in embankments, focused on the vertical displacement of the embankments. The result showed that the settlement of the embankments decreased by nearly 35% by using gravel and geosynthetics. They concluded that the use of geosynthetics sandwiched between gravel would have high resistance against bending deformation due to the overburden load of the embankment. Even though this method does not overcome the occurrence of liquefaction completely, it does alleviate the excessive deformation such as settlement and lateral movement.

3.3 Laboratory Tests on Mitigation of Lateral Ground Movements Induced by Liquefaction with Gravel and Geosynthetic

A series of shaking table tests were performed to determine the influence of gravel and geosynthetics usage to overcome the lateral spreading of the liquefiable ground.

3.3.1 Instruments Used in the Experiment

The sand container used in this laboratory tests has dimensions of 150 cm length, 75 cm width, and 75 cm length. The size was selected to provide enough space for the soil to move laterally towards the downslope. The sand container was built from galvanized steel and acrylic/Plexiglas. In the testing process, some parameters are measured, such as acceleration, water pressure, and ground deformation. The specification of the instruments is shown in **Table 3.1** below. **Figure 3.3** presents the photographs of the instruments.

Table 3.1 Instrument's specifications

Instruments	Type	Capacities	Company
Acceleration transducer	ARF-100A	100 m/s ²	Tokyo Sokki Kenkyujo
Water pressure meter	PMS-5-50K	-50 ~ +50 kPa	Toyota Kohki
Displacement meter	ANR1226	150 mm/5.9 in	Matsushita Electric
Load cell	CLP-10B	10 tf	Tokyo Sokki Kenkyujo

3.3.2 Material Properties

The liquefiable loose sand layer was constructed by pouring the sand through a sieve into the water. The sand that was used in this research was silica sand No. 7. The remedial measures used in this study were gravel and geosynthetics. Crushed stone No. 5 was used to form a model of a gravel layer of 6 cm thick. This type of crushed stone is widely used as gravel in modeling tests, for example, Takahashi et al., 2015, and Murakami et al., 2010.

In this study, two different types of geosynthetic characters (Type I and Type II) including the thickness and tensile strength, were used to determine its influence on ground displacement. Besides, it is also necessary to know the effect of friction between sand and geosynthetic on lateral ground deformation. Therefore, pull-out tests are also carried out to determine the magnitude of friction between sand and geosynthetic, for both geosynthetic types used. The mechanism of the pull-out test performed is explained in **Section 3.3.4**.

Properties of the materials used (silica sand No. 7, crushed stone No. 5, and geosynthetics) in this series of test can be seen in **Table 3.2**. **Figure 3.4** presents the photograph of the materials.

Table 3.2 Index properties of the materials used

Index Properties	Silica sand No. 7	Crushed stone No. 5	Geosynthetic Type I	Geosynthetic Type II
Density, ρ , g/cm ³	2.66	2.56	-	-
Mean grain size, D_{50} , mm	0.17	3.55	-	-
Relative density, D_r , %	50 & 90	-	-	-
Tensile strength, T , kN/m	-	-	6.37	10.43
Tensile stiffness, EA , kN/m	-	-	63.7	233.9
Friction angle, ϕ , °	-	-	23.4	30.2

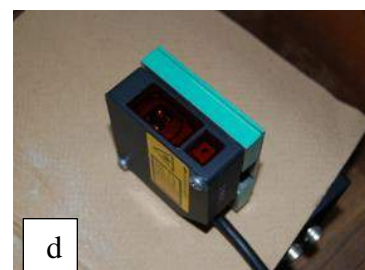
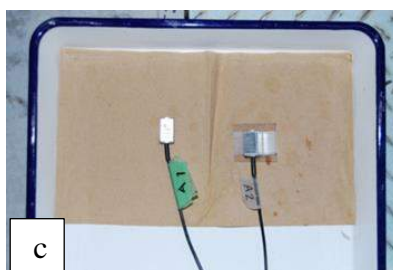
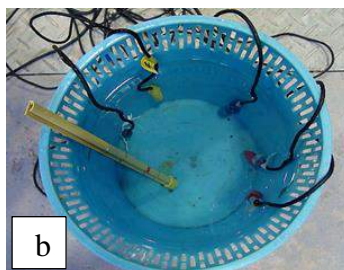
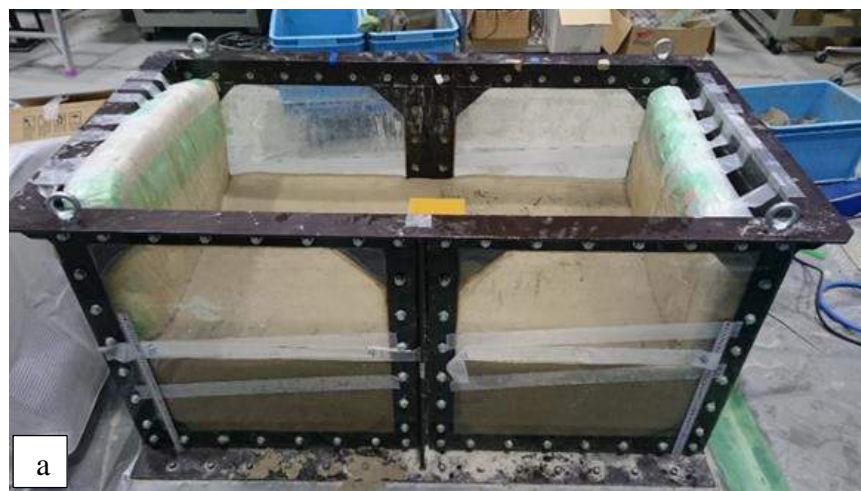


Figure 3.3 The photograph of the instruments used; (a) Sand container, (b) Water pressure meter, (c) Accelerometer, (d) Displacement meter

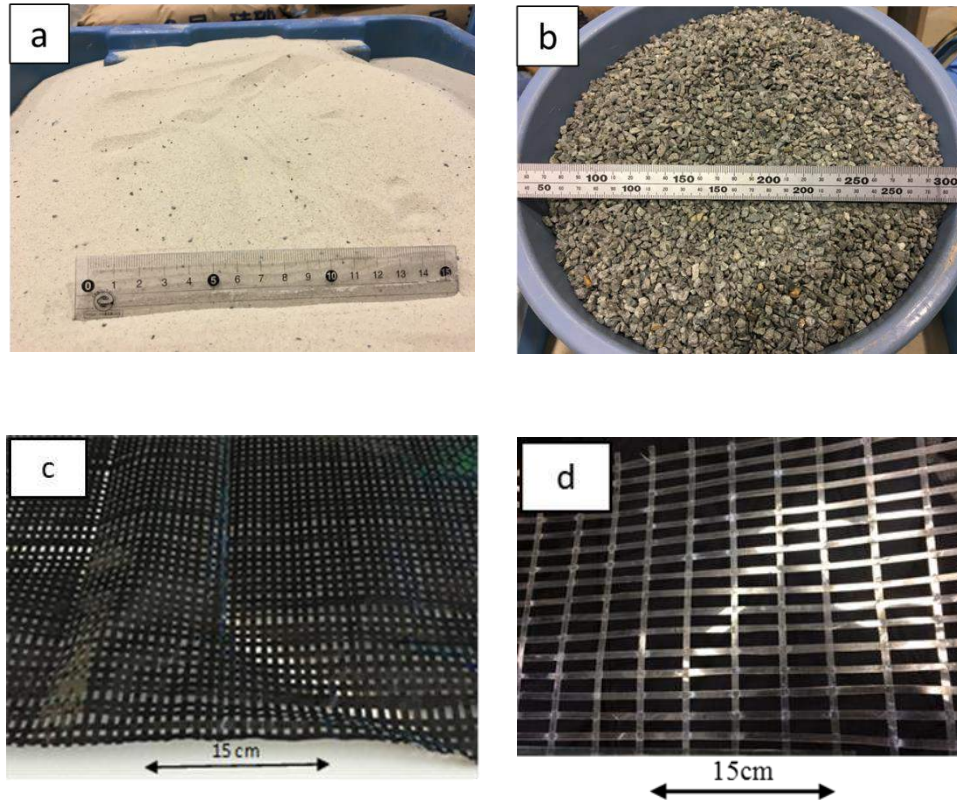


Figure 3.4 The photograph of the materials used
 (a) Silica sand No.7, (b) Crushed stone No.5,
 (c) Geosynthetic Type I, (d) Geosynthetic Type II

3.3.3 Experimental Setup

In this series of tests, input harmonic wave was with frequency 3 Hz, a target maximum input acceleration of around 50 gal, and a shaking duration time was 15 seconds was used. Since the tests carried out were preliminary, these simple characteristics of the input wave were chosen.

Fig. 3.5 shows the plan view and the schematic cross-section of the unreinforced model (Case 1) along with the layout of accelerometers, water pressure meters, and displacement meters. The ground in the model consisted of a liquefiable sand layer with a relative density of around 50 % and a mildly sloping ground surface of around 5% as can be seen in this figure. The slope was selected based on previous studies, for example, Bartlett and Youd (1992) have shown that liquefaction-induced lateral spreading may occur on mild slopes of 0.3-5%. Furthermore, as mentioned by Valsamis et al. in 2010, ground deformation may occur even in the case of a small ground inclination of 2-4%. Therefore, it was decided to examine the occurrence of lateral deformation due to liquefaction on mild slopes of about 5%.

To measure the effectiveness of the mitigation proposed against liquefaction-induced lateral displacement, further tests were conducted. These tests were performed by applying gravel only (Case 2), geosynthetic Type I laid at the bottom of the gravel layer (Case 3), in the middle (Case 4), at the top (Case 5), and geosynthetic Type II located at the bottom of the gravel layer (Case 6). The experimental setup and instrumentation for reinforced models are shown in **Fig. 3.6**.

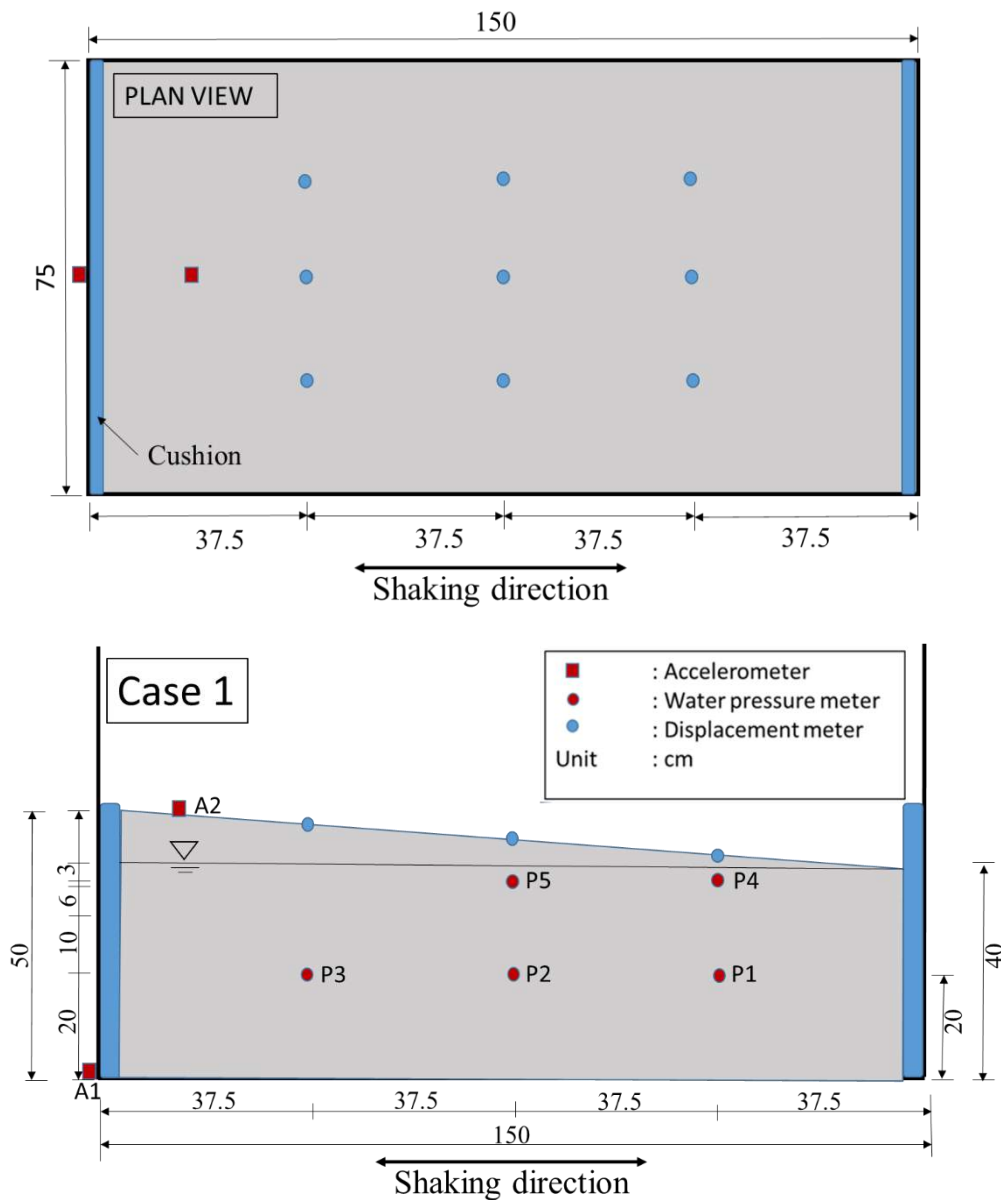


Figure 3.5 The plan view and cross-section of the unreinforced model

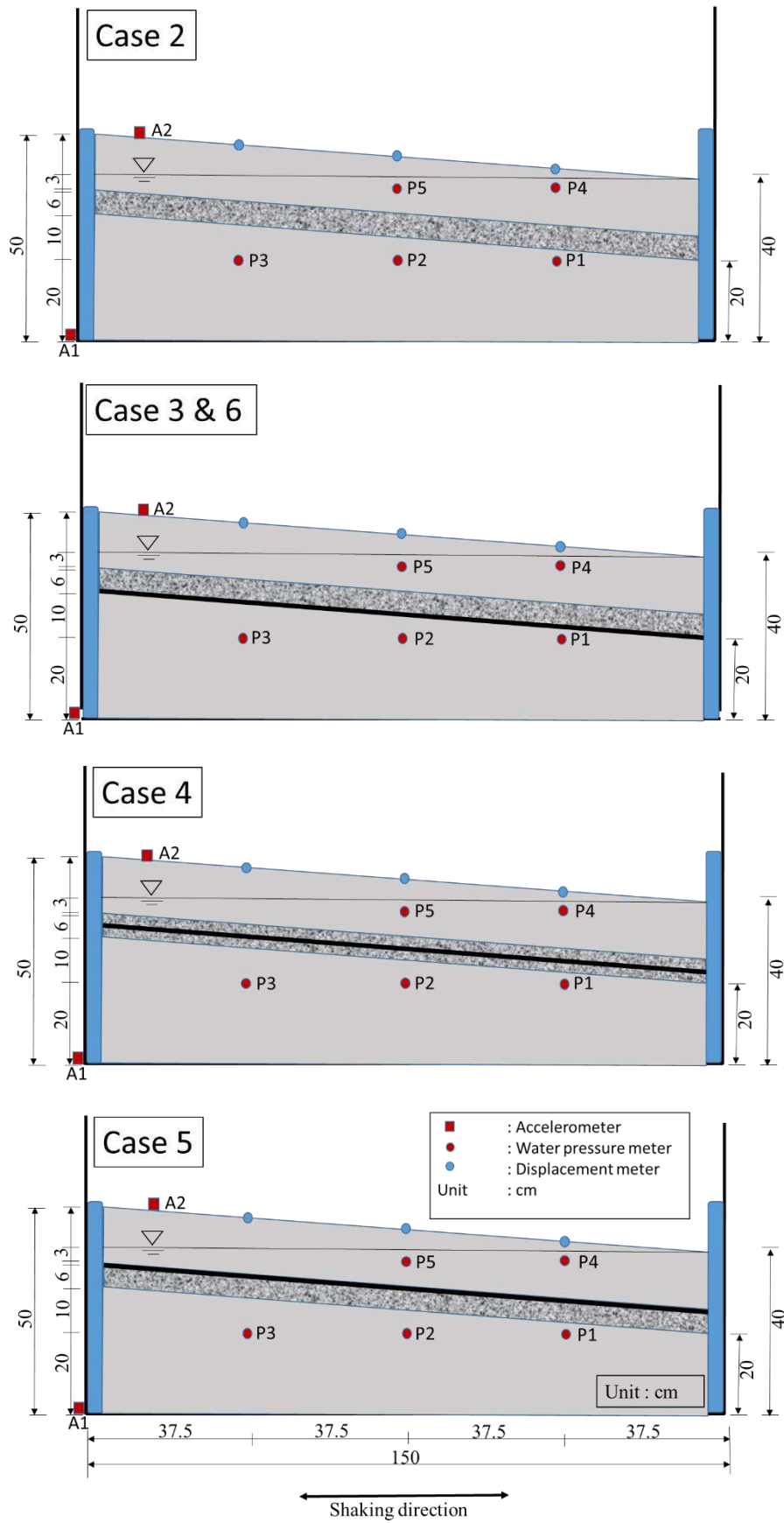


Figure 3.6 The side view of the reinforced models (Case 2 – Case 6)

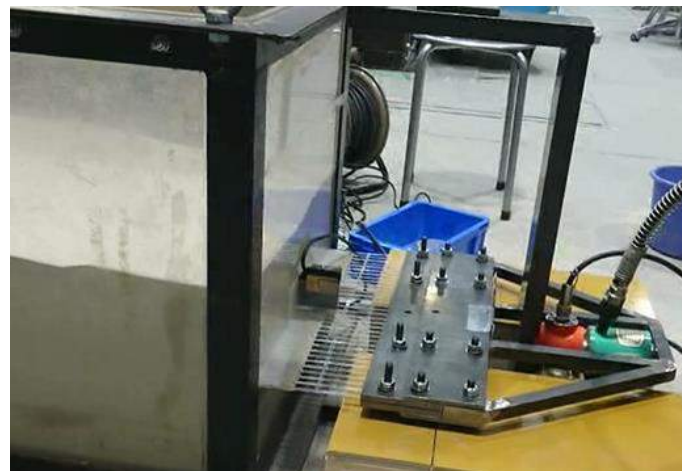
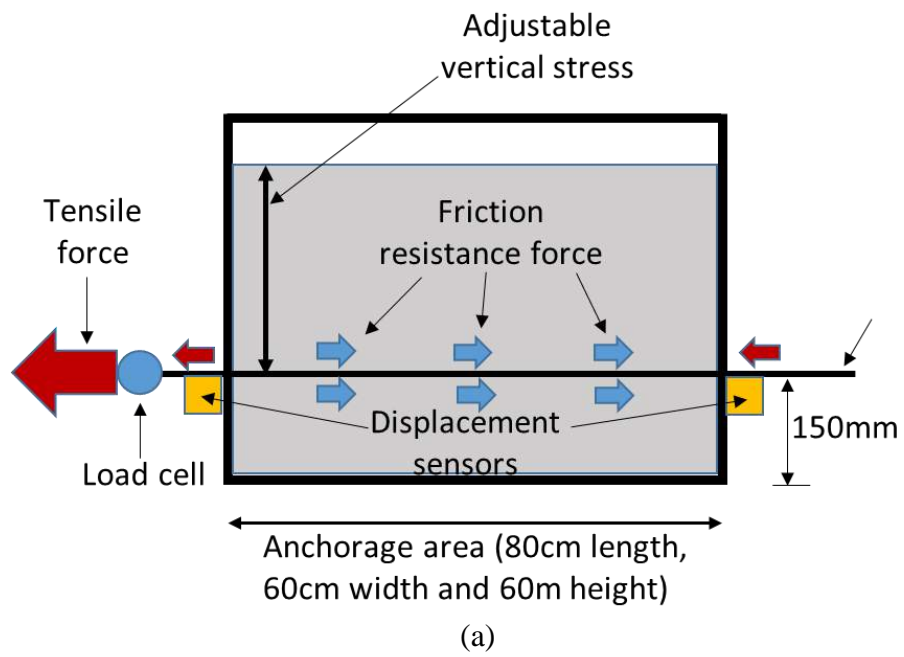
These experiments were the first stage of planned a series of liquefaction mitigation tests using gravel and geosynthetics. The results of these initial experiments are expected to be the initial basis for the development of further experiments, which will eventually result in a method that can be applied to the real conditions in the field to mitigate liquefaction-induced ground deformation problems.

For this purpose, since in this experiment, the mitigation material used was the model of materials used in the actual conditions in the field, whether gravel or geosynthetics, similitude law become one of the consideration. Although similitude law can not be strictly obeyed due to some difficulties encountered, such as the problem of the ratio of gravel grain size between that used in this experimental with the actual size in the field. Nevertheless, it is expected that the results obtained from this experiment can provide an initial depiction of the performance and effectiveness of gravels and geosynthetics to reduce the effects of liquefaction-induced ground deformation, which will be the groundwork for further experimental development.

3.3.4 Pull-Out Test

In order to determine the interaction between soils and geosynthetics, the experiment described as the pull-out test was conducted as well. This test resulted in friction angle which is an important design parameter for soil structures reinforced with geosynthetics where the friction between the soil and reinforcement elements is mobilized. **Fig. 3.7a** shows the side view of the pull-out test apparatus. A photograph of the pull-out test instrument can be seen in **Fig. 3.7b**.

The test tank used in the pull-out test is built from galvanized steel and acrylic with inner dimensions: 80 cm in length, 60 cm in width, and 60 cm in height. The geosynthetics and sand used are the same as those used in the shake table test. Tensile force, displacements and normal stress were observed. The Instruments used in the pull-out test are shown in **Figure 3.8**.



(b)

Figure 3.7 Pull-Out test set up;
 (a) Side view of the pull-out test
 (b) A photograph of the pull-out test



Figure 3.8 Instruments used in the pull-out test;
(a) Hydraulic jack, (b) Load cell

3.4 Experimental Results

A summary of the main data measured during the shaking table test such as excess pore water pressures and lateral ground movements are presented and discussed.

3.4.1 Excess Pore Water Pressure

Pore water pressures were observed by installing five pore water pressure transducers at two different levels. P1, P2, and P3 were located below the gravel layer, around 20 cm from the bottom of the sand container, while P4 and P5 were sited above the gravel layer about 37 cm from the bottom of the sand container. Excess pore water pressure measured were converted to excess pore water pressure ratio by dividing excess pore water pressure with initial vertical effective stress (σ_v'). Excess pore water pressure ratio time histories are shown in **Figures 3.9 – 3.13**.

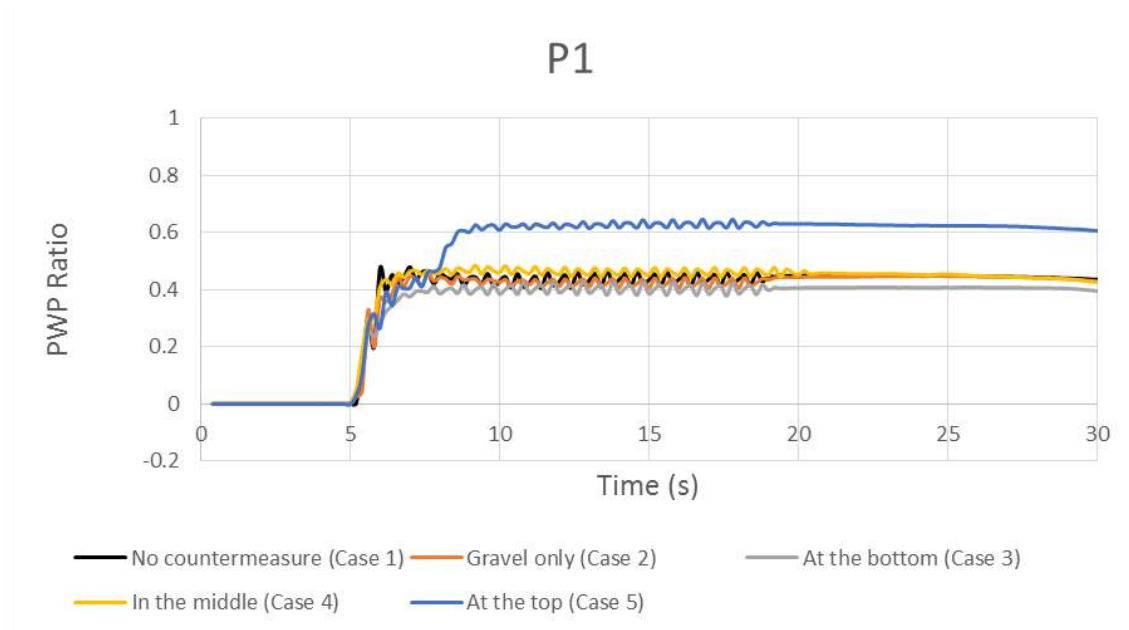


Figure 3.9 Excess pore water pressure time histories for P1

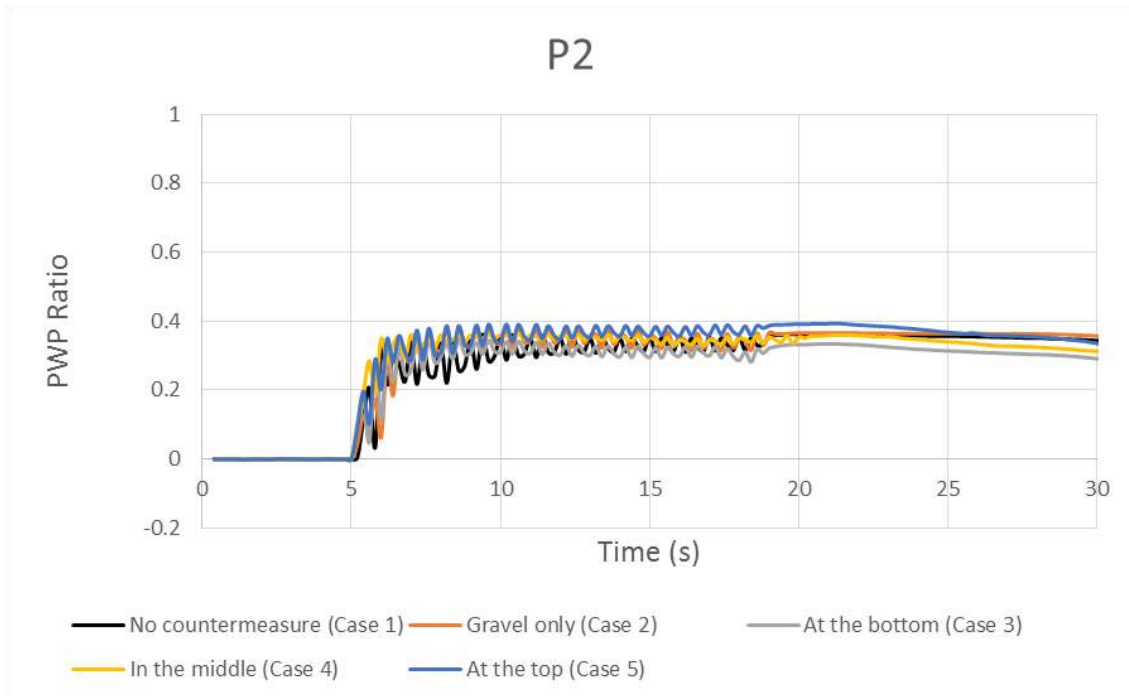


Figure 3.10 Excess pore water pressure time histories for P2

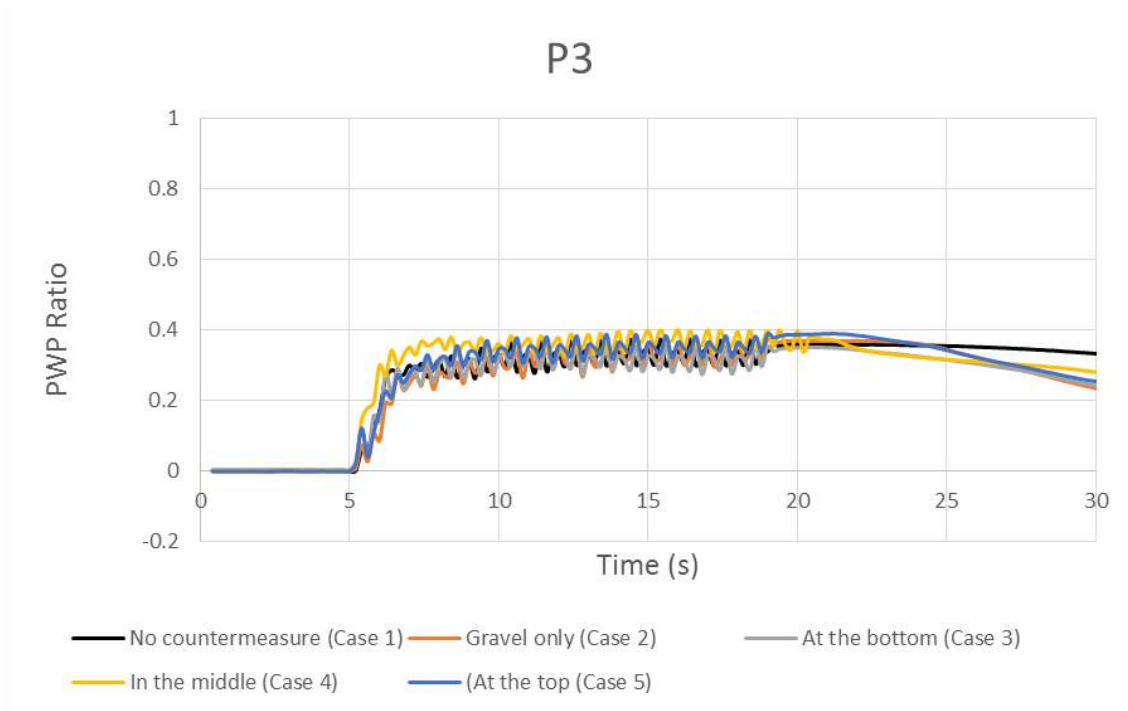


Figure 3.11 Excess pore water pressure time histories for P3

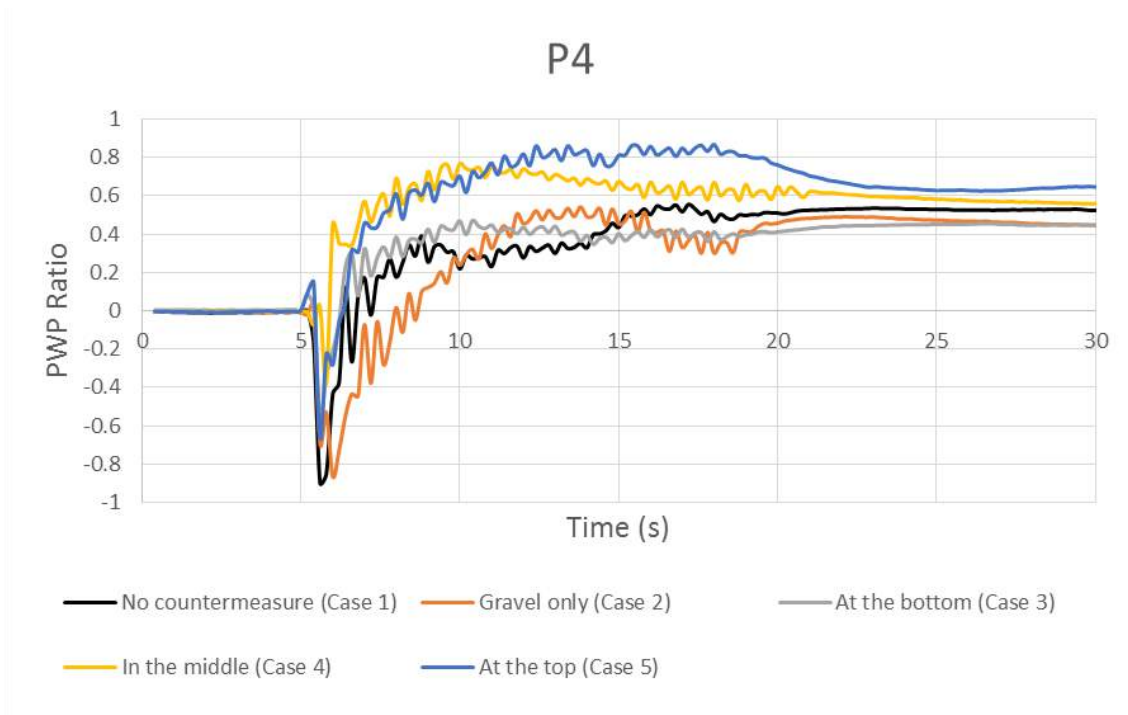


Figure 3.12 Excess pore water pressure time histories for P4

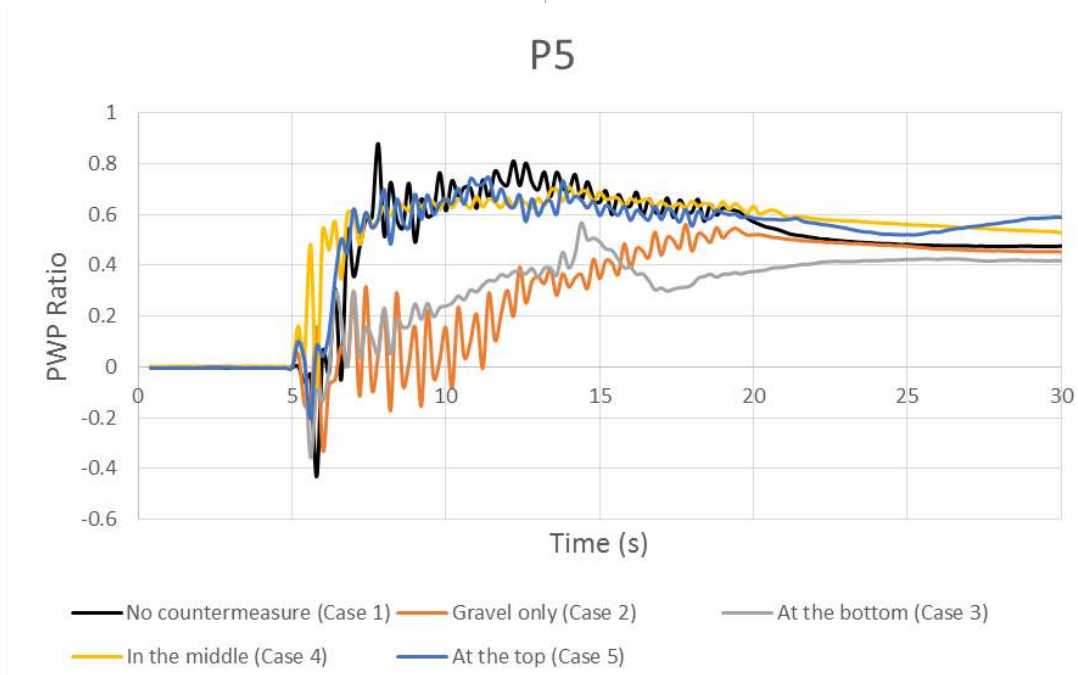


Figure 3.13 Excess pore water pressure time histories for P5

Generally, regarding the value of the excess pore water pressure ratio, the difference for all cases is insignificant. However, for the models with the improvement layer (Case 2 – Case 5), the dissipation of the pore water pressure was observed immediately as the shaking stops, particularly for the P2 and P3 which are located close to the gravel layer. To simplify, the pore water pressure in the graph above is simplified in the **Figure 3.14**.

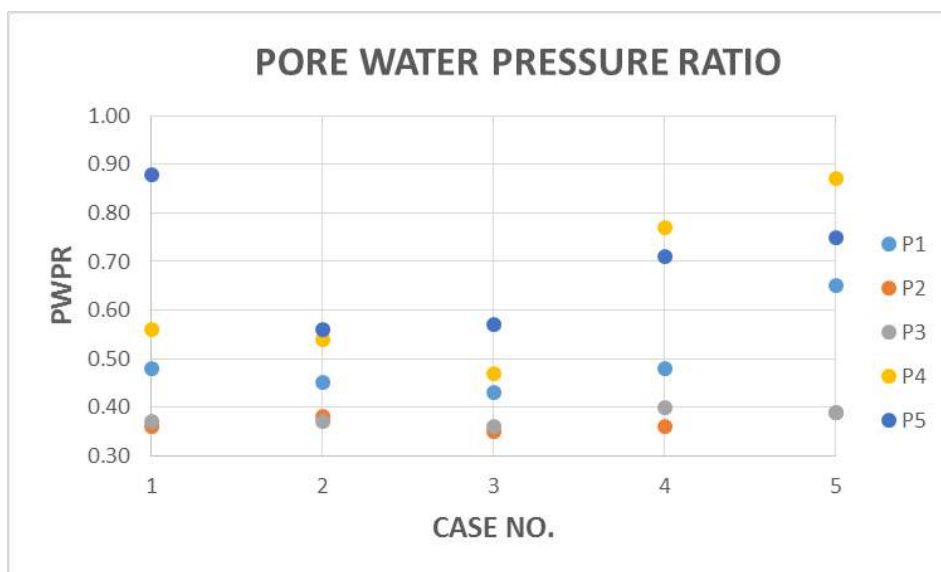


Figure 3.14 Pore water pressure ratio of 5 Cases for P1 – P5

According to the graph, the pore water pressure ratio acquired from Case 3, which is geosynthetic put at the bottom part of the gravel layer, resulting in the lowest pore water pressure ratio compared to other cases, for all transducers (P1 –P5). This is assumed due to by placing geosynthetic under the gravel, the two materials remain united during shaking, even becoming more coherent, and resulting in maximum results in reducing pore water pressure and accelerate the dissipation process.

Conversely, an anomaly appeared in P4 and P5 where the pore water pressure ratio obtained show minus numbers. This is likely due to the dynamics of the pore water pressures and also because of the location of the water pressure transducers which is only 3 cm below the groundwater level. As well as Case 5, which is geosynthetic placed above the gravel, pore water pressure ratio obtained is comparatively higher than any other cases. This is thought due to the gravel grains are heavier than the sand, causing the gravel to spread into the sand during vibration and triggering an increase in pore water pressures.

3.4.2 Lateral Ground Movements

Lateral displacement was measured through nine points on the ground surface for five different states; no countermeasure (Case 1), gravel only (Case 2), and geosynthetic sandwiched at the bottom of the gravel (Case 3), in the middle (Case 4) and at the top of the gravel (Case 5).

Figures 3.15 – 3.19 display the lateral displacements obtained from the measurement on the ground surface for all five cases. Firstly, comparisons of the lateral displacement measured at 9 points on the ground surface were made between case 1 and case 2. Even though case 2 shows smaller displacement than case 1, but the dissimilarity is not significant. Whereas, in cases 3 and 4, the lateral displacement on the ground surface show significant differences compared with the cases 1 and 2. In contrast, the inconsistencies seen in the results obtained in the case 5, where the results are significantly different from cases 3 and 4, although still slightly lower than the cases 1 and 2.

In order to simplify understanding, the lateral displacements measured are averaged as shown in **Figure 3.20**. It can be observed that based on the average values of the lateral displacement measured, the presence of the proposed mitigation measures could reduce lateral displacement in varying amounts. The good results were obtained in cases 3 and 4, where the deformation was reduced by more than 20% compared to case 1. Conversely, lateral deformation obtained in case 5, as well as case 2, are only slightly decreased compare to case 1, around 4%.

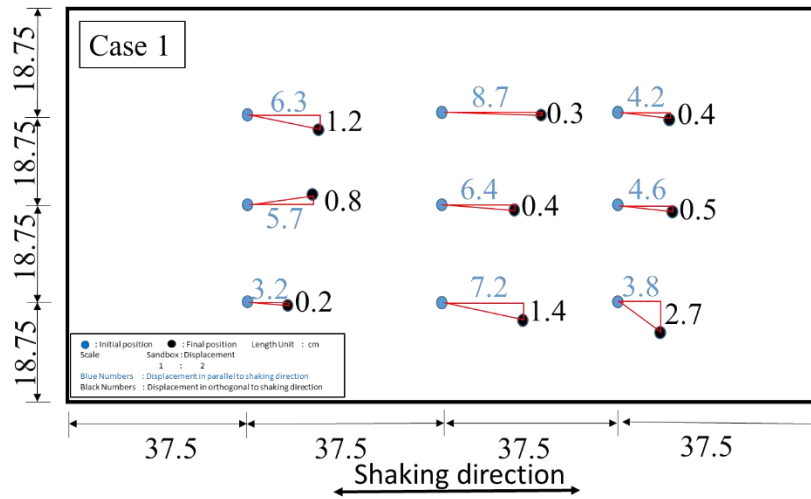


Figure 3.15 Ground surface lateral spreading measured for Case 1

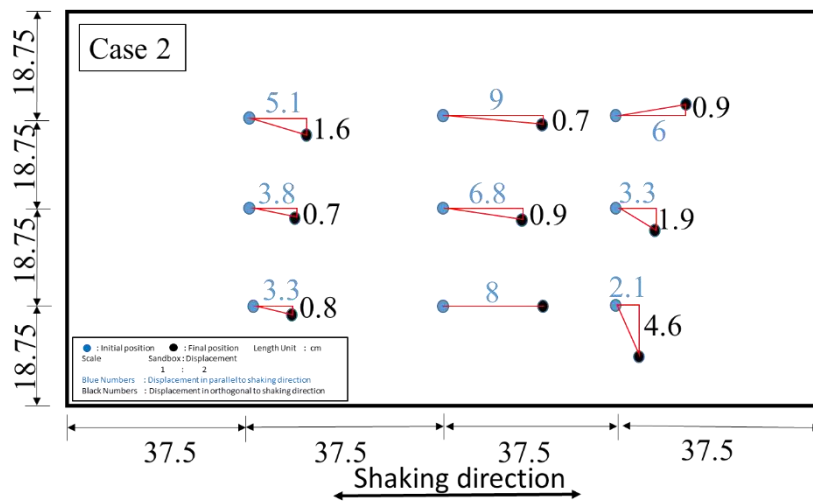


Figure 3.16 Ground surface lateral spreading measured for Case 2

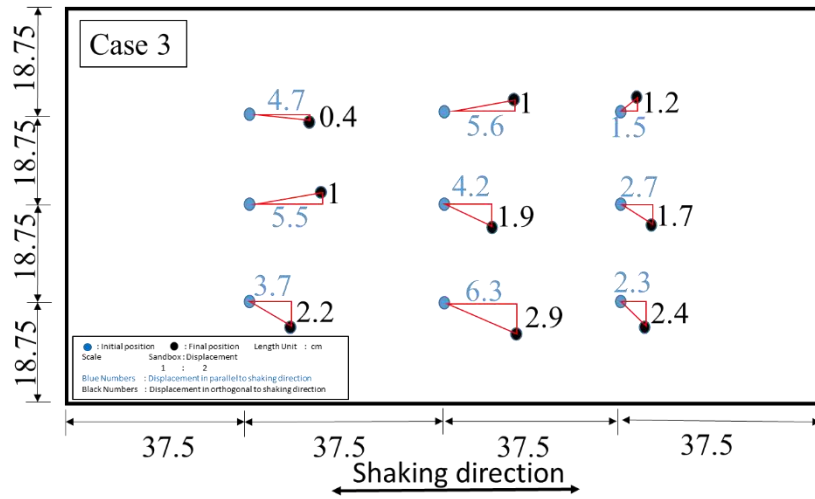


Figure 3.17 Ground surface lateral spreading measured for Case 3

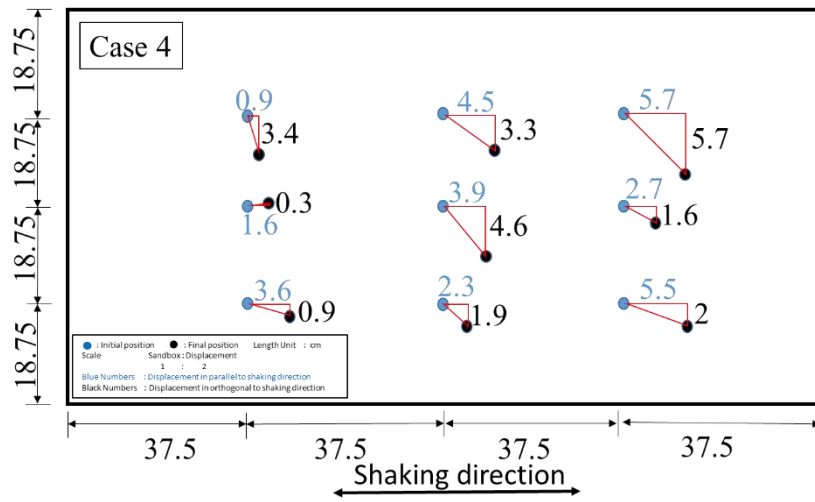


Figure 3.18 Ground surface lateral spreading measured for Case 4

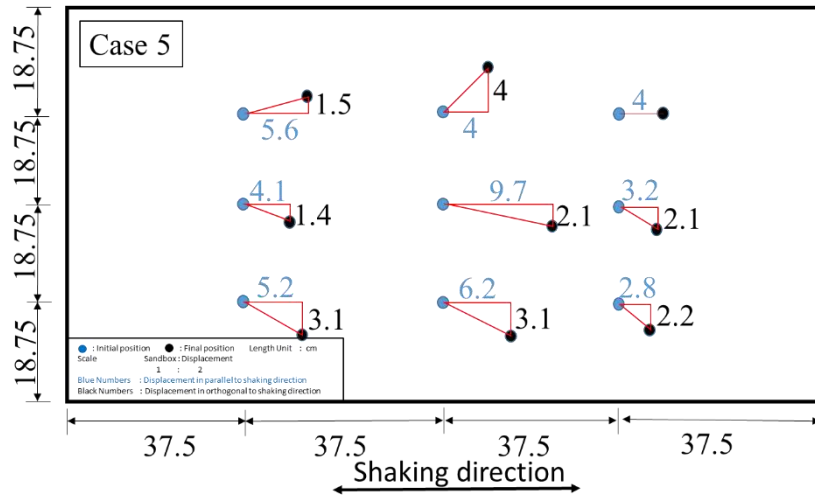


Figure 3.19 Ground surface lateral spreading measured for Case 5

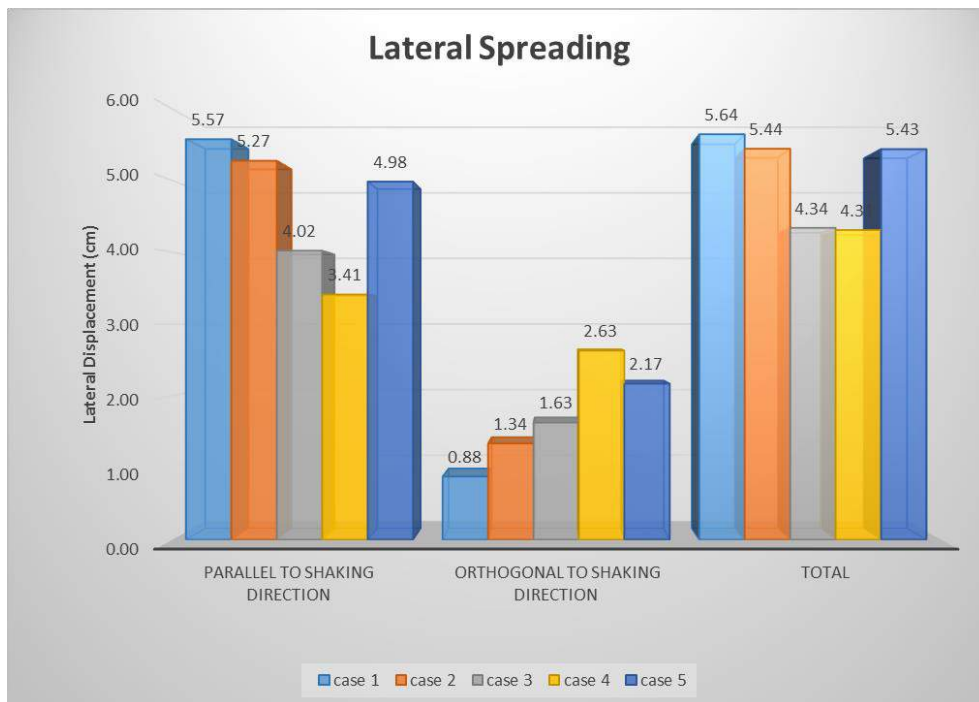


Figure 3.20 Averaged ground surface lateral spreading

The coherence of the gravel layer with its high permeability and high tensile strength provided by geosynthetics were considered as the main reason for this good result. Since the tension generated in the geosynthetics restrain the deformation of the gravel layer and integrally behaves like a board, this reinforcement could reduce the liquefaction-induced

lateral deformation that occurred on the ground surface. This also explains why in case 5 the results obtained are not significant. Regardless of the discrepancy of the lateral deformation orthogonal to shaking direction, lateral ground deformation obtained in parallel to shaking direction and total displacement present analogous results, mainly that the placement of geosynthetics in the middle and at the bottom part of gravel layer effectively reduce the ground lateral displacement of the mildly sloping ground. As a result, this proposed mitigation can be implemented to mitigate the ground surface lateral deformation due to liquefaction.

The test results presented above are tested using geosynthetic Type 1. To determine the effect of geosynthetic with different friction characteristics with the previous type, a shaking table test using geosynthetic type II placed at the bottom of gravel performed (Case 6). Geosynthetic type II is placed under the gravel layer because based on previous testing using geosynthetic type 1, although lateral movement obtained between geosynthetic laying at the bottom (Case 3) and in the middle of gravel (Case 4) give the same results, but the measurement of pore water pressure in the Case 3 gives the lowest pore water pressure of all cases. **Figure 3.21** presents the ground surface lateral movements measured in Case 6. **Figure 3.22** displays the averaged lateral spreading for three specific cases, i.e., no countermeasures (Case 1), geosynthetic type I placed at the bottom of the gravel layer (Case 3), and geosynthetic type II put under the gravel layer (Case 6). As seen on **Figure 3.22**, geosynthetic type II resulted in more significant result compared to geosynthetic type I, so it can be concluded that the friction angle of the geosynthetics affects the lateral movements of the ground. By using geosynthetic type 1 with a friction angle of 23.4° , the lateral spreading obtained is 4.34 cm (decreased by 23% compared to Case 1), while using geosynthetic type II that has a friction angle of 30.2° , lateral spreading occurred only 3.08 cm (reduced around 45% compared with case 1). This is thought due to the higher the angle friction of the geosynthetic, the stronger the bond between geosynthetic with sand and gravel, and making it more effective in reducing lateral spreading.

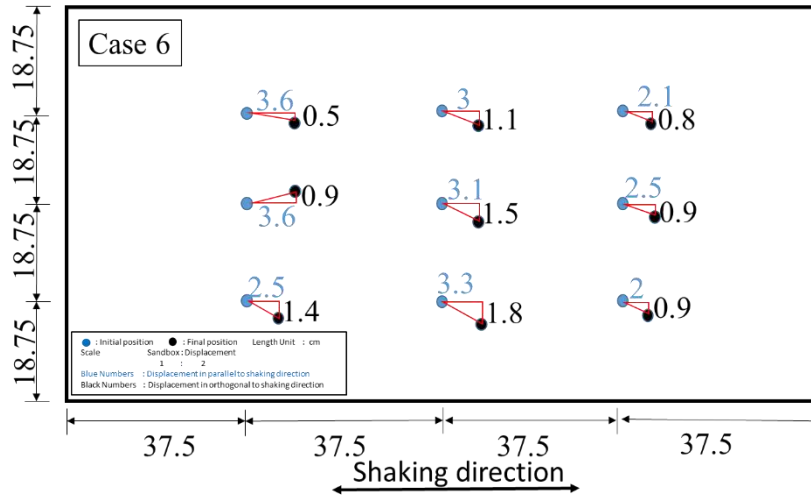


Figure 3.21 Ground surface lateral spreading measured for Case 6

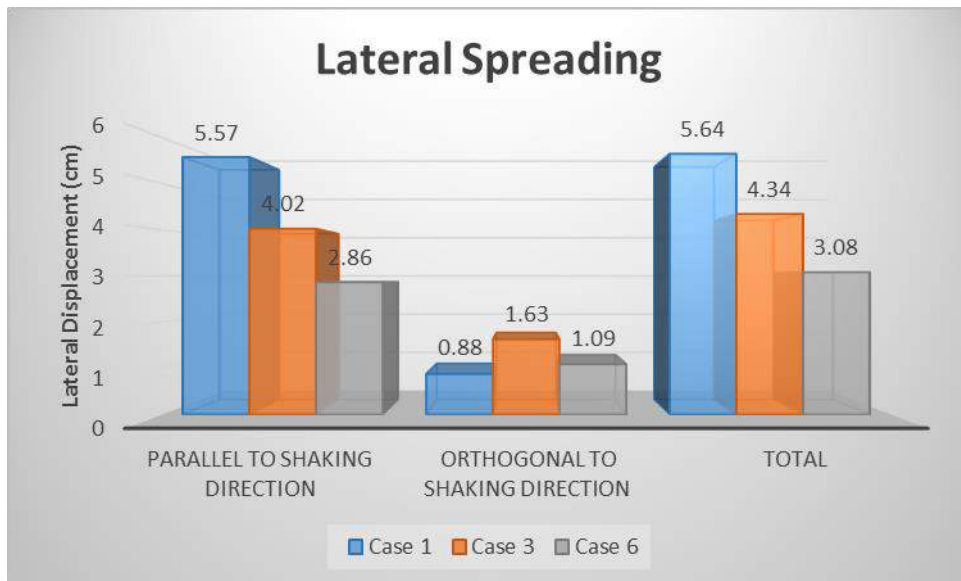


Figure 3.22 Averaged ground surface lateral spreading of Case 1, Case 3, and Case 6

3.4.3 Pull-Out Test

Figure 3.23 shows the results obtained by pull-out tests for geosynthetics used in this study subjected to various overburden pressures. According to the laboratory test results, as shown in this figure, the test using geosynthetics type II provides the higher friction angle,

which is around 30.2° , compared to geosynthetics type II of only about 23.4° . This can be justified due to the thicker and the larger aperture of geosynthetics Type II compared to Type I. This advantage combined with its high tensile strength and tensile stiffness, resulting geosynthetics type II more cohesive when blended with other materials, for example, sand and gravel.

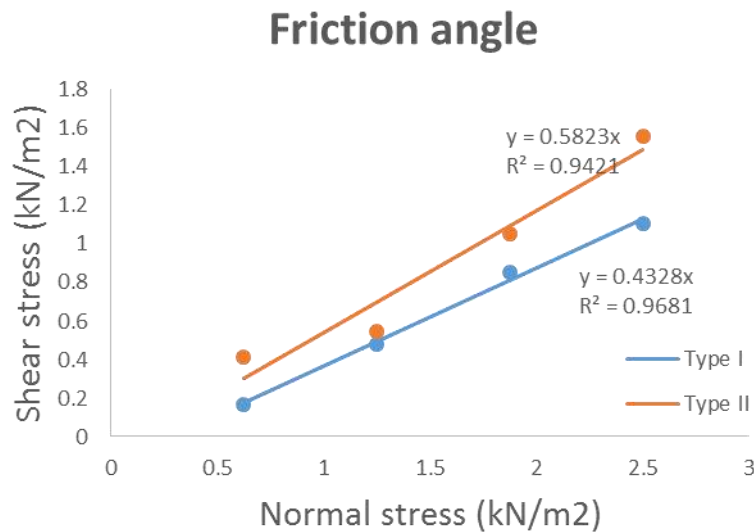


Figure 3.23 Friction angle of the geosynthetics used

According to the Eternal Preserve Ltd. Company, as a company that produces the two geosynthetic types used in this experiment, the geosynthetic Type I in the actual condition is Paralink type 300 L with the tensile strength T_{max} 300 kN/m, and the model used in the experiment is Tiretek BK-85 with tensile strength 6.4 kN/m, hence, the correlation between the model and the actual ones is around 1/50. Furthermore, the geosynthetic type II in the actual condition is Adem type HG-200 with a tensile strength 200 kN/m, and the model around 7.97 kN/m, hence the ratio is around 1/25.

Since the correlation between the model used and the actual condition of these two geosynthetics type is different, this also becomes one of the difficulties that result in similitude law cannot be strictly obeyed. However, as one of the main aims of this study is to mitigate liquefaction-induced ground deformation of a planar road, the experiment performed without loading pressure, and as a result, geosynthetics with higher modulus elasticity and frictional properties with gravel will be more advantageous.

3.5 Conclusions

In order to measure the effectiveness of gravel and geosynthetics remediation to reduce the liquefaction-induced lateral spreading of liquefiable soils, a series of shaking table tests were performed. Based on the results obtained from the tests carried out, the following conclusions are obtained. It is confirmed that the existence of gravel and geosynthetics effectively reduce the ground lateral displacement of liquefiable ground due to the permeability of the gravel and tension strength of the geosynthetics. The test results showed ground improved with geosynthetics type II (with friction angle 30.2°) placed under the gravel layer (Case 6) produced the maximum reduction of lateral ground deformation compared to other cases, decreased by around 45% compared to no countermeasures model. Even though previously this proposed mitigation was poorly investigated in order to restrain liquefaction-induced lateral displacement on the surface of the mildly sloping ground, based on these experimental results, in the future, the use of geosynthetics along with gravel could be recommended and becomes an established liquefaction countermeasure method, in particular, for detached residential houses/buildings and planar roads.

3.6 References

- Bartlett, S. F., and Youd, T. L.: Empirical analysis of horizontal ground displacement generated by liquefaction-induced lateral spreads, Technical Report, NCEER-92-0021, National Center for Earthquake Engineering Research, 1992.
- Boominathan, A. and Hari, S.: Liquefaction strength of fly ash reinforced with randomly distributed fibers, *J. Soil Dynamics and Earthquake Engineering* 22, pp. 1027-1033, 2002.
- Chang, W. J., Chang, C. W. and Zheng, J. K.: Liquefaction characteristics of gap-graded gravelly soils in K_0 condition, *J. Soil Dynamics and Earthquake Engineering* 56, pp. 74-85, 2014.
- Cubrinovski, M. and Robinson, K.: Lateral spreading: Evidence and interpretation from the 2010-2011 Christchurch earthquakes, *J. Soil Dynamics and Earthquake Engineering*, 2016.
- Morikawa Y., Maeda K. and ZHANG F.: Effectiveness of Crushed Tile in Countermeasure Against Liquefaction, *Journal of GEOMATE*, Vol. 7 No. 1 (S1. No. 13), pp. 1003-1008, 2014.
- Motamed, R. and Towhata, I.: Mitigation measures for pile groups behind quay walls subjected to a lateral flow of liquefied soil: Shake table model tests, *J. Soil Dynamics and Earthquake Engineering* 30, pp. 1043-1060, 2010.
- Murakami, K., Kubo, M., Matsumoto, T. and Okochi, Y. : Study on the effect of deformation control embankment during liquefaction by using geosynthetic sandwiched between gravel, *Geosynthetics Engineering Journal*, Vol. 25, pp. 133-140, 2010.

- Noorzad, R. and Amini, P. F.: Liquefaction resistance of Babolsar sand reinforced with randomly distributed fibers under cyclic loading, *J. Soil Dynamics and Earthquake Engineering* 66, pp. 281-292, 2014.
- Orense, R. P., Morimoto, I., Yamamoto, Y., Yumiyama, T., Yamamoto, H. and Sugawara, K.: Study on wall-type gravel drains as liquefaction countermeasure for underground structures, *J. Soil Dynamics and Earthquake Engineering* 23, pp. 19-39, 2003.
- Takahashi, A., Seki, S., Pramadiya, A., Kurachi, Y., Aung, H. and Kubo, M., Dynamic centrifuge model tests for a liquefaction-induced deformation control method by utilizing geosynthetics, *The 50th Geotechnical Research Presentation (Sapporo)*, 2015.
- Valsamis, A. I., Bouckovalas, G. D., Papadimitriou, A. G. : Parametric investigation of lateral spreading of gently sloping liquefied ground, *J. Soil Dynamics and Earthquake Engineering* 30, pp. 490-508, 2010.
- Vercuil, D., Billet, P. and Cordary, D.: Study of the liquefaction resistance of saturated sand reinforced with Geosynthetics, *J. Soil Dynamics and Earthquake Engineering* 16, pp. 417-425, 1997.

4. THE MITIGATION OF LIQUEFACTION-INDUCED VERTICAL GROUND DEFORMATION BY USING GRAVEL AND GEOSYNTHETICS

4.1 Introduction

During earthquakes, the shaking of the ground may cause a loss of strength or stiffness that results in settlement of buildings, landslides, the failure of earth dams, or other hazards. The process leading to such loss of strength or stiffness is called soil liquefaction. It is a phenomenon associated primarily, but not exclusively, with saturated cohesionless soils. Liquefaction takes place when the pore water pressure reaches a particular value which is close to the total stress of soil. One of the consequences that can occur is structures built on top or within the liquefied ground may fail due to ground deformation.

Furthermore, the extent of the ground deformation is influenced by several factors, one of which is the relative density (D_r) of the ground. When earthquake-induced liquefaction occurs in the areas with different density, ground differential settlement can take place and may cause damage to a construction built on it, such as the building tilted and roads become uneven/bumpy. Moreover, in the severe condition and significant differential settlement appears, this can lead to, for example, impassable roads. However, for the important roads, such as main roads, emergency evacuation routes, and roads connected to essential facilities, it is necessary to ensure the accessibility of these valuable roads during earthquakes. For that reason, it is necessary to restrain liquefaction-induced ground displacement by an economical and simple to be implemented method. **Figure 4.1(a)** shows the damaged road construction damage of the Joban Motorway near Mito, Ibaraki, due to liquefaction in the Great East Japan Earthquake (Anon 2011a); **Figure 4.1(b)** presents the damaged road caused by liquefaction in the Great Hanshin Earthquake, Kobe, Japan (Anon1995c); **Figure 4.1(c)** displays the tilted residential houses due to liquefaction in the 2016 Kumamoto Earthquake, Japan.

4.2 Previous Studies on Liquefaction-Induced Ground Settlement

Many types of research have been carried out to investigate the ground displacement due to liquefaction phenomenon. For example, it is presented that significant volume changes occur only when there is liquefaction of sand. Otherwise, the settlement is tiny (Ueng et al. 2010). Correspondingly, Maharjan and Takahashi (2013) reported that the results of dynamic centrifugal tests conducted to investigate the liquefaction mechanism in non-homogeneous soil deposits. In the following year, Maharjan and Takahashi (2014)

conducted a study of the liquefaction-induced deformation of earthen embankments on non-homogeneous soil deposits and found that the embankment resting on non-homogeneous soil deposits suffer more damage compared to the uniform sand foundation of same relative density. Harmoniously, Zeybek and Madabhushi (2017) presented a study of the influence of air injection on the liquefaction-induced deformation mechanisms beneath shallow foundations.



Figure 4.1 Damaged constructions due to liquefaction-induced ground displacements;

- (a) In the 2011 Great East Japan earthquake
- (b) In the 1995 Great Hanshin earthquake, Japan
- (c) In the 2016 Kumamoto earthquake, Japan

Among the variety of liquefaction countermeasure methods proposed, the use of gravel, geosynthetics, or geosynthetics in conjunction with gravel attracted some attention due to their effectiveness and relatively low cost. This method is thought to be a good technique to mitigate liquefiable soil problems. As presented by Murakami et al. (2010), a combination of geosynthetics and gravel to restrain liquefaction in embankments, focused on the vertical displacement of the embankments. The result showed that the settlement of the embankments decreased by nearly 35% by using gravel and geosynthetics. They concluded that the use of geosynthetics sandwiched between gravel would have high resistance to bending deformation due to the overburden load of the embankment. Even though this method does not overcome the occurrence of liquefaction completely, it does alleviate the excessive deformation such as settlement and lateral movement. Accordingly, some other research also showed corresponding results, for example by use gravel presented by Orense et al. (2003), Morikawa et al. (2014), and Chang et al. (2014), and geosynthetics utilized reported by Verduil et al. (1997), Boominathan and Hari (2002), and Noorzad and Amini (2014).

4.3 Laboratory Test of the Liquefaction-induced Vertical Ground Movements

4.3.1 Material and Instrument utilized

Experiments were conducted using materials and instruments such as a sand container, sands, gravel, and geosynthetics, are the same as those used in the experiments mentioned in the previous chapter.

Input harmonic wave used were as follows: a frequency of 5 Hz, a target maximum input acceleration of around 80 gal, and a shaking duration time of 15 seconds.

4.3.2 Experimental Set-up

Figure 4.2 – Figure 4.5 shows the plan view, and the cross-section of the unreinforced model (Case 1), reinforced with gravel (Case 2) and gravel accompanied by geosynthetics type I and type II (Cases 3 and 4) along with the layout of accelerometers, water pressure meters, and displacement meters. The ground in the model composed of a liquefiable layer with a relative density around 50%, non-liquefiable part with a relative density of 90% in dense condition, and dry sand on the ground surface.

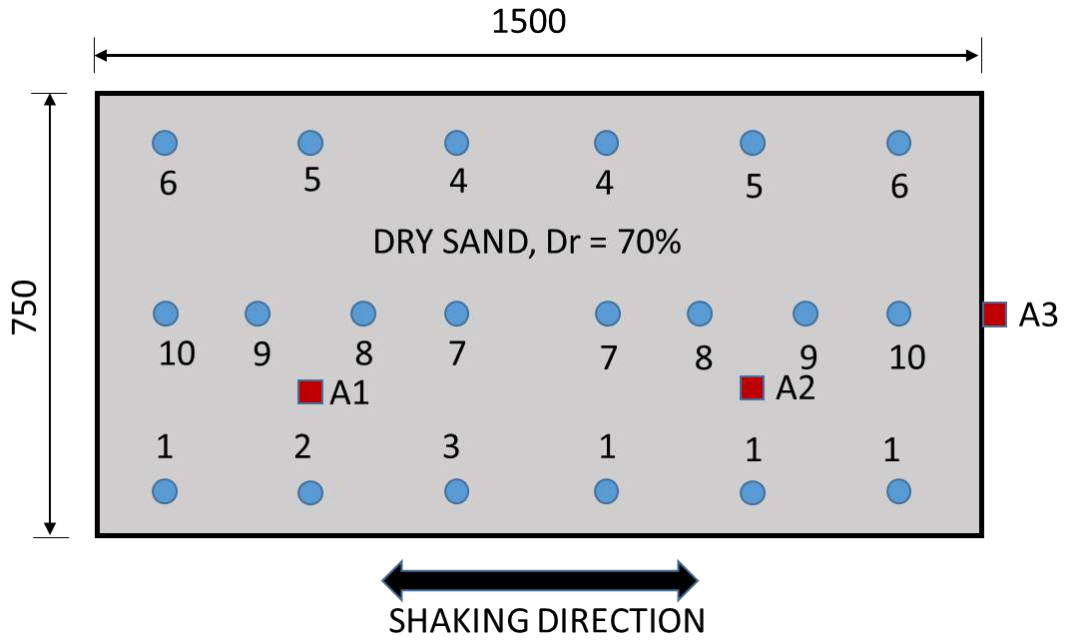


Figure 4.2 The top view of the sandbox

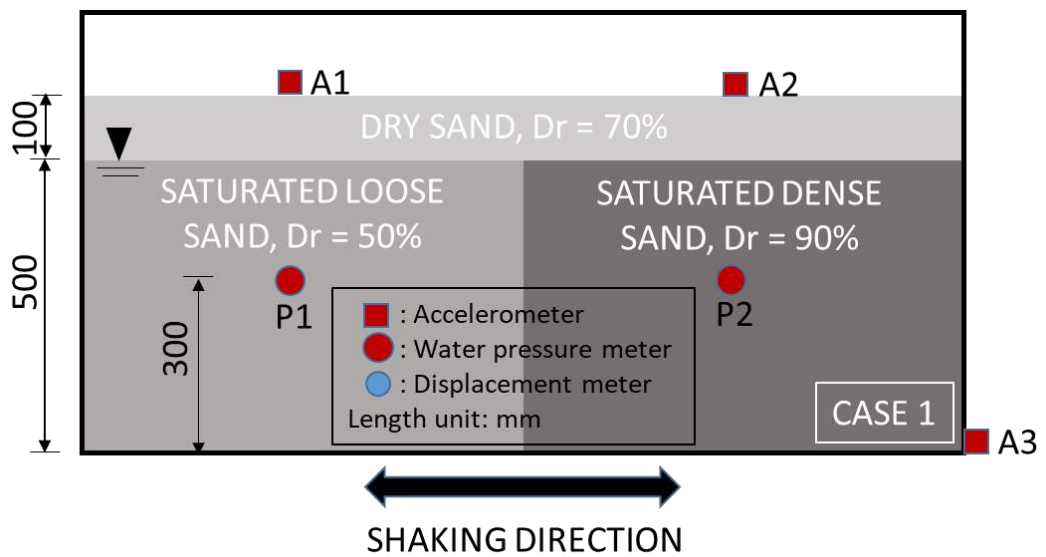


Figure 4.3 The side view of the unreinforced ground (Case 1)

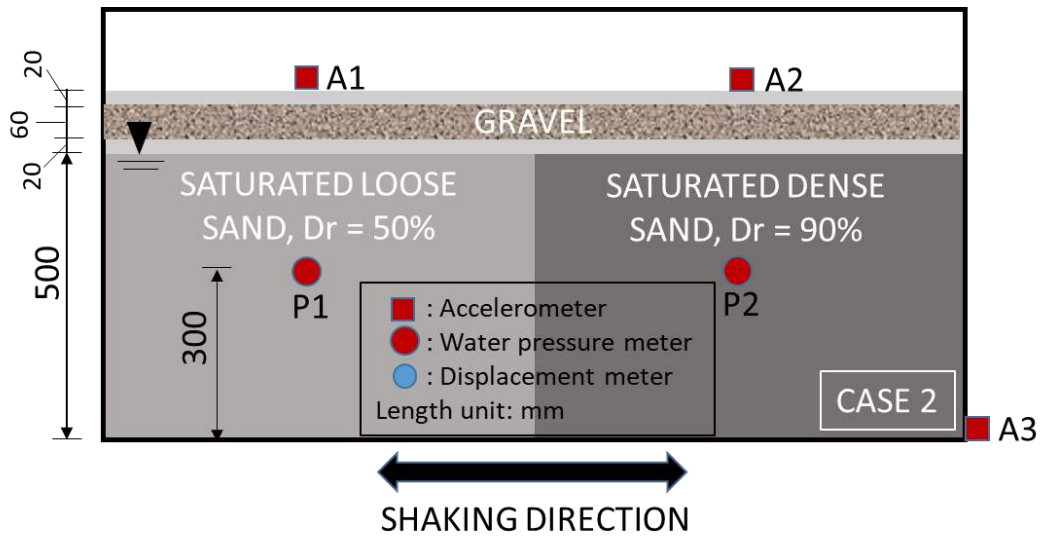


Figure 4.4 The side view of the gravel-reinforced ground (Case 2)

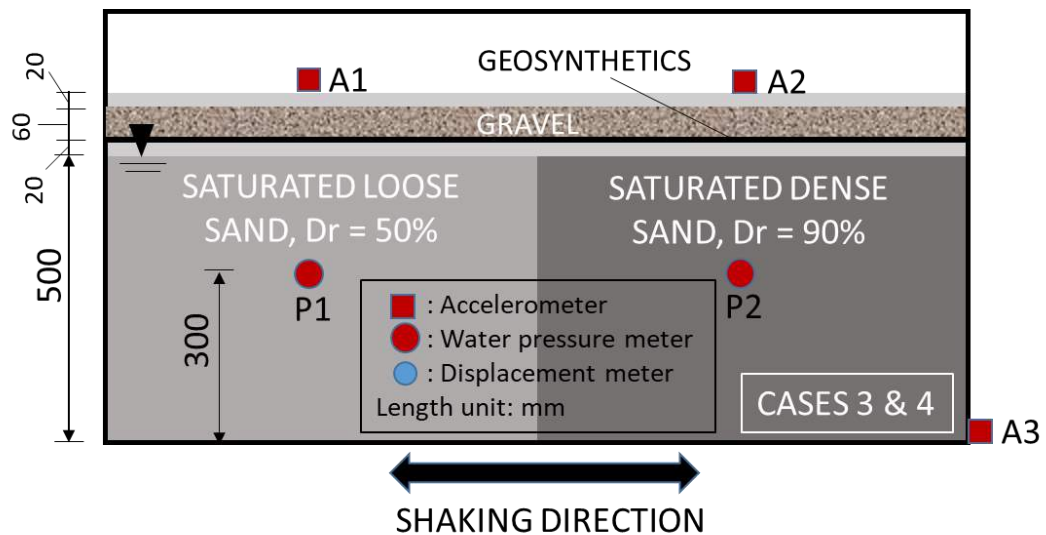


Figure 4.5 The side view of the gravel and geosynthetic (type I and II) reinforced ground (Cases 3 & 4)

4.4 Experimental Results and Discussion

A summary of the primary data measured during the shaking table test such as excess pore water pressure, acceleration, and settlement of ground surface is presented and discussed.

4.4.1 Pore Water Pressures

Pore water pressure was observed by installing two pore water pressure transducers at 30 cm from the bottom of the sandbox, either for the loose sand or dense sand parts. Excess pore water pressure measured was converted to pore water pressure ratio (PWPR) by dividing excess pore water pressure with initial vertical effective stress (σ_v'). Pore water pressure ratio time histories are shown in **Figures 4.6** and **4.7**.

Generally, the results obtained show an insignificant difference in all cases, both for P1 and P2. As can be seen in **Figures 4.6**, for water pressure meter placed in the loose sand zone (P1), although the maximum PWPR obtained is around 1 for Case 2, but the maximum value in Cases 1 and 3 is also immensely close to 1, around 0.97, which indicate that liquefaction occurred. In Case 4, the maximum PWPR is only slightly lower and showed a faster water pressure dissipation, compared to other cases. Correspondingly, as shown in **Figure 4.7**, for the dense sand state (P2), the maximum PWPR acquired is almost similar for all cases of about 0.4, even though the highest PWPR in Case 4 is little higher compared to other cases. These results signify that no liquefaction occurred in this zone.

According to the results, it can be said that the effect of the use of gravel and geosynthetics on pore water pressure is insignificant in these experiments. Since the main purpose of pore water pressure measurement is to determine the occurrence of liquefaction in the sand layer, therefore the influence of the use of gravel and geosynthetics on pore water pressure is not a major concern.

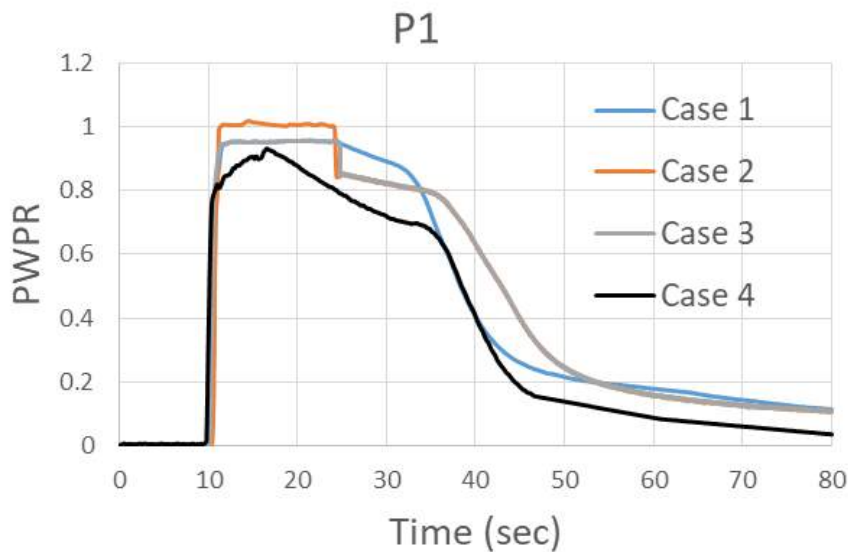


Figure 4.6 Pore water pressures time histories in the loose sand condition (P1)

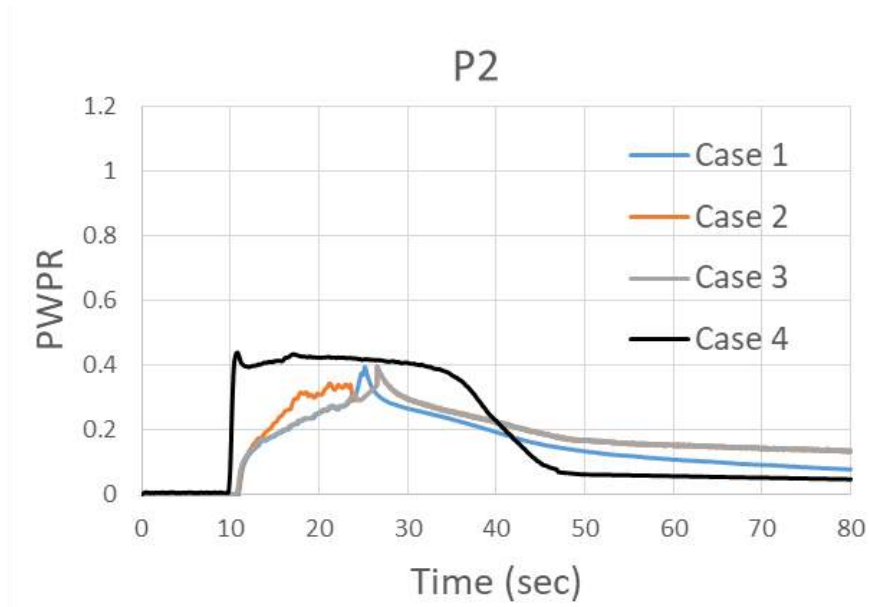


Figure 4.7 Pore water pressures time histories in the dense sand condition (P1)

4.4.2 Acceleration

The acceleration measured are shown in the **Figures 4.8 - 4.11** as follows.

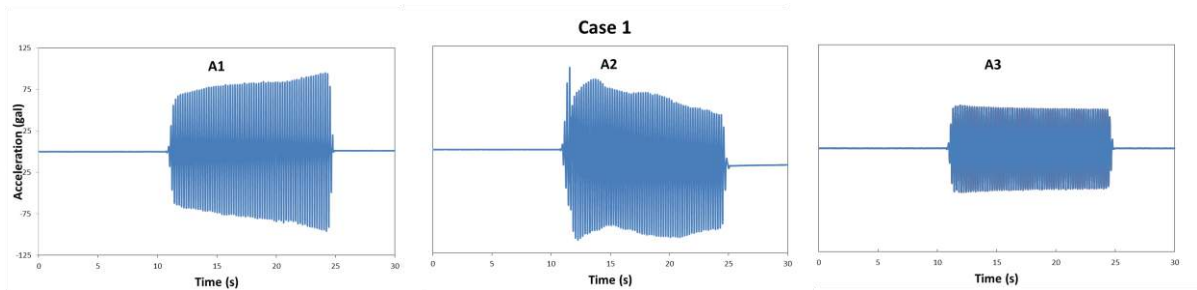


Figure 4.8 Acceleration time histories of no countermeasures ground (Case 1)

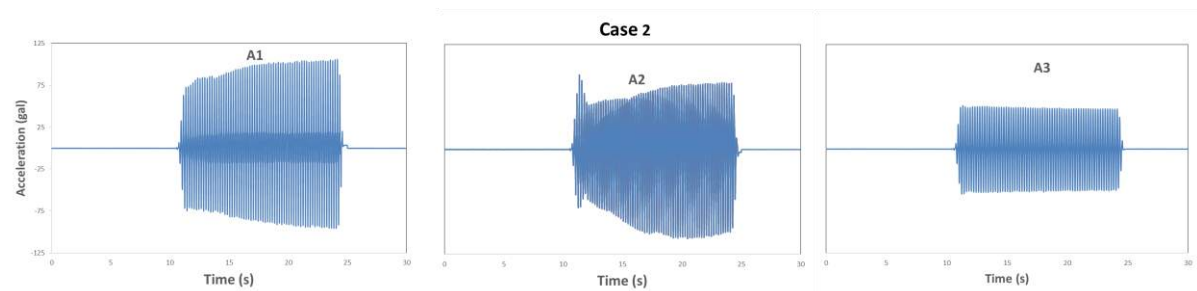


Figure 4.9 Acceleration time histories of gravel-reinforced ground (Case 2)

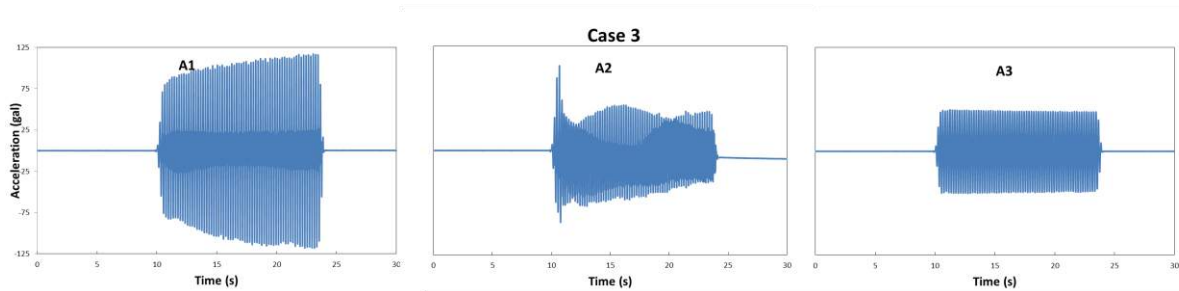


Figure 4.10 Acceleration time histories of gravel & geosynthetic type I-reinforced ground (Case 3)

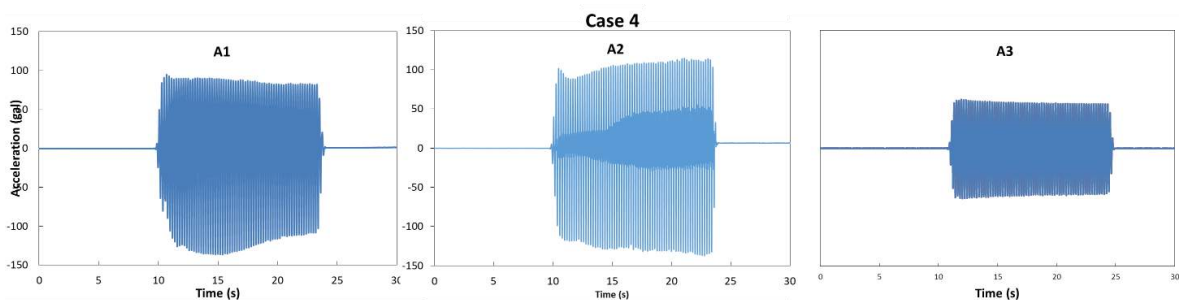


Figure 4.11 Acceleration time histories of gravel & geosynthetic type II -reinforced ground (Case 4)

In the above figures, A1 is the acceleration measured at the loose ground surface, A2 at the dense ground surface, and A3 is an input acceleration. According to the above pictures, it can generally be said that the use of gravel and geosynthetic does not give a significant effect on ground acceleration. Slightly different results were seen in Case 3, where acceleration in the dense sand (A2) showed lower results compared to others. Based on this result it can be said that gravel and geosynthetic used can decrease acceleration amplification, although insignificant. Other than that it appears that the acceleration in loose sand is larger compared to the dense sand, which reveals that the density of the soil also affects acceleration amplification. The increased soil density will be able to reduce acceleration amplification.

To determine the impact of gravel and geosynthetic use on ground acceleration, both on the loose and dense sand, a series of additional tests were performed. The results of this test will be analyzed and will be determined by changes of amplification factors on each test. The amplification factor is the ratio between the amplitude acceleration measured at the ground surface divided by the amplitude of the input acceleration on each test performed. Only 2 cases will be tested on this test, namely case 1 and case 4.

In this additional test series, input harmonic wave used were as follows: frequency of 1 - 30 Hz, a target maximum input acceleration of around 20 gal, and a shaking duration time of 15 seconds.

Figure 4.12 shows the value of the resulting amplification factor ratios in loose sand condition (A1). From this figure, it appears that for the loose sand conditions, the amplification decreases by about 38%, from about 3.7 in Case 1 to 2.3 in Case 4. Similarly, as seen in **Figure 4.13**, in dense sand conditions, although not as significant as loose sand conditions, amplification factor also decreased of about 30%, from 2.7 in case 1 to 1.9 in case 4. According to the results above, it is confirmed that gravel and geosynthetics that used in Case 4 effectively reduce the amplification factor of the ground, both in the loose and dense conditions.

Figures 4.12 and **4.13** also revealed that the effect of gravel and geosynthetic to reduce the acceleration amplification was found more significant in the dense soil conditions than that of the looser one. In the high-density sand, the maximum amplification factor ratios for Case 4 are around 1.9, whereas for Case 1 approximately 2.3. This can be attributed to the more efficient interaction between gravel, geosynthetics, and sand grains at high density. It is speculated that the thickness, apertures, the roughness, and tensile strength of the geosynthetics constituted a stronger interlock with the high-density soils than that of looser one due to loose sand corresponds to a higher void ratio and larger pore diameters. Furthermore, it can also be concluded that the soil density has a significant effect on the acceleration amplification. The looser soil conditions result in larger amplification which thought due to the higher void ratio of the looser soils.

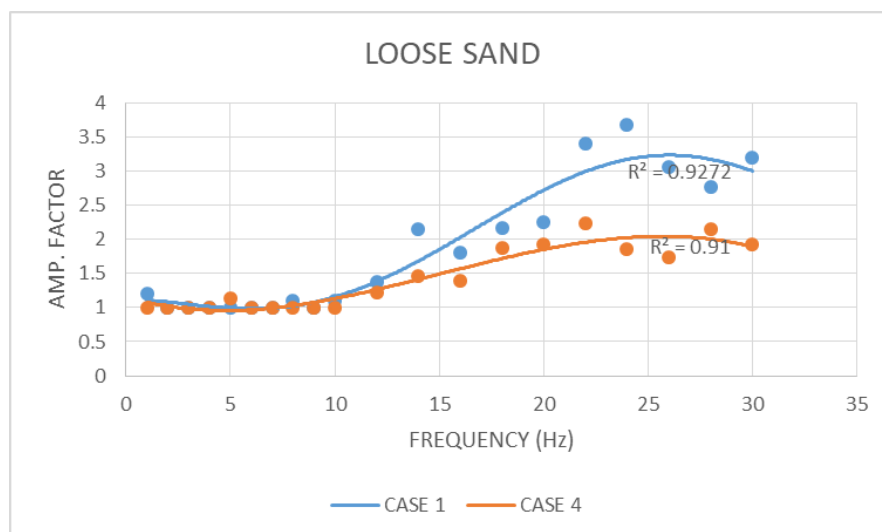


Figure 4.12 Amplification acceleration measured in the loose sand condition (A1)

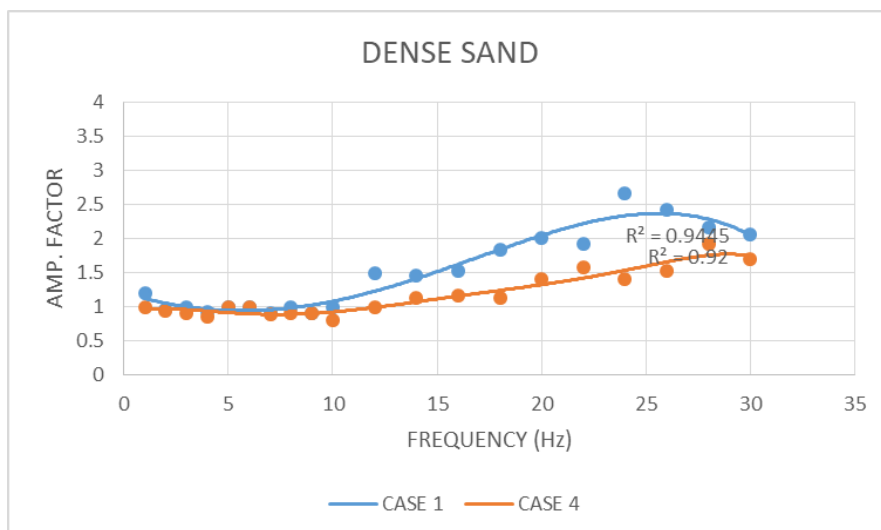


Figure 4.13 Amplification acceleration measured in the dense sand condition (A2)

4.4.2 Vertical Ground Deformation

The vertical ground displacement occurred through ten different points at the ground surface was measured. Tables 4.1 – 4.4 present the residual settlement of all cases.

Table 4.1 Residual settlement for Case 1

POINT NO.	SETTLEMENT (mm)	
	LOOSE	DENSE
1	23.9	10.6
2	20.8	3.7
3	19.1	5.2
4	27.8	3.1
5	21.4	5.4
6	24.3	5.7
7	27.3	14.1
8	11.5	2.1
9	15.9	3.5
10	16.9	2.1
AVERAGE	20.9	5.6
DIFFERENTIAL SETTLEMENT	15.3	

Table 4.2 Residual settlement for Case 2

POINT NO.	SETTLEMENT (mm)	
	LOOSE	DENSE
1	21.9	4.8
2	21.8	8.3
3	17	7.5
4	22.1	1.6
5	13.9	1.2
6	14.2	0.9
7	17.2	2.4
8	3.1	4.1
9	13.5	1.8
10	23.9	4.8
AVERAGE	16.9	3.7
DIFFERENTIAL SETTLEMENT	13.1	

Table 4.3 Residual settlement for Case 3

POINT NO.	SETTLEMENT (mm)	
	LOOSE	DENSE
1	14.6	4.7
2	15.0	9.0
3	16.8	5.6
4	12.8	1.1
5	18.4	2.8
6	13.3	1.5
7	9.5	4.6
8	11.6	6.0
9	10.7	3.0
10	10.5	1.0
AVERAGE	13.3	3.9
DIFFERENTIAL SETTLEMENT	9.4	

Table 4.4 Residual settlement for Case 4

POINT NO.	SETTLEMENT (mm)	
	LOOSE	DENSE
1	12.2	4.8
2	12.4	5.7
3	10.6	6.1
4	11.9	0.3
5	6.1	1.3
6	7.7	3.3
7	10.5	5.3
8	6.4	3.4
9	6.1	1.3
10	10.6	6.2
AVERAGE	9.5	3.8
DIFFERENTIAL SETTLEMENT	5.7	

To simplify understanding, the displacement values are averaged, and the results can be seen in **Figure 4.14**. It can be observed that based on the averaged vertical ground displacement measured, the presence of the proposed mitigation could reduce vertical displacement in various amounts, for example, by use gravel only (Case 2), in the loose sand condition, the settlement was decreased around 4 mm, from 20.9 mm to 16.9 mm, and reach approximately 1.9 mm for the dense condition, from 5.6 mm to 3.7 mm. Moreover, by applying gravel and geosynthetics type I (Case 3), the displacement was reduced up to 7.6 mm and 1.7 mm in the loose sand and dense sand conditions, respectively. Maximum results are shown on reinforcement with gravel and geosynthetics Type II, which the ground settlement lowered around 11.4 mm in loose sand condition and 1.8 mm in the dense sand state, compared to Case 1.

Furthermore, the differential settlement between non-liquefiable and liquefiable zones is compared, as shown in **Figure 4.15**. In the Case 1, the settlement difference is 15.3 mm, while in Case 2 is 13.2 mm, which means decreased 2.1 mm. The differential settlement is reduced up to 5.9 mm and 9.6 mm in Case 3 and Case 4, respectively. The reduction in differential settlements also resulting in the inclination angle at the ground surface at the border line between loose sand and dense sand areas become more gentle as seen on the **Figure 4.16**. In Case 1, the surface angle is around 3.78° , and the angle downgrade becomes 1.40° in the Case 3 and 1.48° in the Case 4.

The coherence of the gravel layer with its high permeability and high tensile strength provided by geosynthetics were considered as the main reason for this good result. Since the tension generated in the geosynthetics restrain the deformation of the gravel layer and integrally perform like a rigid plate with high permeability, this reinforcement could reduce the settlement that occurred on the ground surface. Since the tensile strength and the tensile stiffness of geosynthetics Type II that used in Case 4 is higher compared to type I, this type of geosynthetics could restrain the deformation of the gravel and sand better than Type I, resulting in lower ground vertical displacement compared to geosynthetics Type I that used in Case 3.

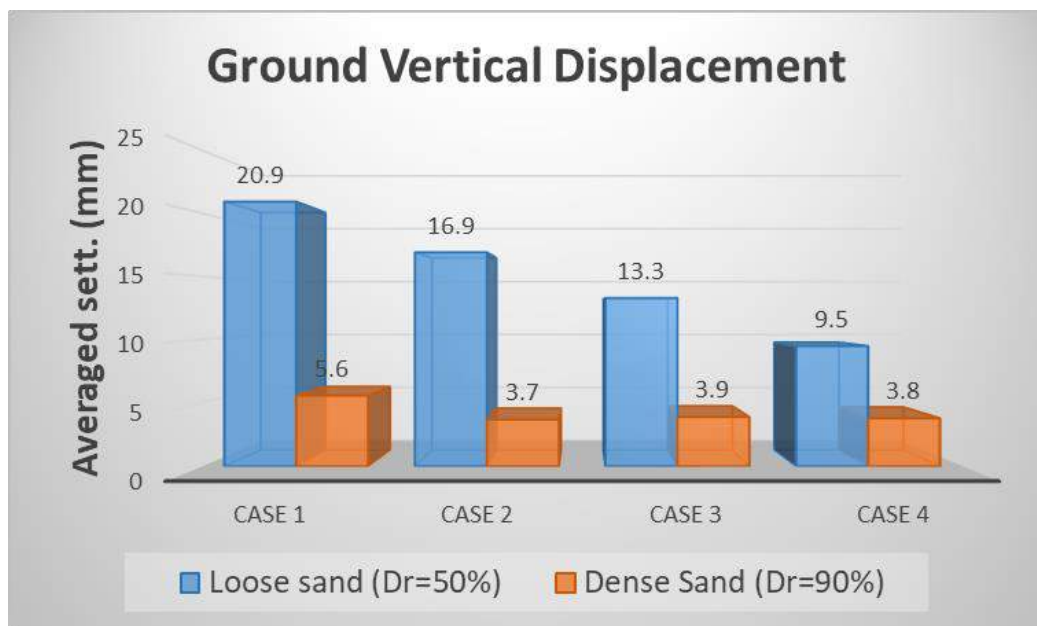


Figure 4.14 Averaged residual vertical ground displacement

Based on the results obtained from laboratory testing, this proposed mitigation can be applied to overcome the liquefaction-induced ground settlement and the resulting damage, such as the impassable roads due to differential settlement appeared caused by the subsoil layer liquefy. This will result in substantial losses if this damage occurs on vital roads. Moreover, tilted houses and building also could be appeared due to liquefaction, for instance as happened in Kumamoto earthquake 2016, Japan, where it was reported that many residential houses and buildings were tilted due to liquefaction (Setiawan et al., 2017). The use of gravel and geosynthetics in those examples mentioned above will be able to lower the settlement and the related-damages caused by liquefaction.



Figure 4.15 Differential settlement between the loose and dense sand zones

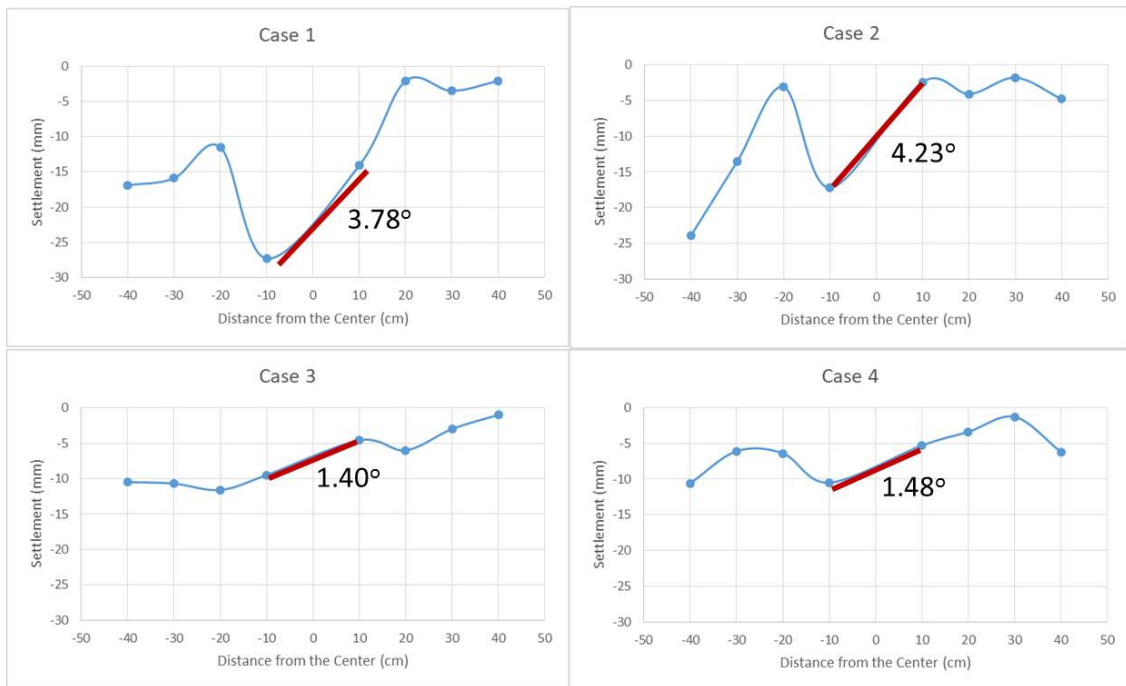


Figure 4.16 The ground surface inclination angle at the border line between loose and dense sand zones

Research related to the use of gravel combined with geosynthetics in order to mitigate ground deformation triggered by liquefaction is poorly investigated. This proposed mitigation method is expected to be widely used to overcome ground settlement due to liquefaction since it has the following advantages; 1) more economical compared to other methods such as vibration or sand piling. According to the Japanese Geotechnical Society (JGS) Kanto branch, ground reinforcement by using the banded geosynthetics type Paralink 300L, the cost is around 1250 JPY/m², whereas by using static clamping sand piling method about 20,000-30,000 JPY/m² and by vibration type SCP method approximately 10,000 JPY/m². 2) more workable, due to this method is simpler to be executed. 3) lower impact on the surrounding environment, by reason of vibration and noise caused by the use of heavy equipment during the installing process is less than other methods. 4) high strength and durability, according to Eternal Preserve Co., Ltd, the tensile strength characteristics of this type of geosynthetics is 309.0 kN/m and is resistant to heat, weather, and chemical effects. 5) in accordance with the results of this study, this proposed mitigation effectively reduced the vertical ground displacement caused by liquefaction.

4.5 Conclusions

The effectiveness of gravel along with geosynthetics remediation to restrain the liquefaction-induced vertical ground displacement had been measured by conducting a series of shaking table tests. According to the results acquired from the tests carried out, the following conclusions are obtained. It is found that the use of gravel and geosynthetics effectively reduce the vertical ground displacement of liquefiable soil due to the permeability of the gravel and tension strength of the geosynthetics. The conjunction of these two reinforcing materials resulted in a permeable layer which behaves like a rigid plate.

The results showed that by using this proposed mitigation, the settlement of the ground surface decreased by around 54% in the liquefiable zone and up to 32% in the non-liquefiable zone. It is also observed that the differential settlement between liquefiable sand and non-liquefiable in the same condition decreased about 62%, from 15.3 mm in no countermeasure condition to 5.7 mm when model improved with gravel and geosynthetics Type II. In the future, gravel in conjunction with geosynthetics could be recommended and becomes an established liquefaction countermeasure mitigation due to its advantages above and effectivity to reduce the liquefaction-induced ground vertical displacement.

4.6 References

- Anon. 2011a. Damaged road due to liquefaction in The Great East Japan Earthquake. Available at: <https://www.telegraph.co.uk/news/worldnews/asia/japan/8377742/Japan-earthquake-and-tsunami-as-it-happened-March-11.html>. Accessed 29 March 2018.
- Anon. 1995b. Tilted building due to liquefaction in The Great Hanshin Earthquake Japan. Available at: <http://web.ics.purdue.edu/~braile/edumod/eqphotos/eqphotos2.htm>. Accessed 29 March 2018.
- Anon. 1995c. Damaged road due to liquefaction in The Great Hanshin Earthquake Japan. Available at: <http://1crankyteacher.blogspot.jp/2013/04/kobe-earthquake-of-1995.html>. Accessed 29 March 2018.
- Boominathan, A. and Hari, S. (2002) Liquefaction strength of fly ash reinforced with randomly distributed fibers, *J. Soil Dynamics and Earthquake Engineering* 22, pp. 1027-1033.
- Chang, W. J., Chang, C. W. and Zheng, J. K. (2014) Liquefaction characteristics of gap-graded gravelly soils in K_0 condition, *J. Soil Dynamics and Earthquake Engineering* 56, pp. 74-85.
- Morikawa Y., Maeda K. and ZHANG F. (2014) Effectiveness of Crushed Tile in Countermeasure Against Liquefaction, *Journal of GEOMATE*, Vol. 7 No. 1 (S1. No. 13), pp. 1003-1008.
- Murakami, K., Kubo, M., Matsumoto, T. and Okochi, Y. (2010) Study on the effect of deformation control embankment during liquefaction by using geosynthetic sandwiched between gravel, *Geosynthetics Engineering Journal*, Vol. 25, pp. 133-140.
- Noorzad, R. and Amini, P. F. (2014) Liquefaction resistance of Babolsar sand reinforced with randomly distributed fibers under cyclic loading, *J. Soil Dynamics and Earthquake Engineering* 66, pp. 281-292.
- Orense, R. P., Morimoto, I., Yamamoto, Y., Yumiyama, T., Yamamoto, H. and Sugawara, K. (2003) Study on wall-type gravel drains as liquefaction countermeasure for underground structures, *J. Soil Dynamics and Earthquake Engineering* 23, pp. 19-39.
- Setiawan, H., Serikawa, Y., Nakamura, M., Miyajima, M., Yoshida, M. (2017) Structural damage to houses and buildings induced by liquefaction in the 2016 Kumamoto Earthquake, Japan. *Journal of Geoenvironmental Disasters* 4:13. DOI: 10.1186/s40677-017-0077-x.
- Takahashi, A., Seki, S., Pramadiya, A., Kurachi, Y., Aung, H. and Kubo, M. (2015) Dynamic centrifuge model tests for a liquefaction-induced deformation control method by utilizing geosynthetics, *The 50th Geotechnical Research Presentation (Sapporo)*.
- Ueng, T. S., Wu, C. W., Cheng, H. W., and Chen, C. H. (2010) Settlements of saturated clean sand deposits in shaking table tests, *J. Soil Dynamics and Earthquake Engineering* 30, pp. 50-60.
- Vercuil, D., Billet, P. and Cordary, D. (1997) Study of the liquefaction resistance of saturated sand reinforced with Geosynthetics, *J. Soil Dynamics and Earthquake Engineering* 16, pp. 417-425.
- Zeybek, A. and Madabhushi, S. P. G. (2017) Influence of air injection on the liquefaction-induced deformation mechanisms beneath swallow foundations, *J. Soil Dynamics and Earthquake Engineering* 97, pp. 266-276.

5. CONCLUDING REMARKS

In this study, the liquefaction phenomenon and its occurrence during earthquakes are studied and observed. The liquefaction occurrences can be seen in several forms, one of which is ground deformation, either horizontally or vertically deformations. In this study, the occurrences of liquefaction-induced ground deformation and the structural damage of houses and buildings its caused during the 2016 Kumamoto earthquake Japan were observed. Furthermore, the ground deformation induced by liquefaction mitigated by using gravel and geosynthetics. The effect of the proposed method in order to restrain ground movement was observed quantitatively by conducting a series of 1-g shaking table test in the laboratory.

Based on the results of this research study, the following conclusions are made regarding the liquefaction-induced ground deformation:

1. The outcomes of chapter 2 showed that the occurrence of liquefaction in the previous earthquakes caused severe damage to buildings and constructions, including residential houses, roads, bridges, and tailing dams. One of the main causes of this severe damage is the ground deformation triggered by liquefaction, both lateral spreading and ground settlement. This disaster has caused enormous economic losses. Liquefaction case pasts can be perceptive for the development of liquefaction phenomenon as well as to reduce the impacts of liquefaction-induced ground deformation.
2. According to the horizontal ground displacement experiments, it is clarified that the presence of proposed mitigation method effectively decreased the lateral ground spreading. Gravel combined with geosynthetics type I with friction angle around 23.4° reduced the lateral spreading around 23%, whereas gravel along with geosynthetics type II with better friction characteristic (friction angle 30.2°) lowered the lateral spreading almost doubled, up to 45%, compared to the ground with no reinforcement. Moreover, although insignificant, the use of geosynthetics placed under the gravel layer, resulted in the lowest pore water pressure among all ground models condition.

3. Vertical ground displacement laboratory experiments resulted and clarified that the use of projected approach commendably decreased the ground subsidence caused by liquefaction. In the loose ground condition, with a relative density (Dr) of 50%, the settlement decreased up to 36.3% by applying gravel and geosynthetics type I, and even more significant result obtained by utilizing gravel in conjunction with geosynthetics type II, i.e., nearly 54.5%. In the dense sand state ($Dr=90\%$), the ground subsidence reduced by about 32% by adding the suggested reinforcement layer. Furthermore, it is also validated that, the ground subsidence difference between the liquefiable and nonliquefiable areas decreased closely 38% and 62%, in case of the use of gravel and geosynthetics type I and II, respectively.

4. Additional shaking tests were performed in order to determine the influence of ground condition and reinforcing layer on ground amplification. In these tests, it is confirmed that ground amplification is influenced by ground density. The more the soil density, the less ground amplification. Moreover, gravel and geosynthetics decrease the ground amplification as well.

5. By measuring the angle of the residual ground surface at the boundary between loose and dense sands, it is clarified that the presence of gravel and geosynthetics lowered the ground surface slope angle.

According to the results obtained, this proposed method expected to complement the existing methods and become an effective and affordable method to mitigate liquefaction-induced ground deformation, particularly for detached residential houses and planar roads.

Appendix A

STRUCTURAL DAMAGE TO HOUSES AND BUILDINGS INDUCED BY LIQUEFACTION IN THE 2016 KUMAMOTO EARTHQUAKE, JAPAN

A.1 Introduction

In April 2016, Kumamoto city, Japan, and surrounding areas were hit by strong and devastating earthquakes. There were two significant events in this earthquake sequence reported by Japan Meteorological Agency (JMA). First, on April 14th, 2016, at 21:26 Japan Standard Time (JST), a strong earthquake of magnitude Mw6.2 occurred, and followed by an earthquake that hit on April 16th, 2016, at 01:25 JST of magnitude Mw7.0, for foreshock and mainshock, respectively. These earthquakes are resulting in 69 deaths and significant economic losses.

Furthermore, This earthquake sequence induced numerous geotechnical damages, such as landslides, ground displacement, and liquefaction. These geotechnical problems occurred in a wide area in Kumamoto city and caused severe damage to infrastructures, such as roadways, railways, bridges, buildings, and residential houses.

This chapter presents an overview of seismological on the 2016 Kumamoto earthquake, casualties and economic losses, and damage to infrastructure due to geotechnical hazards, and as the main focus, liquefaction-induced structural damage of the buildings and residential houses.

A.2 Seismological Characteristics of the Earthquake

The foreshock, which occurred on April 14th, 2016 of magnitude Mw6.2, struck initiated from the northern part of the Hinagu fault in Kumamoto Prefecture, Kyushu island, Japan. The focal depth was recorded at 11 km below the ground surface. Subsequently, the mainshock hit on the southern part of the Futagawa fault on April 16th, 2016, of magnitude Mw7.0w and focal depth lied at 12km below ground level. Some aftershocks also reported with an intensity greater than Mw5. **Figure A.1(a)** shows the epicenter of the two major earthquakes (Anon., 2016a). The JMA intensity of 7 (the highest intensity in the JMA intensity scale) was recorded in Mashiki Town during the earthquake sequence and caused

many buildings and houses collapsed in this area. **Figures. A.1(b)** and **A.1(c)** present the estimated seismic intensity distribution for the foreshock and mainshock (Anon., 2016b; Anon., 2016c).

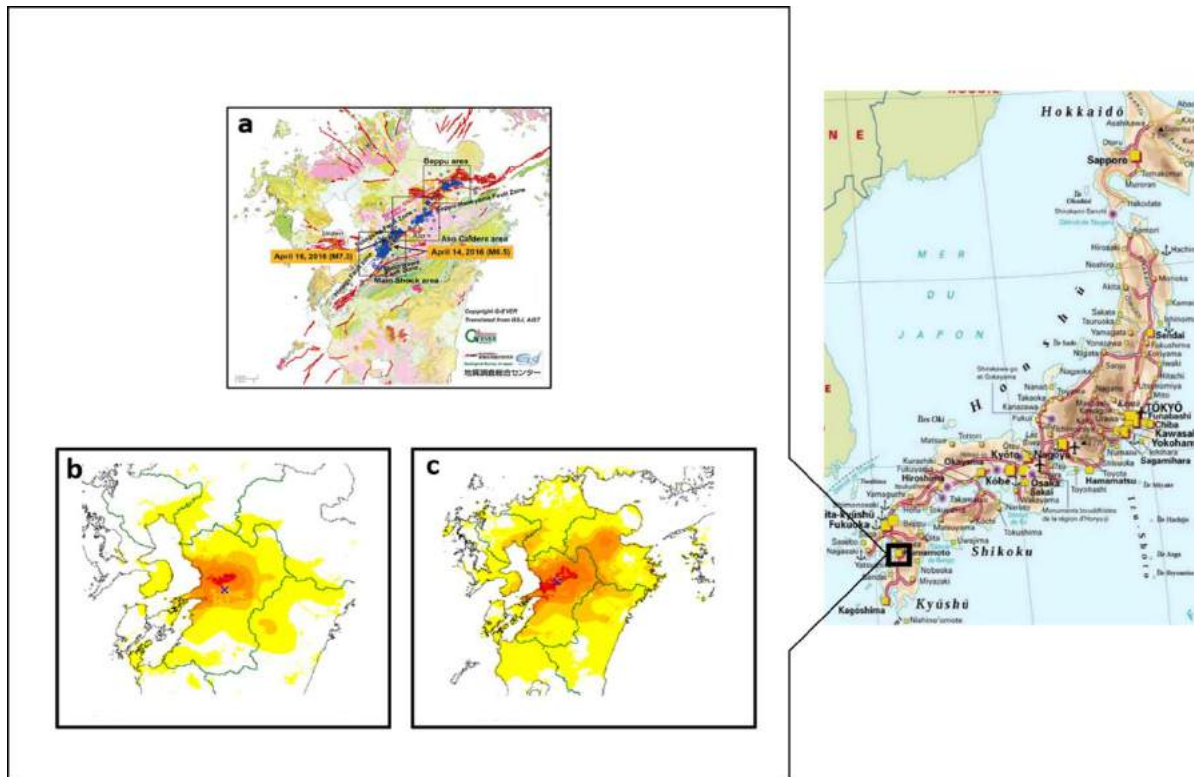


Figure A.1 The seismology of the 2016 Kumamoto earthquake, Japan
 (a) The epicenter foreshock and main-shock
 (b) The estimated seismic intensity distribution for the foreshock
 (c) The estimated seismic intensity distribution for the main-shock

Figure A.2 shows the recorded acceleration, velocity response, and acceleration response at KMMH16 station in Mashiki Town for the foreshock. The maximum acceleration recorded was 1580 gal. Moreover, **Figure A.3** presents the recorded data from KMMH16 station, but for the main-shock, and as shown, the maximum acceleration recorded was 1362 gal (Anon., 2016d).

A.3 An Overview of the Earthquake Damage

The earthquake sequence caused extensive damage, for instance, the total number of fatalities due to the earthquakes is reported 120 (including indirect fatalities), 2337 people injured, and around 177,914 houses and buildings suffered damage with varying level of damage. The total economic loss is projected at approximately 24-46 billion US dollars.

The most severe damage during the earthquakes was focussed in a strip area, approximately 3 kilometers east-west by 1 kilometer north-south along the north side of the valley where the Mashiki residential area situated. The area includes a combination of one and two-story recent and older structures which are generally wood-frame structures with stucco or pre-fabricated

siding. Residential houses in Mashiki Town mostly use tile roofs at the top, which of course a main cause in earthquake damage due to its mass. Commercial buildings and residential apartment buildings are mainly reinforced concrete frame.

The damage of one and two-storey wood frame houses resulted from a combination of strong ground shaking and soil failure including landslides and ground subsidence. **Figure A.4** present the example of severely damaged of residential houses in Mashiki Town.

Furthermore, the earthquakes triggered some geotechnical related hazards, for example, landslides, fault rupture, permanent ground displacement, and liquefaction, which resulting in infrastructure damage as well.

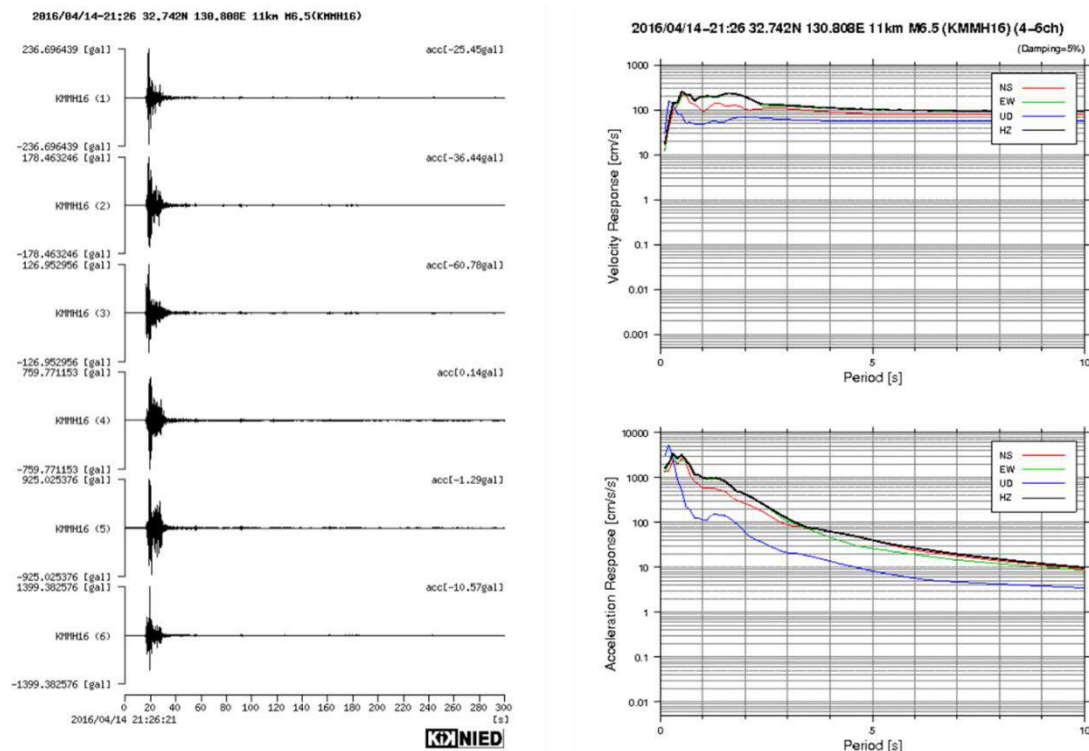


Figure A.2 The recorded acceleration, velocity response, and acceleration response of KMMH16 station at Mashiki town for the foreshock

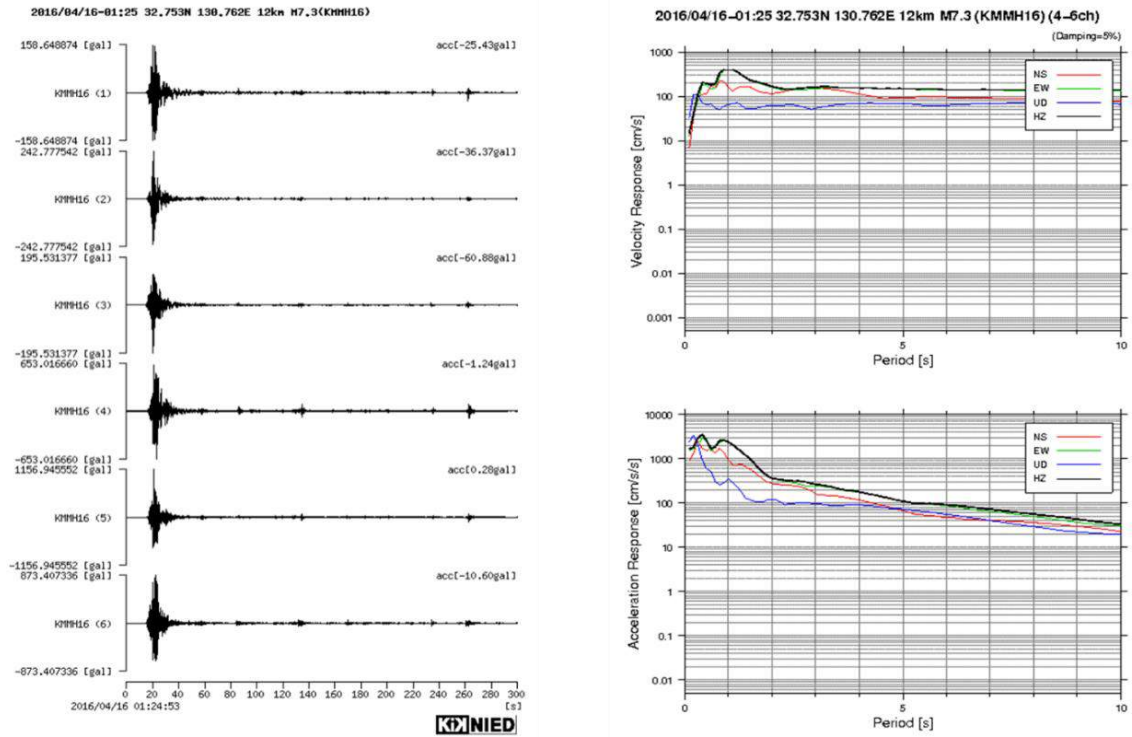


Figure A.3 The recorded acceleration, velocity response, and acceleration response of KMMH16 station at Mashiki town for the main-shock



Figure A.4 The residential houses damage in Mashiki town

A.3.1 Landslides

In the mountainous areas of Kumamoto, landslides occurred and caused severe damages to infrastructure. **Figure A.5(a)** shows earth flow at Aso Ohashi Village. This landslide affected an area of 100 m wide by 600 m long. It is reported that at least five people killed and five houses destroyed (Anon., 2016e). Furthermore, as can be seen in **Figure A.5(b)**, in Minamiaso Kawayo Village, according to the regional development bureau, there were approximately 500,000 cubic meters of soils and other substances in 700 m long and 200 m wide landslide that mopped away the Aso Ohashi bridge (Anon., 2016f).



Figure A.5 The landslides during the 2016 Kumamoto earthquake
(a) The earth flow in Aso Ohashi village
(b) Landslide in Minamiaso, Kawayo village

A.3.2 Fault Movement

Buildings and infrastructures suffered severe damages due to ground deformation in the areas close to the fault. It is reported that up to 2.0 m consistent right-lateral strike-slip is observed on the Futagawa fault. This fault movement appeared as ground surface rupture at many locations. **Figure A.6(a)** displays an aerial photo of the fault movement in a farmland in Mashiki town (Anon., 2016g). **Figure A.6(b)** illustrates the collapsed apartment block situated above the fault crack in Kurokawa Village, Minamiaso (Anon., 2016h).



Figure A.6 The fault movement during the 2016 Kumamoto earthquake
(a) The fault line in Mashiki town
(b) Collapsed apartment block due to fault movement in Kurokawa village

A.3.3 Liquefaction

Due to this earthquake sequence, there is some liquefaction occurrence reported. **Figure A.7** presents the liquefaction sites reported by Bhattacharya et al. (2018). **Figure A.8** shows the example of ground subsidence due to liquefaction that occurred in the surveyed location during this earthquake sequence. More detailed information about liquefaction and the damages occurred due to liquefaction will be presented in the following section.

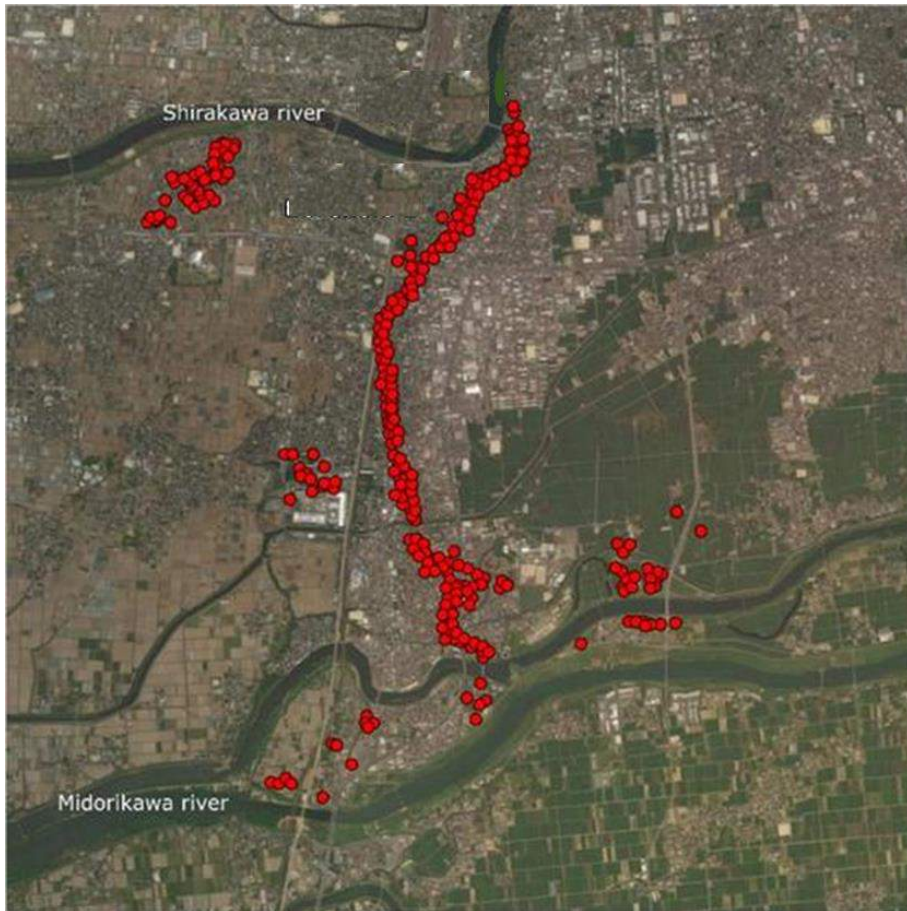


Figure A.7 Liquefaction sites during the 2016 Kumamoto earthquake



Figure A.8 Liquefaction-induced ground subsidence during the 2016 Kumamoto earthquake

A.4 Liquefaction-induced Structural Damage on Residential Houses and Buildings

Liquefaction became one of the serious problems during the 2016 Kumamoto earthquake due to the number of reported liquefaction events and the number of losses incurred. This is possible due to the soil condition in Kumamoto City. **Figure A.9** displays the geologic map of Kumamoto City by the Geological Survey of Japan (Anon., 2016i). As shown on the map, Kumamoto City is located in the north of Kumamoto alluvial plain. The alluvial plain, particularly in its southern and eastern parts are too wet for developing. According to Ishizaka et al. (1975), the Kumamoto plain is an area of active subsidence at a rate of 0.9 mm/year near the coast and 0.45 mm/year in the south of Kumamoto City. With this subsidence rate, 900 m to 450 m sediments are to be accumulated in a million years under the Kumamoto plain. It is very likely this zone of subsidence continues toward east along the Futagawa fault in the south and Mashiki town in the north. Furthermore, **Figure A.10** shows the J-SHIS Japan Seismic Hazard map (Anon., 2016j). According to the map, large site amplification is expected in Kumamoto plain, and intensity higher than 5 is highly forecasted in case of Futagawa-Hinagu fault zone earthquake.

In relation to its significant effects and damages, field reconnaissance was carried out in order to determine the liquefaction that occurred in more detail, and the impact on infrastructure, especially on the building and residential house.

A field investigation was conducted from May 27th – 30th, 2016. An investigation is focused on areas where there are many liquefaction occurrences reported, namely Akitsu, Chikami, and Karikusa areas. **Figure A.11** shows the map of the survey location performed. In these 3 locations, many buildings and houses were found damaged by liquefaction, such as foundation failure and tilted buildings. Firstly, information about the ground condition in the surveyed sites was collected, such as topography information and boring data. **Figure A.12** presents the topography soil classification map of the investigated locations (Anon., 2016k). In this survey, information and data of the damages were obtained by measuring the ground failure such as subsidence, and determine the houses and buildings inclination angle and direction by using a laser rangefinder (Leica DISTO D 510). **Figure A.13** displays the measurement locus of the house. Furthermore, to obtain more comprehensive information of the situation at the time of the earthquake and liquefaction occurred, interview with the residents was also undertaken.

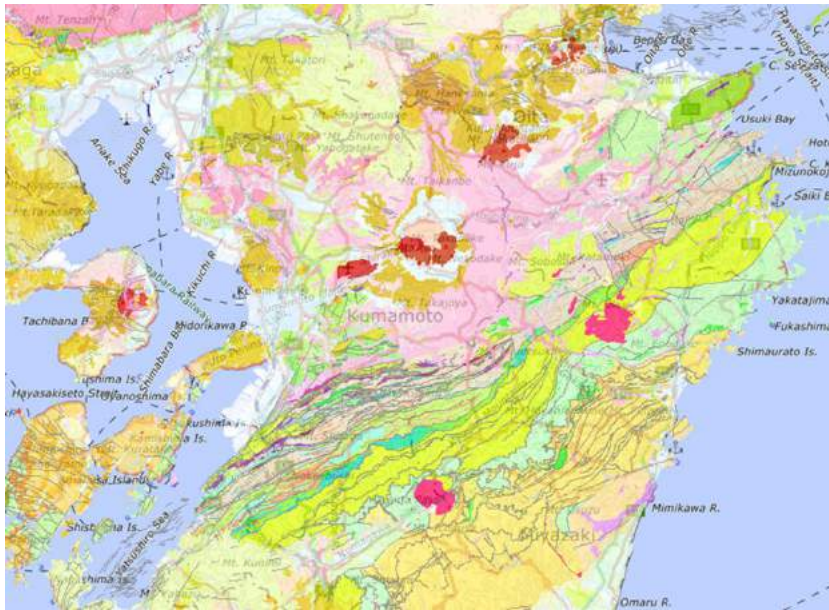


Figure A.9 the geologic map of Kumamoto city



Figure A.10 J_SHIS Japan seismic hazard map



Figure A.11 Location of the field survey

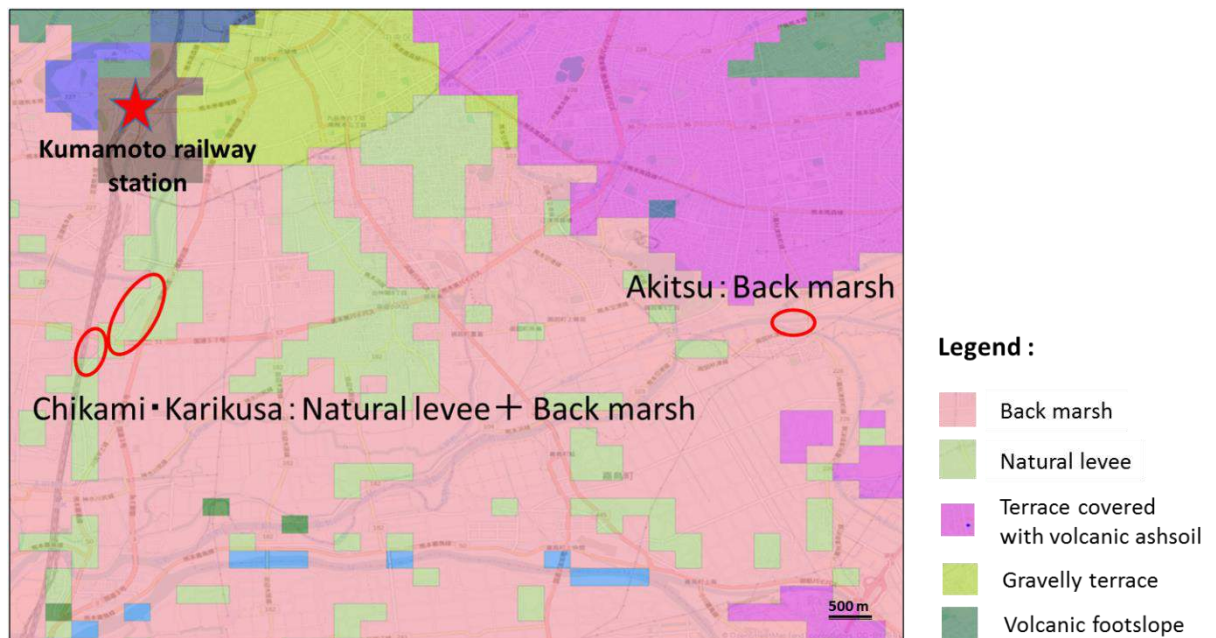


Figure A.12 Topography classification map of the surveyed sites

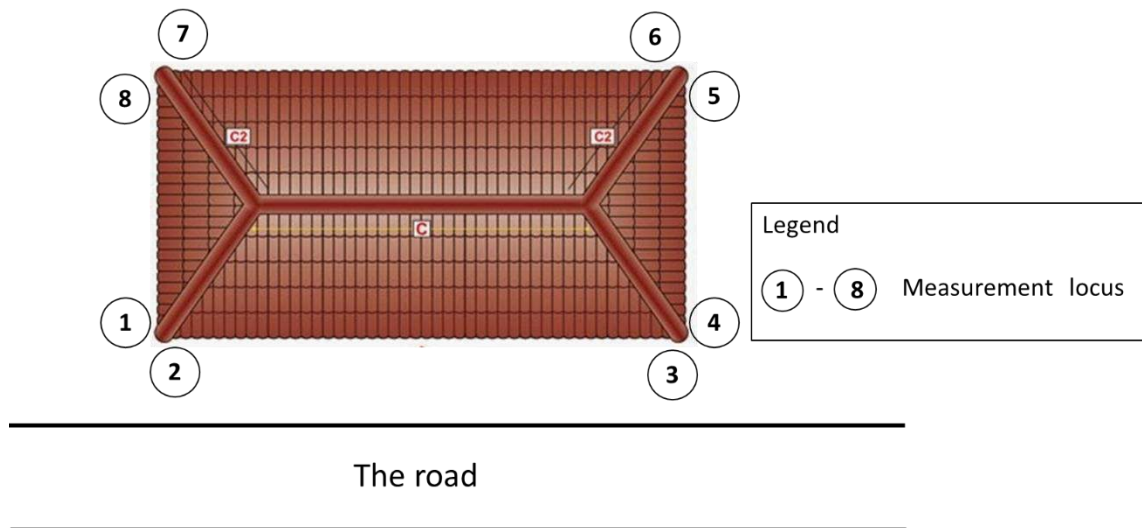


Figure A.13 Measurement locus of the house

A.4.1 Akitsu Town

The first location was Mashima residential complex in Akitsu Town. This housing area situated along the riverbank in the south of Kiyama river. The ground condition of this location observed by using boring data. **Figure A.14(a)** and **A.14(b)** show the location of Mashima residential complex and bore log, and the result obtained from the bore hole. As shown in **Figure A.14(b)**, the groundwater level is 2 meters below the ground surface. The surface layer is a 6.2 meters thick embankment layer, and at a depth ranging from 6.2 meters, the composition of the soil consists of sand and silt. Based on the value of SPT-N obtained can be concluded that the soils are in very loose condition. Although available boring data is only up to a depth of 10 meters, this data is sufficient and can be used to calculate the liquefaction potential of the ground at the site.

Furthermore, by analyzing bore data, including soil classification and SPT-N value, the liquefaction resistance factor, F_L . In this calculating, horizontal seismic intensity (K_{hgL}) of 0.3 is used to determine the liquefaction potential of the ground. **Figure A.14(c)** presents the analysis result of the safety factor against liquefaction, F_L , in Akitsu town. Based on the resultant F_L , the ground in this area highly potential to liquefy at a depth more than 6 meters below the ground surface as the F_L is lower than 1. In contrast, a 5-meter surface layer of ground has a small risk against liquefaction since it has an F_L value is higher than 1 and the groundwater level is below this layer. Although the surface layer is relatively safe against

liquefaction, since the subsoil has a high potential for liquefaction, liquefaction may occur and cause damage to the infrastructures.

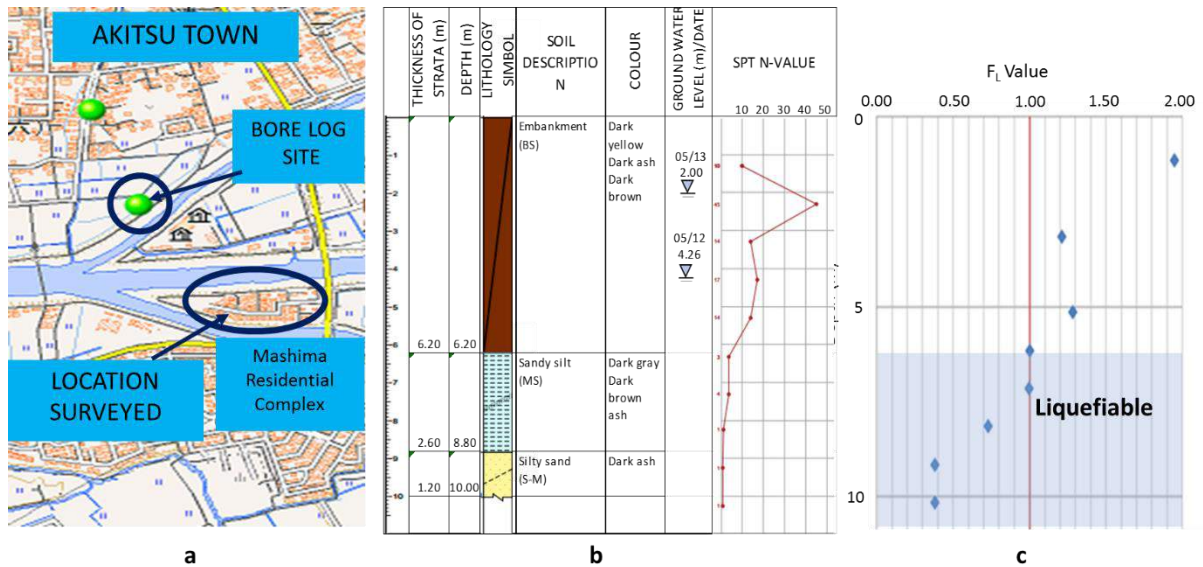


Figure A.14 (a) The location of the survey and the bore hole in Akitsu town
 (b) Boring data obtained in Akitsu town
 (c) Safety factor against liquefaction, F_L

Eight houses were measured in the Akitsu town. **Figure A.15** shows the measurement result of the tilt angle and direction the residential houses in Mashima residential complex, Akitsu town. In this figure, the tilt angle of the house is indicated by the color differences for every 0.5° . The tilt angle used for every single house is the largest angle of all locus measured. As shown on the Figure 2.15, half of the houses measured have a tilt angle higher than 1° . Besides being dangerous in terms of construction safety, according to research, a house with a tilt angle of 1° or higher will cause health problems for the inhabitants. Based on these results, from 8 houses measured in slope, there are four houses that can be categorized as causing health problems. Furthermore, houses assessed in this are were inclined toward the same direction, i.e. tilted toward the location of the Kiyama river. This indicates that the slope of the houses occur because the ground on the side closer to the river has a greater settlement than the other side. This is due to the closer to the river, the higher the potential for liquefaction, which will cause the possibility of ground deformation such as settlement or lateral spreading, also becoming greater.

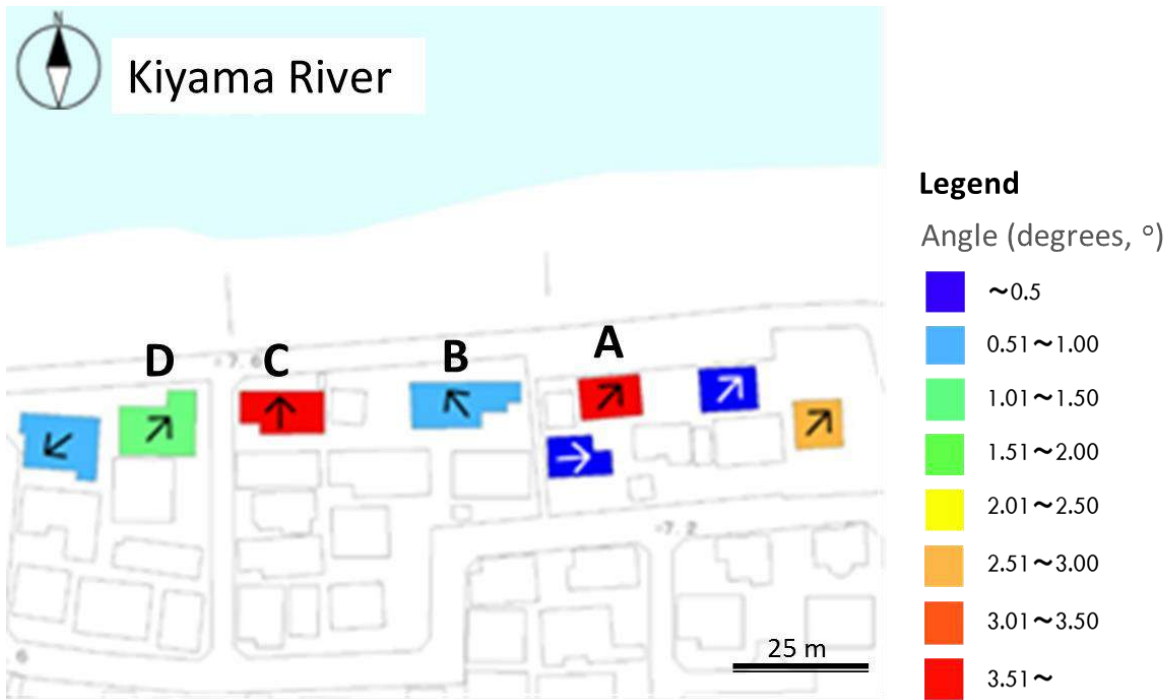


Figure A.15 The tilt angle and tilt direction measured in Akitsu town

Figure A.16 shows the condition of the tilted house surveyed in Akitsu town due to liquefaction during the earthquake. As can be seen, the house is tilted toward the river. Moreover, one of the evidence of liquefaction occurrence around the river is lateral spreading that take place in the river basin, as seen in **Figure A.17**.



Figure A.16 One of the tilted houses in Akitsu town



Figure A.17 The lateral spreading occurred at Kiyama Riverbank, Akitsu town

Figure A.18 presents the resume of the structure type of the houses and the damage in this area. Building A is a 2-story wooden frame building. It is inclined 3.6° to the north and 3.7° to the east. It is observed that ground subsidence occurred on the north side of the building and the foundation suffered differential settlement. Settlement on the north side also appeared in Building C and D, and as a result, these two building tilted to the north as well. In contrary, although ground subsidence appeared, building B only experienced minor inclination due to the insignificant differential settlement of its foundation. This is because this building is supported by pile foundations as shown in **Figure A.19**. Accordingly, it is thought that the degree of inclination of the structures is influenced by the type of the foundation as well.





Building	A	B	C	D
Photo				
Structure Type	Wooden frame, 2 storey	Steel frame, 2 storey	Wooden frame, 2 storey	Wooden frame, 2 storey
Inclination damage	3.6° to the North, 3.7° to the East	Minor inclination (less than 1°)	3.6° to the North	1.5° to the North

Figure A.18 The summary of the structural type and damage level of buildings in Akitsu town



Figure A.19 The pile-supported house which experienced minor inclination in Akitsu town

A.4.2 Chikami and Karikusa Towns

Chikami and Karikusa areas are located in the southern part of Kumamoto city. Figure A.20(a) shows the location investigated and bore log in this area, and **Figure A.20(b)** presents the boring data acquired from the same location. As can be seen, in Chikami and Karikusa, the depth of the groundwater level is as shallow as around 2.15 meters, and the ground up to a depth of about 20 meters mostly composed of sand and silt. Based on the SPT-N value obtained, the ground is in a very loose condition, especially the top soil up to 12.5 meters thick. Furthermore, **Figure A.20(c)** displays the analyzing result of liquefaction resistance, F_L . Based on the graph, it can be determined that the surface layer to a depth of 12.5 meters below the ground surface has a high potential to liquefy due to the F_L is less than 1.

In order to ascertain ground condition in this area, geological profiles of other bore log are observed in the adjacent sites. The results obtained including groundwater level, soil composition, and safety factor against liquefaction, F_L , was much the same, as shown in **Figure A.21**.

It was found that the liquefaction-induced damage in this area was distributed along a longitudinal strip. This phenomenon thoughtful due to the presence of a former river in the north-south direction of Chikami and Karikusa areas.

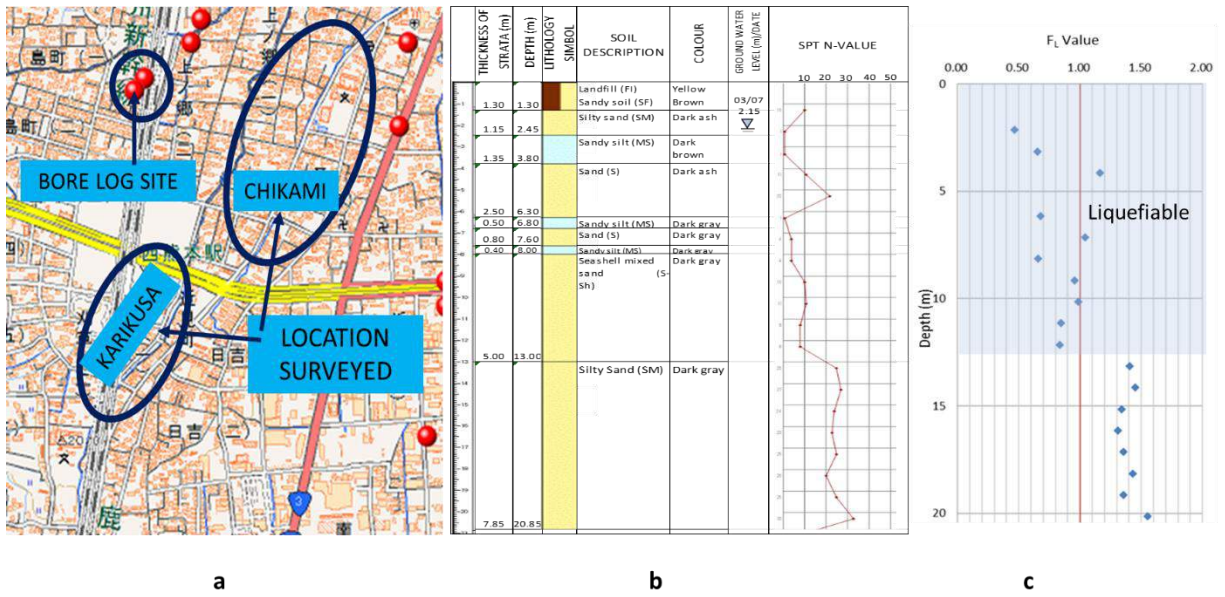


Figure A.20 (a) The location of the survey and the borehole in Chikami-Karikusa towns
 (b) Boring data obtained in Chikami-Karikusa towns
 (c) Safety factor against liquefaction, F_L

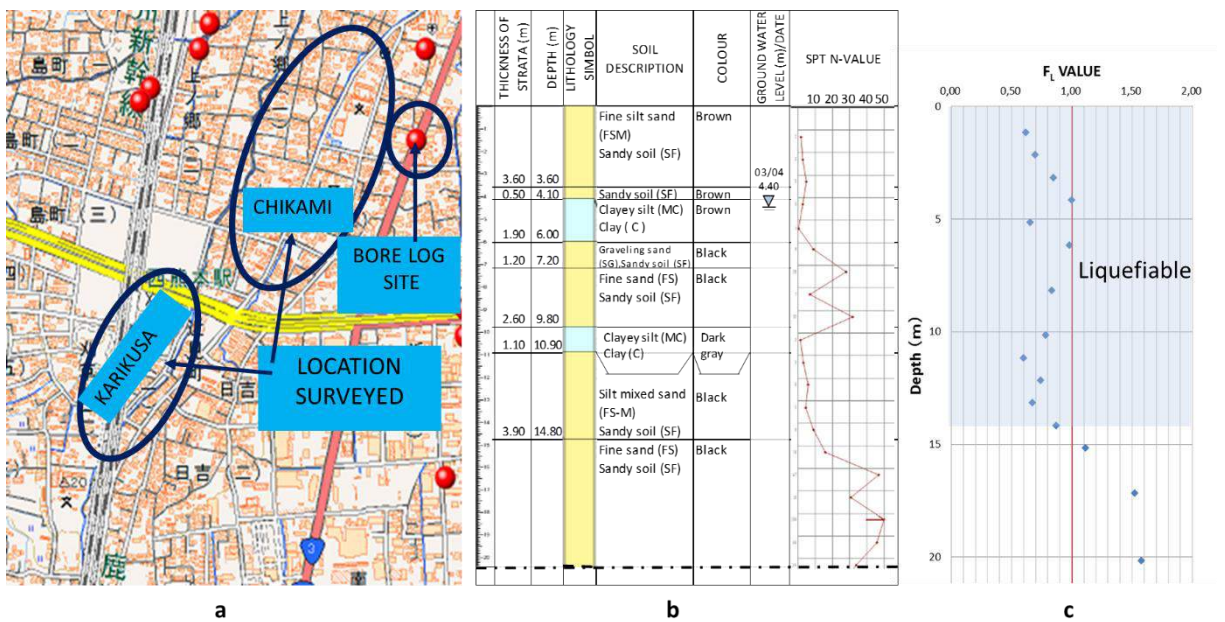


Figure A.21 (a) The location of the survey and the borehole in Chikami-Karikusa towns
 (b) Boring data obtained in Chikami-Karikusa towns
 (c) Safety factor against liquefaction, F_L



Figure A.22 The guiding pillar of former Chikami bridge

Figure A.22 illustrates a guiding pillar at the side of the road and naming it as the Chikami bridge. It convinces the assumption that this area was previously a river and the reason why this area is liquefiable. The liquefiable zone is spread over 5 km in length and 50 to 100 meters in width.

Figure A.23 presents the measurement results of the tilt angle and direction of the buildings and houses in Chikami area. According to the map resulted, there is a tendency that buildings which experienced large tilted angle were located in adjacent locations. Also, it can be seen that the direction of tilted buildings mostly toward to the southeast, where the river used to be. Structure type and building damage in Chikami town are summarized in **Figure A.24**. The four buildings, A, B, C, and D are taller and heavier than other buildings in this site. As a result, the tilt angle and the damage inflicted were more significant than others. Differential settlement occurred in both steel and wooden frame buildings. Buildings B and C were tilted to appear to be attracted to each other. This was probably caused by the combined weight of two adjacent buildings and resulting in a greater settlement on the neighboring side. It also seems that the imbalanced settlement was influenced by the weight of the structures and the position of its mass center.

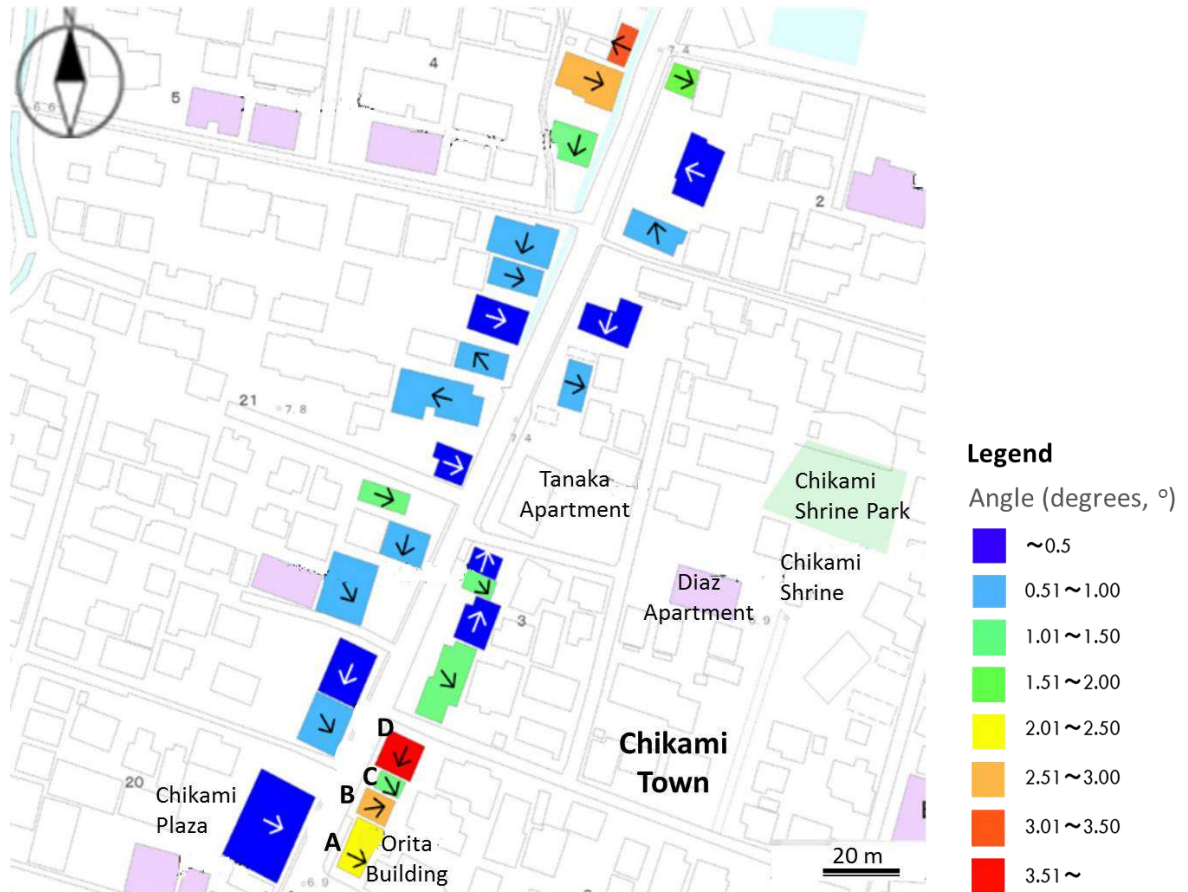


Figure A.23 The inclination angle and direction measured in Chikami town





Building	A	B	C	D
Photo				
Structure Type	Steel frame, 3 storey	Wooden frame, 2 storey	Wooden frame, 3 storey	Wooden frame, 2 storey
Inclination damage	1.5° to the East	2.7° to the East, front wall is damaged	1.3° to the East, first floor is damaged	5.7° to the East, North side wall is damaged

Figure A.24 The summary of the structure type and damage level several buildings in Chikami town

Figure A.25 shows the result of tilt angle and direction of the buildings in Karikusa town. Accordingly, there are many buildings in this area experienced an inclination toward the east side. **Figure A.26** displays the summary of the structural form and building damage in Karikusa town. The building with the largest inclination angle is building B, a one-story building. There is no significant structural damage on building B, but a lot of boiled sands were found around it. Moreover, all these buildings, A, B, C, and D are inclined to the east side as well.

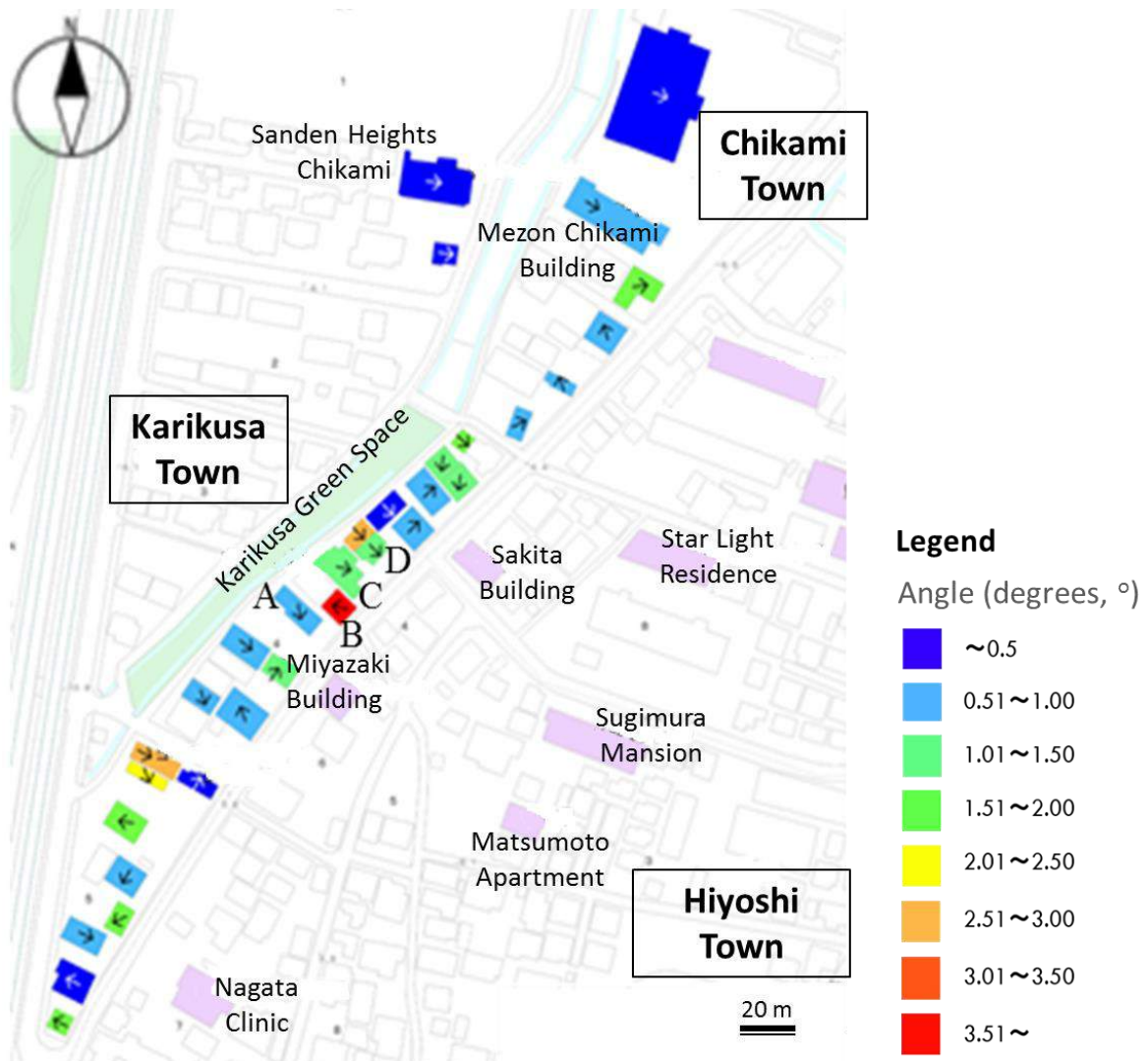


Figure A.25 The inclination angle and direction measured in Karikusa town





Building	A	B	C	D
Photo				
Structure Type	Steel frame, 2 storey	Wooden frame, 1 storey	Steel frame, 2 storey	Wooden frame, 2 storey
Inclination damage	Minor inclination (less than 1°)	3.6° to the West	1.3° to the East	1.3° to the East

Figure A.26 The summary of the structure type and damage level buildings in Karikusa town

A.5 Discussion

In Akitsu town, by analyzing the sounding data, it is found that the ground at a depth of more than 5 meters was categorized as potentially liquefy ground. This analysis is proven during the 2016 Kumamoto earthquake, liquefaction occurred. This liquefaction occurrence mainly triggered by the very loose sand and silt conditions, and the existence of Kiyama river in this area. Lateral spreading appeared on the river basin. Moreover, significant ground subsidence and imbalanced settlement also took place and caused many buildings to tilt.

Furthermore, in Chikami and Karikusa towns, ejected sands trace remained at the roadside and around the buildings surveyed. Sand boiling took place because of the ground surface is mostly composed of the loose sand layer. In addition, the presence of a former river in north-south direction of this areas also causes the opportunity for liquefaction to become larger.

Previously, in the 2011 Great East Japan earthquake, enormous liquefaction damage occurred in Urayasu city, Chiba Prefecture. At that time, approximately 85% of the Urayasu city was damaged due to liquefaction. Since the area affected by liquefaction is enormous, a large-scale liquefaction countermeasure technique was undertaken, in the form of massive underground walls. In contrary, unlike Urayasu city, liquefaction occurrence in Kumamoto city during the 2016 Kumamoto earthquake was not centralized in one large area but scattered in small separate sites. Even though some buildings are situated in the neighboring

locations, the extent of the damage may vary, depend on the aforementioned factors, such as structure type, foundation type, and soil conditions just below the building.

Interviews with residents indicate that some residents prefer to move rather than perform liquefaction countermeasure technique on their homes. The reason is that liquefaction mitigation techniques usually require enormous cost and complex technical implementation. Furthermore, residents felt uncomfortable to live in the tilted house with a tilt angle of 1° or higher, and even worse; the house became hard to live in if the inclination angle is exceeding 2°.

Based on the field reconnaissance results, liquefaction characteristics in Kumamoto city during the 2016 Kumamoto earthquake are different from liquefaction in Urayasu city during the 2011 Great East Japan earthquake. Therefore, liquefaction mitigation that can be applied is also different. For liquefaction characters as happened in Kumamoto, it is thought that will be very useful to devise and develop liquefaction countermeasure technique for detached residential houses and buildings, whether for existing or new houses. These new and simplified methods are expected to be affordable and used to overcome liquefaction in residential houses and constructions that cannot use sophisticated and costly techniques.

A.6 References

- Anon. 2016a. Distribution of epicenters plotted on geological maps in Kumamoto Prefecture. Available at: <http://g-ever.org/updates/p=285> [Accessed November 29, 2016].
- Anon. 2016b. Estimated seismic intensity distribution map (April 14th, 2016). Available at: http://www.data.jma.go.jp/svd/eew/data/suikai/201604142126_741/201604142126_741_1.html [Accessed November 29, 2016].
- Anon. 2016c. Estimated seismic intensity distribution map (April 16, 2016). Available at: http://www.data.jma.go.jp/svd/eew/data/suikai/201604160125_741/201604160125_741_1.html [Accessed November 25, 2016].
- Anon. 2016d. Recorded acceleration, velocity response, and acceleration response at KMMH16 station, Mashiki town. Available at: http://www.kyoshin.bosai.go.jp/kyoshin/share/index_multi.html [Accessed May, 2018].
- Anon. 2016e. Earth flow at Aso Ohashi village. Available at: <https://blogs.agu.org/landslideblog/2016/06/28/new-zealand-society-for-earthquake-engineering-report-1>. [Accessed May, 2018].
- Anon. 2016f. Landslide in Minamiaso, Kawayo village. Available at:

- <https://mainichi.jp/english/articles/20160505/p2a/00m/0na/014000c> [Accessed May, 2018].
- Anon. 2016g. Aerial photograph of the fault movement in the farmland in Mashiki town. Available at: <https://www.japantimes.co.jp/news/2016/04/18/national/questions-and-answers-the-kumamoto-earthquakes/#.Wv1Ne6SFNpg>. [Accessed May, 2018].
- Anon. 2016h. The collapsed apartment block situated above the fault crack in Kurokawa village. Available at: http://www.eqclearinghouse.org/2016-04-15-kumamoto/files/2016/04/NZSEE_Kumamoto_Report.pdf. [Accessed May, 2018].
- Anon. 2016i. The geologic map of Kumamoto city. Available at: <https://gbank.gsj.jp/seamless/seamless2015/2d/index.html?lang=en> [Accessed May, 2018].
- Anon. 2016j. J-SHIS Japan seismic hazard map. Available at: <http://www.j-shis.bosai.go.jp/map/?lang=en> [Accessed November 29, 2016].
- Anon. 2016k. Kumamoto topography classification map. Available at: <http://www.j-shis.bosai.go.jp/> [Accessed November 29, 2016].
- Bhattacharya, S., Hyodo, M., Nikitas, G., Ismael, B., Suzuki, H., Lombardi, D., Egami, S., Watanabe, G., and Goda, K. 2018. Geotechnical and infrastructural damage due to the 2016 Kumamoto earthquake sequence. *Soil Dynamics and Earthquake Engineering Journal*, Vol. 104, January 2018, 390-394.
- Cubrinovski, M., Henderson, D., and Bradley, B. 2012. Liquefaction Impacts in Residential Areas in the 2010-2011 Christchurch Earthquakes. *One year after 2011 Great East Japan Earthquake: International Symposium on Engineering Lessons Learned from the Giant Earthquake*, pp.1–14.
- Koseki, J., Wakamatsu, K., Sawada, S., and Matsushita, K. 2015. Liquefaction-induced damage to houses and its countermeasures at Minami-Kurhashi in Kuki City during the 2011 Tohoku Earthquake, Japan. *Soil Dynamics and Earthquake Engineering* 79: 391–400.
- Rasouli, R., Towhata, I. & Hayashida, T. 2015. Mitigation of seismic settlement of light surface structures by installation of sheet-pile walls around the foundation. *Soil Dynamics and Earthquake Engineering* 72: 108–118.
- Shigeki, S., Wakamatsu, K., Ozawa, K., and Fujiwara, H. 2016. Liquefied sites during the 2016 Kumamoto Earthquake. Available at: <https://confit.atlas.jp/guide/event-ing/jpgu2016/MIS34-26P87/public/pdf> [Accessed November 29, 2016].
- Tani, K., Kiyota, T., Matsushita, K., Hashimoto, T., Yamamoto, A., Takeuchi, H., Noda, T., Kiku, H., and Obayashi, J. 2015. Liquefaction countermeasures by shallow ground improvement for houses and their cost analysis. *Soil Dynamics and Earthquake Engineering* 79: 401–414.
- Tokimatsu, B.K., Kojima, H. & Kuwayama, S. 1994. Liquefaction-induced damage to buildings in 1990 Luzon earthquake. *Journal of Geotechnical Engineering* 120(2): 290–307.

- Tokimatsu, K. & Katsumata, K., 2012. Liquefaction-Induced Damade To Buildings in Urayasu City During the 2011 Tohoku Pacific Eathquake. *The International Symposium on Engineering Lessons learned from the 2011 Great East Japan earthquake* 665–674.
- Yoshida, M., Miyajima, M. & Numata, A., 2012. Proposal of liquefaction countermeasure technique by log piling for residential houses. In *Proceedings of the Tenth International Symposium on Mitigation of Geo-disasters in Asia in Matsue Conference* 55–67.